EFFECTS OF CALMODULIN ON THE FUNCTION OF CARDIAC AND SKELETAL RYANODINE RECEPTORS

Ye Wint Oo
MSc

A thesis submitted in fulfillment
of the requirements for the degree of
Doctor of Philosophy
August 2016

School of Biomedical Sciences and Pharmacy
University of Newcastle

Statement of Originality

This thesis contains no material which has been accepted for the award of any other degree or diploma in any university or other tertiary institution, and to the best of my knowledge and belief, contains no material previously published or written by another person, except where due reference has been made in the text. I give consent to this copy of my thesis, when deposited in the University Library, being made available for loan and photocopying subject to the provisions of the Copyright Act 1968.

…….

School of Biomedical Sciences and Pharmacy
University of Newcastle

Statement of Collaboration

I hereby certify that the work embodied in this thesis has been done in collaboration with other researchers or carried out in other institutions. I have included as part of the thesis a statement clearly outlining the extent of collaboration, with whom and under what auspices.

Ca^{2+} wave and frequency measurements of permeabilised cardiomyocytes in **Chapter 3** are given by **DrBC Knollmann** (School of Medicine, Vanderbilt University, Nashville TN USA.).

…….

School of Biomedical Sciences and Pharmacy

University of Newcastle

Statement of Authorship

I hereby certify that the work embodied in this thesis contains a published paper/s/scholarly work of which I am a main author. I have included as part of the thesis a written statement endorsed by my supervisor, attesting to my contribution to the joint publication/s/scholarly work.

Oo, Y. W., Gomez-Hurtado, N., Walweel, K., van Helden, D. F., Imtiaz, M. S., Knollmann, B. C., & Laver, D. R. (2015). Essential role of Calmodulin in RyR inhibition by dantrolene. *Molecular pharmacology*, *88*(1), 57-63.

…….

School of Biomedical Sciences and Pharmacy

University of Newcastle

Dedication

This thesis is dedicated to my parents U Khin Maung Oo and Daw Khin Hla, who have always supported me throughout my life and, by their example, have taught me to work hard for the goals that I aspire to achieve. In addition, this work is also dedicated to my wife Khin Moh Moh Latt, who has been a constant source of support and encouragement during my studies.

Acknowledgements

This thesis is a result of a long journey accompanied by the support and encouragement of others. Along the journey, I feel blessed to have had great mentors over the years. I would like to sincerely express my immense gratitude to my primary supervisor A/P Prof. Derek Laver for his positive encouragement, academic support and inspiring personal advice throughout my study. He is one of the shining lights on my academic journey. In particular, I would like to thank him for the extension of my scholarship in the last few months of the Ph.D. studies.

For thoughtful advice and support, I would like to thank my supervisors Prof. Dirk van Helden and Dr. Mohammad Imtiaz. For great friendship and for always sharing experiences, I want to thank my colleague Dr. Kafa Walweel, and to Paul Johnson for his assistance with the laboratory work. I must acknowledge to all of those people and other work colleagueswho are not named here, I thank you from the core of my heart.

I would also like to extend warm thanks to Myo Nyunt Maw for never doubting me over the many years of our friendship and for proofreading of my thesis.

Finally, my heartfelt thanks and appreciation go to my parents and my wife who have been supporting me unconditionally throughout my studies from the other side of the world. This work would not have been possible without them.

Publications

Journal articles

1. **Oo, Y. W.**, Gomez-Hurtado, N., Walweel, K., van Helden, D. F., Imtiaz, M. S., Knollmann, B. C., & Laver, D. R. (2015). Essential role of calmodulin in RyR inhibition by dantrolene. *Molecular pharmacology*, *88*(1), 57-63.

2. Bupha-Intr, T., **Oo, Y. W.** & Wattanapermpool, J. (2011). Increased myocardial stiffness with maintenance of length-dependent calcium activation by female sex hormones in diabetic rats. *American Journal of Physiology-Heart and Circulatory Physiology*, *300*(5), H1661-H1668.

3. **Oo, Y. W** K., van Helden, D. F., Imtiaz, M. S., Knollmann, B. C., & Laver, D. R. (2016). Inhibitory effects of dantrolene on skeletal ryanodine receptor. *Anaesthesiology Journal (Manuscript in preparation)*

Oral presentations

1. **Y.W. Oo** , D.F. vanHelden , M. S. Imtiaz, and D.R. Laver
   "Inhibitory effect of dantrolene on skeletal muscle RyR in the presence of calmodulin"
   AuPS, Hobart, Tasmania, Australia (Nov 29 - Dec 2, 2015)
2. **Y.W. Oo**, N. Gomez-Hurtado, D.F. van Helden , M.S. Imtiaz , B.C. Knollmann and D.R. Laver
   "Dantrolene inhibition of RyR2 requires calmodulin"
   Gordon Research Seminar, Newry, Maine, USA (May 30-31, 2015)

3. **Y.W. Oo** , D.F. van Helden , M. S. Imtiaz , B.C. Knollmann and D.R. Laver
   "Inhibitory effect of dantrolene on cardiac RyR2 in the presence of calmodulin"
   AuPS, Brisbane, Queensland, Australia (Nov 30 - Dec 3, 2014)

Poster presentations

1. **Y.W. Oo**, D.F. van Helden , M. S. Imtiaz and D.R. Laver
   "Dantrolene inhibition of skeletal muscle RyR in the presence of CaM"
   Biophysical Society 60th Annual Meeting, Los Angeles, CA, USA. (Feb 27 - -Mar 2, 2016)
2. **Y.W. Oo**, N. Gomez-Hurtado, D.F. van Helden, M.S. Imtiaz , B.C. Knollmann and D.R. Laver
   "Dantrolene inhibition of RyR requires calmodulin"
   Gordon Research Conference, Newry, Maine, USA (May 31- - June 6, 2015)
3. **Y.W. Oo**, D.F. van Helden , M.S. Imtiaz , B.C. Knollmann and D.R. Laver
   "Dantrolene inhibition of RyR2 requires calmodulin"
   Biophysical Society 59th Annual Meeting, Baltimore, MD, USA (Feb 7 - 11, 2015).
4. **Y.W. Oo**, D.F. van Helden , M. S. Imtiaz and D.R. Laver
   "Effects of calmodulin on calcium activation of cardiac ryanodine receptor"
   IUPAB, Congress, Brisbane, Australia (Aug 3 - 7, 2014)
5. T. Bupha-Intr, **Y.W. Oo**, J. Wattanapermpool
   "Potential diastolic myocardial dysfunction in ovariectomized rats complicated with diabetes"
   ISHR meeting,North American Section,(2009)

Abbreviations

ADP	adenosine diphosphate
ATP	adenosine triphosphate
apoCaM	apocalmodulin
AMP	adenosine monophosphate
BAPTA	1, 2-bis [o-aminophenoxy] ethane-*N*, *N*, *N*', *N*'- tetraacetic acid
CaCaM	Ca^{2+}/calmodulin
CaM	calmodulin
CaMKII	Ca^{2+}/calmodulin-dependent protein kinase II
CICR	calcium-induced calcium release
CPVT	cCatecholaminergic polymorphic ventricular tachycardia
CSQ2	calsequestrin
CsMS	cesium methanesulfonate
DR	divergent region
E-C	excitation-contraction
FKBP	FK506-binding proteins
FRET	fluorescence-resonance-energy-transfer
MH	malignant hyperthermia
mM	millimolar (mmol/l)
ms	millisecond
NaF	sodium fluoride
NCX	Na^{+}/Ca^{2+} exchanger
nM	nanomolar (nmol/l)
PC	phosphatidylcholine
PDE4D3	type 4 phosphodiesterase
PE	phosphatidylethanolamine
PKA	cyclic AMP-dependent protein kinase
PP1	protein phosphatase 1
PP2A	protein phosphatase 2A
RyR	ryanodine receptor
s	second
SA	sino-atrial

SERCA2a	sarcoplasmic/endoplasmic reticulum Ca^{2+}-ATPase
SR	sarcoplasmic reticulum
T-tubules	transverse tubules
µl	microliter
µM	micromolar (µmol/l)

Contents

Abstract

Dantrolene is a muscle relaxant that has been used clinically for the treatment of the malignant hyperthermia (MH) response to volatile anaesthetics such as halothane. Interestingly, it has been recently found to protect against heart failure and arrhythmias caused by spontaneous Ca^{2+} release. Assays of Ca^{2+} release in intact myocytes and cell homogenates indicate that dantrolene inhibits Ca^{2+} release from the sarcoplasmic reticulum (SR) of skeletal and cardiac muscle. However, its mechanism of action has remained controversial because single channel studies did not find any effect of dantrolene on the RyR Ca^{2+} release channel. Realizing that the physiological RyR binding partner calmodulin (CaM) readily dissociates from RyRs during incorporation into lipid bilayers, and that endogenous CaM is absent during single channel recordings, it was hypothesized in this thesis that CaM was required for dantrolene inhibition. RyR1 and RyR2 from rabbit skeletal muscle or sheep and human hearts were isolated and incorporated into artificial lipid bilayers and their open probability (P_o) was measured using single channel recordings. In the presence of exogenous 100 nM CaM (100 nM cytoplasmic [Ca^{2+}] + 2 mM ATP), dantrolene caused an allosteric inhibition of the RyR1 (rabbit skeletal muscle) and the RyR2 (sheep heart) in single channel assays showing a maximum relative P_o (E_{max}) of 52 ± 4 % of control values. In saponin-permeabilized mouse cardiomyocytes supplemented with 100 nM CaM, dantrolene similarly reduced Ca^{2+} wave frequency (IC_{50} = 0.42 ± 0.18 µM, E_{max}= 47 ± 4 %) and amplitude (IC_{50} = 0.19 ± 0.04 µM, E_{max}= 66 ± 4 %). Together, the results demonstrate that CaM is essential for dantrolene inhibition of RyR1s and RyR2s and that its absence explains why dantrolene inhibition in single channels has not been previously observed. This study also presents the first demonstration of dose-dependent dantrolene inhibition of RyR2s with an IC_{50} of 0.16 ± 0.03 µM in the presence of exogenous 100 nM CaM. The study also aimed to characterize dantrolene inhibition on RyR1s in the presence of exogenous CaM. The effects of dantrolene on RyR1s differentially regulated by CaM were measured at various cytosolic and luminal Ca^{2+} concentrations. It was then tested whether dantrolene could restore the channel activity affected by activating substances such as ATP, halothane and the interdomain domain destablising peptide DP4.which mimics the effects of inherited mutations underlying MH susceptibility. Dantrolene inhibited the RyR1 with identical hyperbolic dose-responses with an IC_{50} of 0.20 ± 0.02

μM and a maximum P_o of 50 ± 2 % of controls in the presence of exogenous 100 nM CaM (100 nM cytoplasmic [Ca^{2+}] + 2 mM ATP). In the absence of dantrolene, the RyR1 has a bell-shaped cytoplasmic Ca^{2+} activation curve with half activation at 1.7 ± 0.4 μM (H_a = 1.3 ± 0.2), half inhibition at 0.22 ± 0.01 mM (H_i = 2.7 ± 0.5) and a peak P_o = 0.93 ± 0.04. Dantrolene reduced P_o in sub-activating and inhibiting [Ca^{2+}] but failed to reduce the peak P_o. Dantrolene significantly inhibited RyR1 activity at luminal [Ca^{2+}] of 0, 100 and 1000 μM in the presence of exogenous CaM regardless of the trans-membrane voltages. Dantrolene caused a 50-60% reduction in P_o of RyR1s activated by cytoplasmic Ca^{2+} alone (100 nM) or in conjunction with ATP (2mM), halothane (5 mM) or DP4 (10 μM). Dantrolene equally inhibited RyR1 activity (50-60%) in the absence and presence of 20 and 50 μM cytoplasmic Mg^{2+}.

To conclude, dantrolene inhibited the RyR1 activity by decreasing RyR1 sensitivity to Ca^{2+} activation and increasing sensitivity to Ca^{2+} inhibition. Because dantrolene decreased channel activity both in the absence and presence of modulators such as halothane and DP4, this suggests the action of dantrolene inhibition of RyR1 activity could be independent of halothane and DP4.

Regulation of RyR1s by Ca^{2+}, Mg^{2+} and ATP is well characterised. However, there is minimal data on these regulation processes in the presence of CaM. Therefore, the effects of CaM on cytosolic Ca^{2+} activation and inhibition of the RyR1, as well as its regulation by luminal Ca^{2+} and inhibition by cytoplasmic Mg^{2+} were investigated in this thesis using single channel recordings. In addition, the effects of CaM on RyR1s altered by ATP, halothane and DP4 were tested. CaM increased the P_o of RyR1s to ~150% of control at a cytoplasmic [Ca^{2+}] of 0.1 μM, whereas it reduced the P_o of RyR1s to 50 % of control at 1 μM and concentrations higher than 500 μM. Notably, CaM failed to have any impact on RyR1 activity at cytoplasmic [Ca^{2+}] of 10-100 μM. CaM increased the P_o of RyR1 by ~140% at 0 and 100 μM luminal [Ca^{2+}] whereas it was inhibited by 25-35% at 1000 μM luminal [Ca^{2+}] regardless of the voltage. At cytoplasmic [Ca^{2+}] of 0.1 μM, CaM equally activated RyR1s by 150-200% in the absence and presence of 20 and 50 μM cytosolic Mg^{2+}. ATP did not affect CaM activation at cytoplasmic [Ca^{2+}] of 0.1 μM. However, CaM inhibited the channel activity only in the absence of ATP at cytoplasmic [Ca^{2+}] of 100 μM. CaM activation of RyR1s was not affected by halothane and DP4.

Chapter 1

General Introduction

1.1 Introduction

1.1.1 Cardiac cycle and excitation-contraction (E-C) coupling

Cardiac excitation-contraction (E-C) coupling is the process by which electrical stimulation causes mechanical contraction [1]. In this event, Ca^{2+} acts as a second messenger that binds to myofilaments to generate the contraction [2]. The summation of the contraction of the cardiac muscle cells causes the contraction of the whole heart to pump blood, a process called *systole*. Relaxation of the cardiac muscles allows the refilling of blood to the heart during the *diastole* period. Thus, any abnormality in calcium handling by cardiac myocytes is associated with a contractile dysfunction [3].

In the mammalian heart, a group of specialized pacemaker cells present in the sino-atrial node (SA node) generates the action potential. The cardiac myocytes form an electrical syncytium due to gap junction coupling. Thus, the action potential from the SA node travels through the cellular syncytium through a network of conducting cells and then into the muscle. The cardiac action potential causes the influx of calcium into the cell via voltage gated calcium channels (L-type Ca^{2+} channels).

The cardiac L-type Ca^{2+} channels in the transverse tubule (T-tubules, which are invaginations of the plasma membrane) oppose clusters of Ca^{2+} release channels (ryanodine receptors, RyR) in the sarcoplasmic reticulum (SR) membrane at narrow junctions between the SR and T-tubule (dyads) [4]. During diastole, the cytosolic free calcium concentration is around 100 nM [5]. When cardiac myocytes are activated during systole, Ca^{2+} flux via L-type channels triggers RyR2s to open and release Ca^{2+} from the SR;this released Ca^{2+} further activates the calcium release channel as shown in Figure 1.1. This process is called Ca^{2+}-induced Ca^{2+} release (CICR). The combination of Ca^{2+} influx and release leads to the Ca^{2+} concentration rising to 100 μM in the dyad cleft and 1 μM in the bulk cytoplasm [1, 6]. There are several Ca^{2+} release phenomena arising from the SR. A calcium spark is caused by the release of Ca^{2+} from a cluster of RyR2s in a dyad cleft [7]. It is called a calcium spark because it appears as a burst of light given by fluorescent Ca^{2+} under confocal microscopy [7]. The summation of calcium sparks from about 10^4 Ca^{2+}-release sites results in a global transient increase in

intracellular Ca^{2+} of ~ 1 μM [2, 6]. In addition, the diffusion of Ca^{2+} between Ca^{2+} release sites can trigger neighboring RyR2s to form a Ca^{2+} wave that propagate along the cell. During E-C coupling, a single myocyte may evoke approximately 10^4 Ca^{2+} sparks within a few tens of milliseconds. [7].

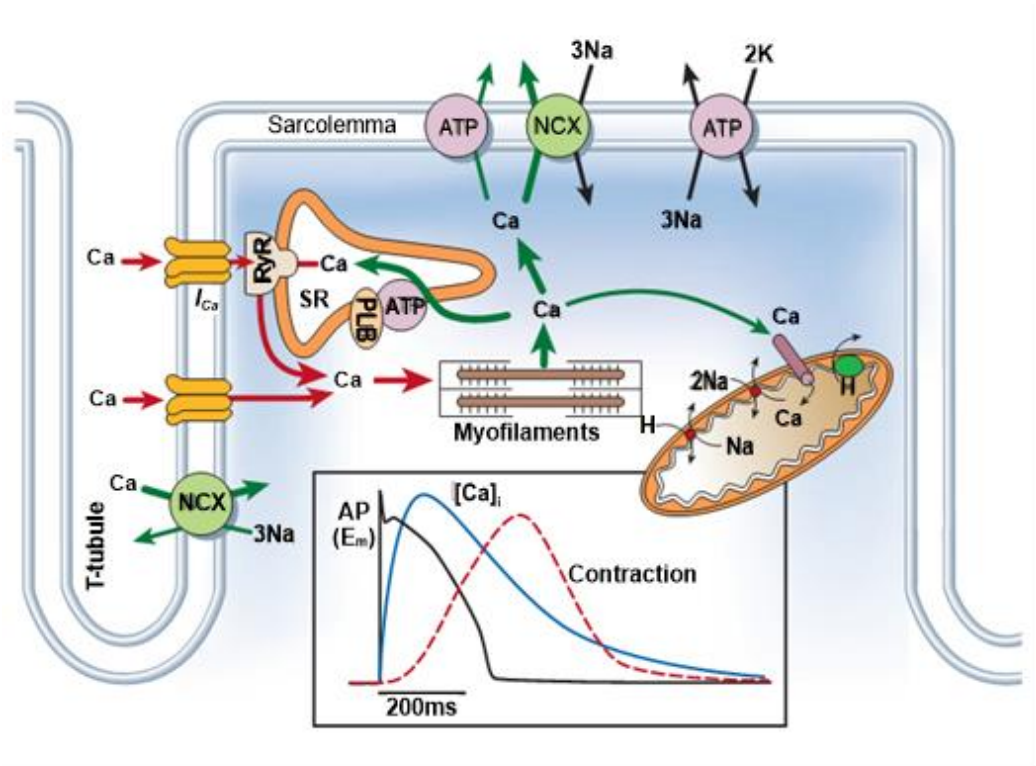

Figure 1.1 Excitation-contraction coupling of cardiac myocytes [1]. The depolarization waves propagate over regularly occurring invaginations of the plasma membrane called transverse tubules (T-tubules). The initial spread of depolarization from the propagating action potential, triggers an action potential in the T-tubule via the opening of voltage-gated Na^+ and L-type calcium channels, triggering the opening of Ca^{2+} release from the SR and causing a further increase in the cytoplasmic [Ca^{2+}]. The increased [Ca^{2+}] initiates and activates contractile machinery. For relaxation, SR Ca^{2+} ATPase sequesters Ca^{2+} back into the SR to reduce [Ca^{2+}]. The sodium-calcium exchanger (NCX) uses the Na^+ gradient to power the removal of Ca^{2+}. Figure adapted from Bers (2002) [1].

Following each contraction phase, the heart enters diastole (relaxation) as Ca^{2+} release from the SR terminates and cytosolic Ca^{2+} concentration declines. This action is normally the consequence of Ca^{2+} uptake into the SR by SR Ca^{2+} ATPase (SERCA2a), an ATP-dependent process. The SERCA2a is responsible for pumping two Ca^{2+} ions into the lumen by using one ATP molecule [8]. Activity of this pump is reduced by phospholamban (PLB) [9]. The degree of inhibition depends on phospholamban phosphorylation by Ca^{2+}/calmodulin-dependent kinase II (CaMKII) at threonine-17 and cyclic AMP (cAMP)-dependent protein kinase A (PKA) at serine-16 which both reduce the inhibition of PLB to increase the pump activity [9].

In addition, in the steady state condition there is an efflux of Ca^{2+} across the cell plasma membrane that balances Ca^{2+} entry via voltage gated L-type calcium channels. This efflux is controlled by the NCX removing 10-30 % of the systolic $[Ca^{2+}]_I$, depending on species [1]. The Ca^{2+}ATPase in the cell plasma membrane and mitochondrial Ca^{2+} uniporter extrudes about 1% of Ca^{2+} [1].

1.1.2 (E-C) coupling in skeletal muscle

The mechanism of E-C coupling in cardiac and skeletal muscle is fundamentally different. L-type Ca^{2+} channels have two isoforms, $Ca_v1.1$ and $Ca_v1.2$ for skeletal and cardiac muscle respectively. L-type Ca^{2+} channels have multiple subunits: α_1, α_2/δ, β and γ (as yet unidentified) for $Ca_v1.1$ and α_1, α_2/δ, β for $Ca_v1.2$. The α_1 subunit is essential for E-C coupling and functions as the voltage sensor as a pore forming subunit. Cardiac E-C coupling is dependent on extracellular Ca^{2+} and the functional coupling that depends on the spatial proximity between $Ca_v1.2$ and the RyR2. E-C coupling in skeletal muscle can occur for long periods in the absence of extracellular Ca^{2+} due to the physical interaction between $Ca_v1.1$ and RyR1 [10, 11].

In cardiac muscle L-type Ca^{2+} channels are loosely clustered with RyR2s in a dyadic junction between the surface membrane and the terminal SR (dyad) [12]. The ratio of two channels is 3:10 although it can vary among the species [13]. However, in skeletal muscle L-type Ca^{2+} channels form as “tetrads” [14, 15] as a result of the direct interaction of L-type Ca^{2+} and RyR1 channels. The ratio of RyR1s to tetrads is nearly 0.125 according to morphological and biochemical studies [13]. This physical

interaction permits the transduction of conformational changes of L-type Ca^{2+} channels to the opening of the RyR1s, and, the release of Ca^{2+} from the SR by relieving the Mg^{2+} inhibition of RyR1s [16, 17]. Mg^{2+} has a very strong inhibitory effect on the release channel in a skeletal muscle under resting conditions [18-21]. It has been shown in experiments on cut and skinned fibres that when Mg^{2+} inhibition is reduced by lowering free [Mg^{2+}] from its physiological concentration (~1 mM) to 0.05 mM, the Ca^{2+} release channels spontaneously open and all of the Ca^{2+} is lost from the SR [17, 22]. In these experiments, L-Type Ca^{2+} channels can potently activate the channels in the presence of physiological concentration free [Mg^{2+}], possibly by overcoming or bypassing the strong inhibition of [Mg^{2+}] [17].

Skeletal muscle contraction does not require CICR. Rather, direct communication between RyR1 channels and L-type Ca^{2+} channels in the transverse tubule membrane plays an essential role in E-C coupling of skeletal muscle. Depolarization of the transverse tubule causes a voltage-dependent conformational change of the L-type channel within its II-III loops that has been detected as a charge movement [23]. This conformational change is communicated by a direct physical interaction to the RyR1 channels causing SR Ca^{2+} release. Physical interaction between the transverse tubule L-type Ca^{2+} channel and the RyR1 is required for skeletal muscle excitation-contraction coupling. This interaction has been suggested to involve an orthograde signal by which the L-type Ca^{2+} channel signals the RyR1 to open and a retrograde signal by which the RyR1 prevents L-type channel inactivation [24]. However, the actual interactions between the two proteins are complex, involving more than one domain and being subject to allosteric modulations [25]. One of the approaches to mapping interaction sites on the RyR1 and the L-type channel is to prepare chimeras of RyR1s and RyR2s [26] or α_{1c} and α_{1sk} subunits of the voltage dependent Ca^{2+} channels [27, 28]. This approach is based on the findings that RyR1s but not RyR2s can restore mechanical coupling in RyR1-deficient myotubes [26], and α_{1sk} but not α_{1c} can restore skeletal type E-C coupling in DHPR deficient myotubes [27, 28]. This approach has provided evidence that the II-III loop of the L-type Ca^{2+} channel α_{1sk} subunit is required for mechanical excitation-contraction coupling. A region between amino acids 1635 and 2636 of the RyR1 is required for both orthograde and retrograde signalling, whereas a second region between amino acids 2659 and 3720 of the RyR1 is required for retrograde signalling [26].

1.2 Ryanodine receptor

1.2.1 Structure and function

The ryanodine receptor is a tetrameric protein with a molecular weight of 2260 kDa (MW 565 kDa per monomer) and to date, it is the largest known ion channel [29]. The ryanodine receptor derives its name from ryanodine, a potent paralytic agent, that binds to skeletal and cardiac muscle RyRs because it can cause intracellular Ca^{2+} to leak by locking the RyR channel in an open state.

RyRs enable calcium release from the SR and are found in a wide variety of cell types such as neurons, exocrine cells, epithelial cells and lymphocytes[30]. There are three isoforms of Ryanodine receptors in mammals, each one encoded by a separate gene. As noted above, RyR1 is the main isoform in skeletal muscle cells and was the first to be cloned [31, 32] whereas RyR2 is the main isoform that is expressed in cardiac myocytes [33, 34]. A third type, the RyR3 isoform, was first cloned from rabbit brain and hence it is termed a brain isoform [35].

The N-terminal of the ryanodine channel, comprising 80% of the RyR polypeptide chain, exists as a multi-domain cytoplasmic assembly, playing the role of a scaffold protein and interacting with numerous regulatory enzymes and binding proteins to modulate the RyR channel function [36]. This cytoplasmic domain is the major part of RyR, forming a “foot like” domain that is close to the location of L-type Ca^{2+} channels in the junctional SR. The C-terminal, comprising another 20% of the RyR2 poly peptide chain, forms the transmembrane and luminal domains. [37-39].

RyR isoforms share ~70% sequence identity [32, 35]. The main differences in amino acid composition between the RyR isoforms are found in three regions called the divergent regions (DR): DR1 (residues 4254-4631 in RyR1); DR2 (residues 1342-1403) and DR3 (residues1872-1923) [40] (Figure 1.2).

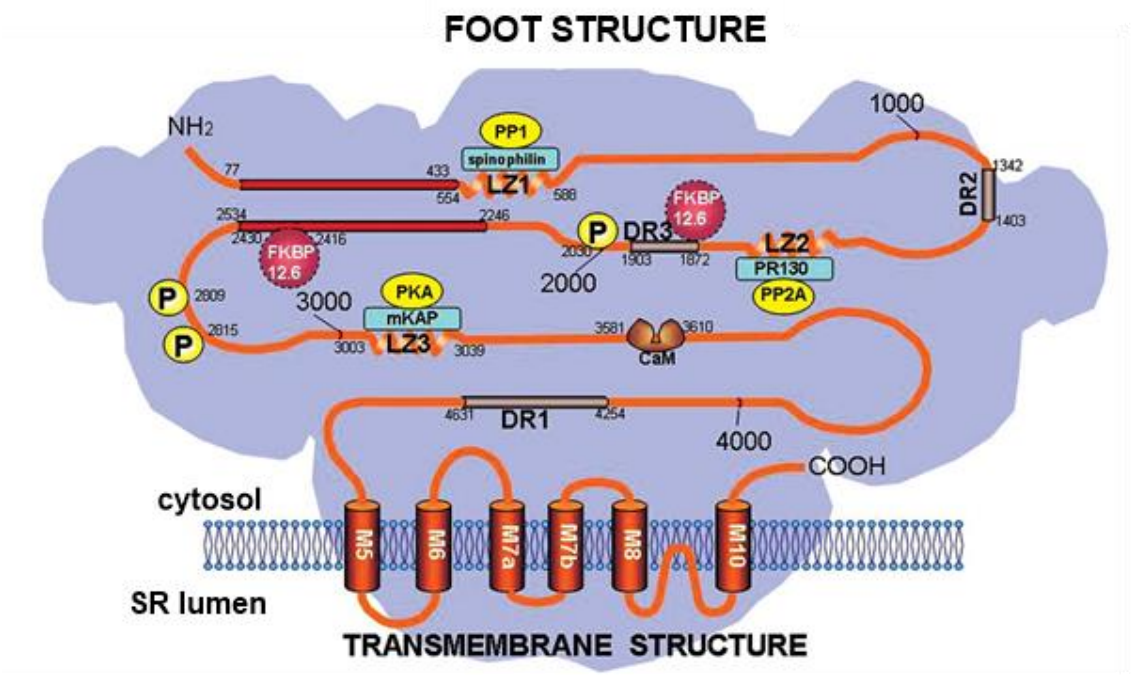

Figure 1.2: The RyR2 cytoplasmic domain known as the 'foot structure'. Figure adapted from Yano (2008) [41].

Electron microscopy has been used to study the structure of RyR1s [42-46]. RyRs were initially identified in the electron microscopy negative-staining imagines of muscle cells where the presence of "feet" between the T-tubule and SR was revealed [47]. Efremov et al. (2015) determined the architecture of the rabbit RyR1 at a resolution of 6.1 Å [48]. To date, the highest overall resolution achieved for the RyR1 is 10Å which showsa mushroom-shaped architecture and a transmembrane domain that is believed to resemble the $K_V2.1$ channel [46]. Moreover, crystal structure of the amino-terminal fragments and a phosphorylation hot-spot domain have been reported [49]. The structure of a closed state RyR1 in complex with FK506-binding proteins (FKBP12) at 3.8 Å has been determined using direct electron detection and advanced image processing [50-52]. Recently, near-atomic resolution was achieved at the channel domains (residues 4545-5037) and its adjoining domain the cytoplasmic region which is sufficient for building a *de novo* atomic model [53]. The tertrameric RyR1 has an appearance of a pyramid with a square base of 270 x 270Å and a height of 160Å as shown in **Figure 1.3**. The backbone of 3685 residues and more than 3100 specific side

chains were assigned in each protomer [53]. Recently, nine distinct domains have been resolved in the cytoplasmic region of each protomer. They include the N-terminal domain (NTD), three SPRY domains, the P1 and P2 domains, and the handle, helical and central domains (**Figure 1.4**). The handle and helical domains are connected in both primary sequences and spatial arrangements.

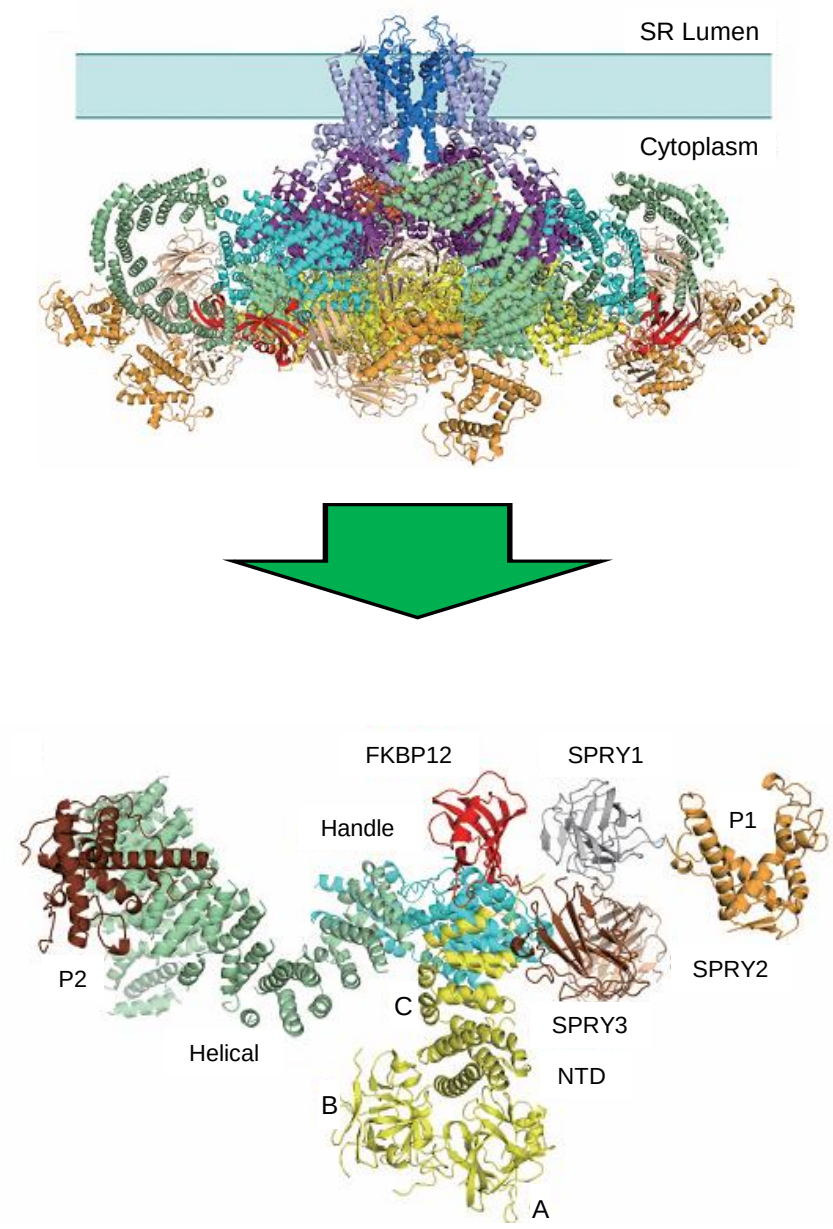

Figure 1.3: Pyramidal structure of the tetrameric rabbit RyR1. Side views of RyR1 structure are presented with the SR lumen side on the top. The significance of the colour coding is given in **Figure 1.4**. Figures are adapted from Zhen et al., 2015 [53].

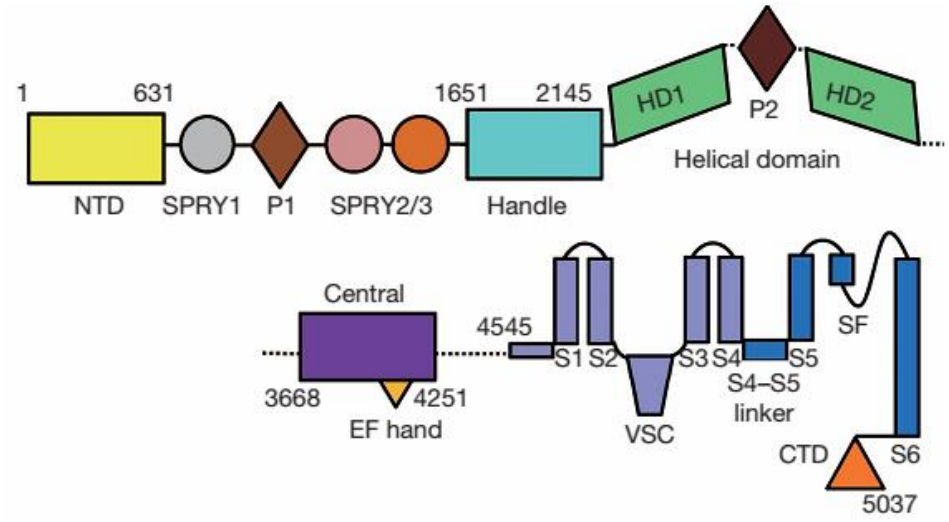

Figure 1.4: A schematic diagram of domain organization in one RyR1 protomer showing spatial arrangement of the cytoplasmic domains proceedings the central domain within one RyR1 promer from the cytoplasm. Figure adapted from Zhen et al. (2015) [53].

The architecture of the RyR1 has four protomers that surround a central transmembrane pore corresponding with the four-fold symmetry axis of the tetramer. Each protomer is built around an extended scaffold of α-solenoid repeats [54]. This scaffold is comprised of thirty-seven repeats in three segments with a total of 2217 residues of the ordered residues in the polypeptide. It was found that the α-solenoid scaffold is capped at the amino terminus by two β-trefoil domains - N-terminal domain (NTD) NTD-A and NTD-B [55]. The six-transmembrane (6TM) superfamily of ion channels includes the voltage-gated sodium and potassium channels and the transient receptor potential (TRP) channels (**Figure 1.5)** [55]. The alpha-solenoid scaffold has five major domains: three SPRY domains (SPRY 1-3) and two pairs of RyR repeats (RY12 and RyR34). In addition, several smaller insertions, including a previously predicted EF-hand pair, were also identified (**Figure 1.5**) [55].

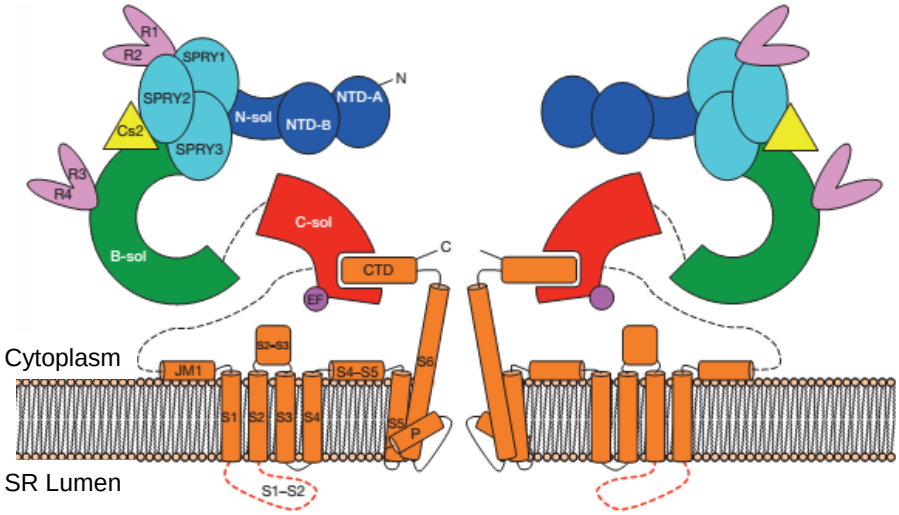

Figure 1.5: A schematic diagram of the RyR1 showing colour-coded representations. N-terminal domains (cyan) SPRR1-3 (salmon), clamp region (RY 12 repeats, blue) and the phosphorylation domain (RY34 repeats, blue) . Calstabin is shown in yellow, the bridge solenoid scaffold is shown in green and the core solenoid in red. The transmembrane and C-terminal domains are shown in orange and putative Ca^{2+} binding domains are purple. Dashed lines are the major disordered segments. Figure adapted from Zalk et al., 2015 [55].

The CaM-like domain inserted within the core solenoid was suggested to play a role as a Ca^{2+} sensor [56]. This region is highly conserved among RyRs. In addition, it shares about 26% sequence identity with the C-lobe of human CaM [55]. Interestingly, six out of eight residues coordinating Ca^{2+} in CaM are also conserved in the putative Ca^{2+} binding domain of RyR1s. Moreover, this putative Ca^{2+} binding domain is adjacent to the S2-S3 and CTD [55]. Therefore, the authors suggested a mechanism for Ca^{2+}-mediated gating in which Ca^{2+}-dependent changes in the conformation of the Ca^{2+} binding domains, are transmitted to the pore by physically contacting with the S2-S3 loop and the CTD. This could lead to a conformational change that alters the cytosolic aperture of the channel [57].

1.2.2 The role of intracellular Ca^{2+}, Mg^{2+} and ATP

The modulators/ligands that play an important role in the regulation of RyRs are Ca^{2+}, Mg^{2+} and ATP on both the cytoplasmic and luminal sides of the SR [20, 58-61]. It is noted that there are differences in RyR1 and RyR2 regulation that underlie the different characteristics of E-C coupling in cardiac and skeletal muscle [62, 63].

Measurements of SR Ca^{2+} release from skeletal and cardiac muscles [18, 64] and single channel studies in bilayers, show that micromolar concentrations of cytoplasmic Ca^{2+} increase the open probability of both RyR1s and RyR2s via cytoplasmic activation sites (A-sites) [19, 60], whilst millimolar concentrations reduce the open probability of these channels [61] via cytoplasmic-facing Ca^{2+} inhibition sites (I-sites). Luminal Ca^{2+} activation of RyR1 and RyR2 is attributed to a luminal-facing Ca^{2+} activation site [58, 65-68] and also to the flux of luminal Ca^{2+} through the RyR1 and RyR2 channels to the cytoplasmic activation and inhibition sites [58, 69-71]. This mechanism is known as "Luminal-Triggered Ca^{2+} Feed-Through" [58, 71]. The biphasic regulation of the RyR is demonstrated by the bell-shaped Ca^{2+} concentration dependence curve [19, 72]. It is noted that inhibition of the RyR2 occurs at a higher cytoplasmic [Ca^{2+}] than the RyR1 [61].

Mg^{2+} strongly inhibits SR Ca^{2+} release and reduces RyR activity [73-78] by altering the cytoplasmic and luminal [Ca^{2+}] dependencies of RyR activity in the cell [59, 64]. It is believed that Mg^{2+} inhibits RyRs by two mechanisms: by competing with Ca^{2+} for the A-sites, and/or by binding to I-sites that have no apparent specificity between Ca^{2+} and Mg^{2+}. Interestingly, luminal Mg^{2+} flows through the channel and binds to the A-site thus terminating the channel opening. It is noteworthy that I-sites of RyR2s exhibit tenfold lower affinity for divalent ions than RyR1s even though regulation of RyR1 and RyR2 by Ca^{2+} and Mg^{2+} are very similar.

Thus, in summary, four Ca^{2+}/Mg^{2+} regulation sites have been identified in RyR2s and their location and binding affinities are summarized in **Figure 1.6** [58]. The first two, A and L sites, are involved in activation of channels and the other two, I1 and I2 sites, are involved in inhibition [71]. When Ca^{2+} binds to the high-affinity cytoplasmic facing Ca^{2+} binding site called the A-site (1 μM affinity), the channel is usually activated [64]. Another lower affinity Ca^{2+} activation site (60 μM affinity) lies on the luminal site (L-site) [71]. On the other hand, Ca^{2+} can cause inhibition of the RyR channel by 1), high

$[Ca^{2+}]_c$ via the I1 low affinity inhibitory site (10 mM affinity), and 2), the I2 inhibition site that has a high affinity for Ca^{2+} (e.g. 1 μM); both sites are located on the cytosolic side [61]

ATP is an activator for all ryanodine receptors. Lipid bilayer studies indicate that ATP increases both RyR1 and RyR2 open probability with a half-activating concentration (K_a) of 0.22 mM [62, 79]. Millimolar levels of ATP in the range 1 – 2 mM generally maximally activate RyRs [62, 79]. However, in RyR2, ATP activation is reduced by 15% when its concentration is increased from 2mM to 10mM [79]. In general, ATP activates all ryanodine receptors but the mechanism of activation is slightly different between skeletal and cardiac muscle. ATP activates RyR1s both in the absence and in the presence of Ca^{2+} [73, 74, 76]. In contrast, ATP activates RyR2s only in the presence of Ca^{2+} [71, 80, 81]. In the absence of Ca^{2+}, at least 2 molecules of ATP are required to activate the RyR1 channel [62]. In the presence of Ca^{2+}, ATP activates RyR1s and RyR2s by stabilizing the Ca^{2+}-induced channel open state and destabilising the channel closed state [80]. It has been shown that by-products of ATP hydrolysis such as AMP and ADP are less effective in activating RyRs [79]. ATP also increases luminal Ca^{2+} dependence of the RyR2 opening rate without altering the Ca^{2+} binding affinity of the L-site [71].

In skeletal muscle at rest, ATP would be an activator of RyR1s except that this is prevented by Mg^{2+} which is a strong inhibitor [82]. During release, Mg^{2+} inhibition is reduced 10-fold by L-type channels, allowing ATP to activate Ca^{2+} release [82, 83]. In a cardiac muscle in diastole, the RyR2 is not so strongly activated by ATP and Mg^{2+} acts as an inhibitor of RyR2s. Ca^{2+} concentration increase due to L-type channels is sufficient to active RyR2s even in the presence of Mg^{2+} (Mg^{2+} inhibition is not as strong as in skeletal muscle) [17].

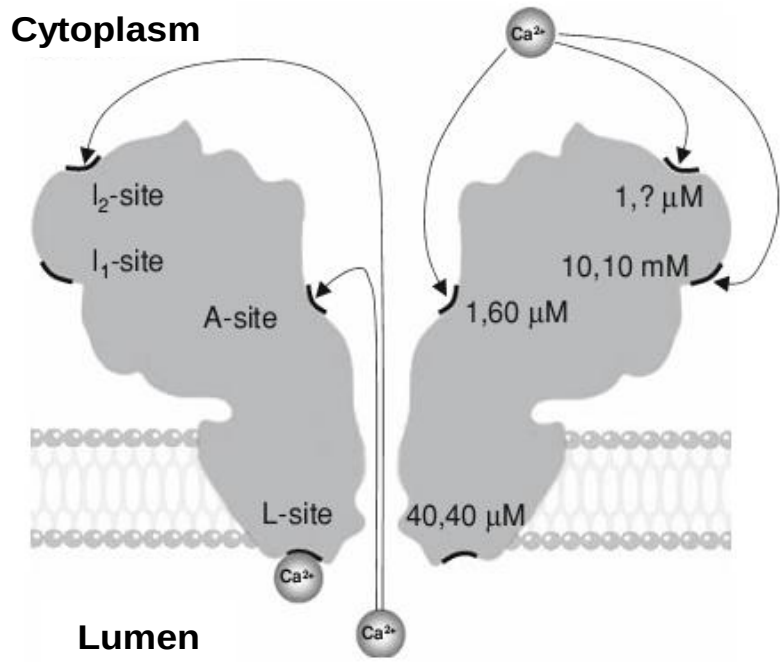

Figure 1.6 Activation and inhibition sites of divalent ions on the cardiac ryanodine receptor. The names of the sites on the left correspond to Ca^{2+}-Mg^{2+} concentration affinities shown on the right side. The arrows show the ability of cytoplasmic and luminal Ca^{2+} to access Ca^{2+} binding sites on the cytoplasmic site of the RyR (Figure adapted from Laver,

2009)[58].

1.3 Regulatory Proteins

1.3.1 FK506-binding protein

FK506-binding proteins (FKBP) or FK506-binding immunophilin proteins were initially discovered as they were tightly bound to RyR1s [84, 85]. FKBP exists in two isoforms with molecular weights of 12.0 kDa and 12.6 kDa for skeletal and cardiac muscle, respectively [86]. FKBP12.6 shares approximately 85% sequence homology with FKBP12 [87]. They bind tightly to the cytoplasmic domain of the RyR at amino acids 2416-2430 [88]. The stoichiometry of binding is one FKBP per RyR subunit (4 FKBP molecules per RyR tetramer) [89]. Although FKB12 and FKB12.6 are believed to bind to the same sites on RyRs [90], the locations of the FKBP binding sites remain controversial. A valyl-prolyl motif (aa 2461 and 2462) was reported for FKBP12/

FKBP1.26 binding in RyR1s [91], but an isoleucyl-propyl motif (aa 2427 and 2428) was reported for FKBP12.6 binding in RyR2s [92]. However, mutations of either site did not have any impact on FKBP12.6 binding [93].

In a cardiac muscle, FKBP12 and FKBP12.6 are both present [94-96]. In most species, including human, the amount of FKBP12 expressed in cardiomyocytes is 10 times higher than that of FKBP12.6 [88]. However, FKBP12.6 is preferentially associated with RyR2s due to its higher affinity [96]. The dissociation of this protein has been implicated in heart failure and arrhythmia [92, 97]. FK506 or rapamycin (an immunosuppressant) can dissociate FKBP12.6 from RyRs and loss of FKBP12.6 from RyRs by the addition of FK506 or rapamycin leads to increased channel activity [98]. FKBP12.6 removal using FK506/rapamycin treatment or gene-targeted deletion increased RyR2 channel activity and induced multiple sub-conductance states in artificial lipid bilayer studies [99-101]. Normal activity of the RyR2 could be restored by the addition of exogenous FKBP12.6 [38, 102]. It has been reported that hyperphosphorylation of RyR2 by PKA in failing hearts caused the depletion of FKBP12.6 from the RyR complex [92, 103], leading to an abnormal Ca^{2+} leak from RyR2 [104, 105]. However, phosphorylation of RyR2 by CaMKII at serine 2815 seems to activate the channel without affecting FKBP12.6 [106].

1.3.2 Protein kinase A (PKA)

PKA binds to the cardiac RyR via an A-kinase anchoring protein (AKAP) [92, 107]. PKA, a cyclic AMP (cAMP) dependent protein kinase, is a tetramer composed of two catalytic subunits and two regulatory subunits. cAMP binding causes conformational changes of the regulatory subunits and dissociation from the catalytic subunits, leading to activation of the kinase activity of the catalytic subunits. The targeted proteins of PKA in cardiac myocytes are L-type calcium channels, phospholamban, the Na^{+}/Ca^{2+} exchanger and RyR2. PKA phosphorylation increases the activity of RyR2 [108-114]. PKA-dependent phosphorylation is believed to alter RyR2 gating in bilayers. PKA was shown to slightly decrease RyR2 open probability at 100 nM $[Ca^{2+}]$, whereas it greatly increased peak open probability in response to a rapid photolytic increase of $[Ca^{2+}]$ [109]. PKA also accelerated the subsequent decline in open probability. By contrast,

PKA-dependent phosphorylation at Ser-2809 enhanced the steady state open probability of single RyRs in bilayers [92, 107]. Subsequent bilayer studies reported that PKA phosphorylation activates RyR2s by increasing the RyR2 sensitivity to luminal Ca^{2+} [113, 114].

In a skeletal muscle, PKA phosphorylates RyR1 at Ser-2843 and regulates the binding of FKBP12 to the channel [115]. However, it was not clear whether the activation of RyR1 by PKA phosphorylation was caused by dissociation of FKBP12 from RyR1. Single channel recordings of mutant RyR1s-V2461I which cannot bind FKBP12 [116], were compared to those of PKA phosphorylated WT RyR1s to examine the PKA effects on channel activity. PKA equally increased the open probability of both mutant and WT channels [115], indicating the direct effect of PKA phosphorylation on RyR1.

1.3.3 CaMKII

CaMKII is known to have three domains, each of them with an individual function [117]. The amino-terminal catalytic domain is responsible for enzymatic catalysis. The central regulatory domain regulates CaMKII function and the carboxy-terminal association domain takes part in oligomerization [118-120]. CaMKII can be autophosphorylated as a result of CaM binding, maintaining 100% activity of CaMKII even when cytoplasmic [Ca^{2+}] is low. After that, autophosphorylated CaMKII remains partially active even after CaM dissociation at resting cytoplasmic [Ca^{2+}] [121-124]. CaMKII phosphorylation alters the channel activity of the RyR. However, the effects of CaMKII on RyR2 gating in bilayers are controversial, with both an increase [106, 108, 125] and a decrease [126] in RyR2 activity reported. When more intact cellular systems were used, the effect of CaMKII-dependent RyR2 phosphorylation was to increase the amount of SR Ca^{2+} release for a given content of SR Ca^{2+} [127].

CaMKII is regulated by changes in the concentration of intracellular Ca^{2+} [128, 129]. CaMKII phosphorylation has been identified on the same residues on RyR1 as PKA and it phosphorylates other proteins such as troponin I, sarcolemmal Ca^{2+} channels and phospholamban [30].

1.3.4 Protein phosphatases

Protein phosphatase 1 (PP1) has a molecular weight of 35-38 kDa. PP1 consists of one catalytic subunit and one regulatory subunit [130]. The regulatory subunit plays a role in targeting the PP1 catalytic subunit to specific subcellular locations and regulates substrate specificity or acts as substrate. The catalytic subunit has binding sites for Mn^{2+} and Fe^{2+}. The binding of these two ions facilitates PP1 activation. Inhibitory proteins such as I-1 regulate PP1. For example, phosphorylation of I-1 at Threonine-35 inhibits the activity of PP1 [131, 132].

Phosphatase 2A (PP2A) is believed to have two forms: the heterodimeric core enzyme and the heterotrimeric holoenzyme [130]. The PP2A core enzyme has a scaffold subunit and a catalytic subunit. Holoenzyme is formed when PP2A core enzyme binds with various regulatory subunits.

PP1 is targeted to skeletal ryanodine receptors (RyR1) via the targeting proteins known to bind to highly conserved leucine/isoleucine zipper motifs on the channel [107]. RyR1 is dephosphorylated by protamine by activating PP1 that is bound to RyR1s [115].

1.3.5 Calsequestrin, junctin and triadin

Calsequestrin (CSQ), a major Ca^{2+} binding protein in the SR, is localized at the junctional region of the SR membrane [38, 133]. It has two isoforms: CSQ1 for skeletal muscle and CSQ2 for cardiac muscle [134]. CSQ binds to RyRs via triadin and junctin. Single channel recordings indicate the association between CSQ and RyR is disrupted by high luminal [Ca^{2+}] (>=10mM) and increased ionic strength (~500 mM).[135, 136]. CSQ contributes to SR Ca^{2+} storage since it is a high capacity and low affinity luminal Ca^{2+} buffer [134]. The binding capacity of CSQ differs depending on the isoforms: CSQ binds 20 calcium ions are bound in cardiac muscle, whereas it binds 40 calcium ions in skeletal muscle [137]. CSQ, which usually exists as a monomer at low luminal [Ca^{2+}], undergoes conformational changes becoming condensed when the luminal [Ca^{2+}] is increased to 10 µM. When the luminal [Ca^{2+}] is further increased to between 10 and 100 µM, CSQ firstly undergoes dimerization followed by polymerization [38,

134, 138]. It is the CSQ polymer that is anchored to the SR membrane and the RyR via triadin and junctin. However, this CSQ association with SR membrane and RyRs can be disrupted if luminal [Ca^{2+}] is further increased above 10 mM [134, 136, 139, 140].

CSQ functions both as a Ca^{2+} buffer site and as a RyR regulator. CSQ regulates RyR2 activity directly via protein-protein interactions involving triadin and junctin. CSQ regulates RyR2s in a luminal Ca^{2+}-dependent manner and it inhibits RyR2s at low (<1 uM) luminal [Ca^{2+}]. However, increasing the luminal [Ca^{2+}] can reduce this inhibition via the dissociation of CSQ from the RyR2. One study using gene-targeted CSQ2 knock-out mice suggested that CSQ2 has a role in protecting the heart against premature spontaneous SR Ca^{2+} release and triggered arrhythmia. [141]. Interestingly, contractile function was not impaired by the loss of CSQ2 [141].

Some studies have suggested that CSQ1 and CSQ2 regulate RyR1 and RyR2 differently. Whereas CSQ1 inhibitedRyR1 function upon association with the RyR1 [135]dissociation of CSQ1, or removal of inhibition, was required to activate RyR1s [142]. In contrast, interaction with triadin and junctin mediate the association of CSQ2 with RyR2. Its strong interaction with triadin and junctin at luminal [Ca^{2+}] lower than 20μM results in the binding of CSQ2 to RyR2s and subsequent inhibition of the receptor activity.. However, when the luminal [Ca^{2+}] is increased from 20 μM to 5 mM the inhibition of CSQ2 on RyR2 is decreased by a reduction in the binding of CSQ2 to triadin and junctin. The inhibition is totally abolished by its dissociation from the RyR2 when luminal [Ca^{2+}] is increased above 5 mM [143].

Transmembrane proteins, triadin and junctin, are integral proteins in the junctional SR and interact with each other, calsequestrin and RyR, constituting the luminal components of the RyR complex [38, 134, 136]. The interaction of CSQ with triadin and junctin is highly dependent on luminal [Ca^{2+}]; a decrease in luminal [Ca^{2+}] strengthens CSQ binding to triadin and junctin [38, 136]. Based on lipid bilayer studies it was suggested that the complex of CSQ, triadin and junctin contributes to RyR2 sensitivity to luminal [Ca^{2+}] [143]. Only one type of triadin (MW 95kDa) is expressed in skeletal muscle. In contrast, three types of triadin (MW 35,40 and 92kDa) are expressed in cardiac muscle although the type 1 is the major isoform representing 95% of the total [38]. Triadin increased RyR2 sensitivity to luminal [Ca^{2+}] and enhanced SR Ca^{2+} release in lipid bilayer and isolated cardiac myocyte studies [143, 144]. A mouse

heart triadin knock-out study suggested that triadin is essential to maintain structural and functional integrity of Ca^{2+} release units [141, 145].

Junctin, a small protein of MW 26kDa, is expressed in both cardiac and skeletal muscles [38, 136]. Junctin regulation of RyR gating is still controversial. Addition of exogenous junctin to purified RyR2s increased the RyR2 open probability in single channel recordings [143]. On the other hand, an inhibitory effect of junctin on RyR activity has been suggested since ablation or overexpression of junctin enhanced or decreased SR Ca^{2+} release in Ca^{2+} spark measurements in intact cardiac myocytes [146, 147].

1.3.6 Sorcin

Sorcin, a ubiquitous MW 22kD Ca^{2+}-binding protein, has five EF-hands that have been reported to associate with cardiac RyR and L-type Ca^{2+} channels [148, 149]. Sorcin interacts with the cytoplasmic domain of RyR2 at higher cytoplasmic [Ca^{2+}] [150]. Sorcin reduced the open probability of RyR2 in bilayer studies and [^{3}H]-ryanodine-binding assays [151]. This inhibition of RyR2 activity by sorcin could be reversedby PKA-mediated phosphorylation of sorcin [151]. Sorcin was also reported to depress myocyte Ca^{2+} transients [150, 152] and reduce Ca^{2+} spark frequency in permeabilized myocytes [150, 152]. In intact rabbit ventricular myocytes, over-expression of sorcin reduced Ca^{2+} transients and the SR Ca^{2+} load, an effect thought to be attributed to increased Ca^{2+} extrusion by Na^+/Ca^{2+} exchange [152]. Thus, sorcin may act as an endogenous inhibitor of SR Ca^{2+} release but this effect can be relieved at low $[Ca^{2+}]_i$ or by PKA-dependent phosphorylation [153]. When sorcin is phosphorylated by CaMKIIδC, sorcin inhibition of RyR2 is abolished. Sorcin significantly but equally inhibited both recombinant and native CaMKIIδC when phosphorylated by CaMKIIδC [154]. Interestingly, dephosphorylated sorcin could inhibit CaMKII activity, suggesting alternative regulation of sorcin in addition to its regulation via phosphorylation [154].

1.3.7 S100A1

The S100 family of proteins also has EF-hands. These proteins were originally isolated from bovine brain and discovered to be soluble in 100% ammonium sulfate, hence their name 'S100' [155, 156]. EF-hands of S100 proteins can bind Ca^{2+}, followed by binding to target proteins such as CaM [157, 158]. Unlike CaM lobes, the first EF-hand of each subunit is considered a "pesudo" EF-hand since it has an extremely weak Ca^{2+} binding affinity with K_d=1-50 μM[157]. Glutathionylation and the presence of target proteins can increase the overall apparent Ca^{2+} affinity [159, 160].

In skeletal muscle, S100A1 is highly abundant at a concentration of 0.5-15 μM, which is higher than the concentration of CaM [161]. S100A1 and CaM were shown to compete for a common binding site on RyR1 that is encoded by residues 3614-3643 [159, 162]. However, [^{3}H]-ryanodine studies have recently shown that CaM and S100A1 do not compete for the binding site although they bind to and regulate both skeletal and cardiac channels [163]. In cardiomyopathic hearts, the knockout of S100A1 increased the incidence of heart failure [164, 165]. In cardiac muscle fibres, knockout of S100A1 decreased Ca^{2+} transients upon electrical stimulation [166]. Since it enhances cardiac contractility, S100A1 has been suggested as a possible target for the treatment of heart failure [167].

1.3.8 Calmodulin

1.3.8.1 Structure and function

Calmodulin (CaM) is a cytosolic calcium-binding protein [148 amino acids, 16.7 kDa]. It is acidic and it is highly conserved throughout eukaryotic evolution [168]. Free [CaM] in myocytes is only 1% of the total [CaM] when it was measured in adult rabbit cardiac myocytes using two modified null-point titration methods [169]. CaM has been known to activate about forty types of enzymes or channels. *CAM* genes are absent in some 50 completed bacterial or archaeal genomes. However, at least one *CAM* gene is present in eukaryotes [170] and the *CAM* sequence is extremely conserved. CaMs are identical for all known vertebrates and essentially the same for all metazoans. The CaM of *Paramecium* has 94% homology to mammalian CaM and *Aspergillus* (a fungus) has 92 % homology [170]. In mammals, each species has three *CAM* genes that have 80%

identical nucleotide sequences,however, they encode CaM protein that is 100% identical [170].

CaM is known to function as a monomer with two pairs of EF-hands; its structure has been identified using both X-ray crystallography and NMR [171, 172]. CaM consists of a roughly symmetrical N-terminal pair (EF hand I and II) and C-terminal pair (III and IV) joined by an eight-turn α-helix giving the dumbbell appearance [171, 173, 174]. Interestingly, domains I and II of the N terminal display a lower affinity for Ca^{2+} (K_d ~ 10 μM) than domains III and IV of the C-terminal (K_d ~ 1 μM) when CaM is free in solution. CaM regulation has a role in multiple biological functions acting in three distinct forms: as CaCaM (Ca^{2+} bound), apoCaM (Ca^{2+} free) and Ca^{2+} independent or constituently bound CAM [175]. The conformational changes are caused by the binding of Ca^{2+} at the EF hand motifs within CaM's amino and carboxy lobes, exposing hydrophobic residues that transduce the intracellular Ca^{2+} signal [176]. Various ion channels can bind to CaM including RyRs [1, 30, 38, 170]. Calmodulin modulates other proteins in two ways: by a direct binding with its targeted proteins or indirect through the action of CaM-activated protein kinases and protein phosphatases such as calcineurin [117, 170].

The structural basis of RyR2 regulation by CaM has not been clearly defined because 3D mapping of CaM binding by cryo-electron microscopy (cryo-EM) and fluorescence resonance energy transfer (FRET) microscopy have been limited to the RyR1 isoform [30].

Fruen et al. (2000) reported a high affinity CaM binding domain on the RyR2 that is shared by apoCaM and CaCaM [177]. Deletion of the CaM binding sites caused the elimination of the inhibitory effect of CaM on RyR2 at all Ca^{2+} concentrations [178]. It is well known that CaM inhibits all three types of ryanodine receptors above 1 μM $[Ca^{2+}]_c$ [117]. Thus, CaM regulation of RyR1s varies depending on $[Ca^{2+}]_c$ [178], with CaM activating channels at submicromolar cytosolic $[Ca^{2+}]_c$ while inhibiting the channel at higher $[Ca^{2+}]_c$ [179]. Activation by apoCaM does not occur for RyR2s although an inhibition by CaCaM does occur in a very similar way to RyR1 inhibition [64, 177].

1.3.8.2 Calcium binding /CaM-like domains

Ryanodine receptors are activated and regulated by Ca^{2+} during CICR. CaM activation or inhibition of RyR1 channels depends on the free cytosolic Ca^{2+} concentration [162]. Thus, CaM can fine-tune the channel's Ca^{2+} sensitivity by binding to RyRs. The binding region of both apo and Ca^{2+}-CaM on the RyR1 receptor is between residues 3614-3643, and between residues 3581-3612 for the RyR2 receptor [180, 181]. CaM has EF-hand motifs so it can act as aCa^{2+} sensor [182], and it is interesting that the RyR itself also contains several EF-hand motifs. Several regions within RyRs that have homology to CaM, were recently identified through the EF-hand protein sequence [56, 183]. However, only two Ca^{2+} ions could be bound , suggesting not all EF-hands are functional according to the initial biochemical data using equilibrium dialysis [56]. These EF-hands may be involved in CICR as the intrinsic Ca^{2+} sensors of RyR [56, 183].

1.3.8.3 Binding sites of CaM on RyRs

Some controversial findings involving the stoichiometry of CaM binding to RyRs have emerged. Data analysis of the CaM binding properties of RyR2 using metabolically S-labelled CaM, showed that CaM has a stoichiometry of 1 molecule of CaCaM and 4-6 molecules of apoCaM bound per subunit in the presence of 100 μM Ca^{2+} [184]. It was reported that S-CaM binding to SR vesicles and purified RyR1s and RyR2s showed the stoichiometry of CaM binding is 1 mole of CaM/mole RyR subunits regardless of the states (i.e whether Ca^{2+} is bound or not) [180, 184]. It has also been reported that CaM binds to approximately 2 binding sites for each RyR2 subunit in the presence of Ca^{2+} and a single site per subunit in the absence of Ca^{2+} in native cardiac SR vesicles [185]. A possible explanation could be the loss of Ca-CaM binding protein during the purification that induces the conformational changes, covering up the second site [186].

The role of Ca^{2+} binding to CaM in the regulation of various targets was studied using site-directed CaM mutants in which substitution of critical glutamate residues within each EF hand selectively reduces Ca^{2+} binding at each site [187, 188]. These Ca^{2+} insensitive mutants help to define how the number and position of Ca^{2+} ions bound determines the functional interactions of CaM with different targets. [^{35}S]CaM binding

determinations indicate a single high-affinity CaM binding site per RyR1 subunit [177, 180]. In addition, 3D reconstructions show CaM bound within a cleft near the cytoplasmic face of the channel [189]. It was also suggested that the binding sites of apoCaM and Ca^{2+}CaM overlap within the primary sequence of RyR1s [180, 181, 190] and hence this region may play a role in the physical coupling of RyR1 channels with voltage sensing L-type Ca^{2+} channels on the T-tubule membrane [25]. It was proposed that the RyR amino acid sequence 3614-3643 is the site of CaM action and all subsequent effectors are due to downstream changes [178, 191, 192].

It has been recently reported that the CaM binding site on RyR2 in the deep cleft is very similar to the CaM binding site on RyR1 [193]. More specifically, the region of amino acid residues 3614-3643 for RyR1 and residues 3581-3612 for RyR2 are involved in binding CaM [180, 181].

Interestingly, previous cryo-EM and single-particle three-dimensional reconstruction studies reported that the apoCaM and the Ca^{2+}CaM binding sites overlap but are spatially distinct on the cytoplasmic assembly of RyR1s (3-4 nm) [193]. Recently, it has been found that the apoCaM binding site on the RyR2 is similar to the Ca^{2+}CaM binding site on the RyR1 [193]. Since apoCaM weakly activates RyR1 but inhibits RyR2, it has been suggested this inhibition could be due to its binding site that is similar to Ca^{2+}CaM binding site on RyR1.

1.3.8.4 Role of CaM in cell function

CaM binding to the cardiac RyR2 channel isoforms causes a shift in the rightward direction of the steady state [Ca^{2+}]-dependence of RyR2 activation in SR vesicles [177]. CaM also reduces the frequency of Ca^{2+} sparks in permeabilized myocytes [194]. Severe hypertrophy of the heart and early death have been shown to result through the disruption of RyR2 and CaM binding within a core CaM binding sequence in mutant mice [195]. Therefore, it is possible to conclude that RyR2 regulation by CaM is very important for the normal physiology of the heart. However, CaM has many other binding proteins such as calcineurin, CaMKII, and L-type calcium channels [196, 197] so it is difficult to resolve CaM's functional interactions with RyR2s. This problem was addressed using a CaM that has a mutation on the domain that specifically binds to a

highly conserved RyR CaM binding site. The authors found that CaM regulates RyR1 and RyR2 receptors by binding to a single highly conserved CaM binding site [178]. In one *in vivo* study, the role of CaM regulation of RyR2 was investigated using a transgenic mouse model with the replacement of 3 amino acids (RyR2-W3587A/L3951D/F3603A) [RyR^{ADA}] in the RyR2 gene. Mouse survival, physiological function of the heart, Ca^{2+} release from RyR2, calcium dynamics, and gene expression associated with cardiac hypertrophy were investigated. It was concluded that impairment of CaM regulation on the RyR caused aberrant SR Ca^{2+} release and defective regulation of genes associated with cardiac hypertrophy and early death in homozygous mutant ($RyR2^{ADA/ADA}$) mice [195].

RyR2 activity is inhibited by CaM binding to a site that has been known as a conserved site among RyRs [30]. It was reported that CaM lowered RyR2 channel opening probability at all Ca^{2+} concentrations by reducing the number of channel events and increasing the duration of close time [198]. However, the detailed mechanism by which CaM regulates RyR2 still needs to be resolved to unravel the physiological importance of CaM regulation.

1.3.8.5 CaM and the different sensitivities of skeletal and cardiac ryanodine receptors

CaM activation of RyR1s in the presence of nanomolar Ca^{2+} concentrations suggested that CaM-dependent activation of RyR1 is not dependent on Ca^{2+} dependent channel activation. In contrast, Fruen et al. studied the relationship between the CaM and Ca^{2+} dependent mechanisms of RyR channel activation using skeletal and cardiac muscle SR vesicles, reporting that CaM activation of RyR1s is likely to operate by increasing the sensitivity of the Ca^{2+}-dependent activation mechanism [177]. In addition, their results showed that CaM's effect on Ca^{2+} sensitivity of the channel is far more pronounced in RyR1 than RyR2 receptors [177], suggesting that Ca^{2+} dependence of SR Ca^{2+} release is different in the two isoforms possibly because of the differential interaction of CaM with RyR1 and RyR2 channels.

The conversion of CaM from an activator to an inhibitor of RyR1 is due to Ca^{2+} binding within the C-terminal domain of CaM [199], accounting for the enhanced sensitization of the RyR1 channel to both activation and inhibition by Ca^{2+} in CaM containing media [185, 200]. It was suggested that the role of CaM regulation is distinct for RyR1 and

RyR2 although the detailed mechanisms of the different regulatory mechanisms remain unclear [177, 184]. Balshaw et al. (date) reported that apoCaM and Ca^{2+} CaM inhibited RyR2 activity [184], suggesting that the consequences of CaM binding may account for major differences in the Ca^{2+} sensitivities that characterize skeletal and cardiac RyRs [177, 184, 200].

The conversion of wtCaM from an activator (apoCaM) to an inhibitor (Ca^{2+}-CaM) required high [Ca^{2+}] ($\geq$ 1uM) [201], indicating that Ca^{2+} binding to CaM may be the main determinant for its interaction with both RyR1 and RyR2 isoforms. In contrast, the cardiac RyR2 isoform was inhibited by wtCaM at all physiologically relevant Ca^{2+} concentrations (100 nM to 1mM) [201]. This finding was consistent with other findings that both apoCaM and Ca^{2+}CaM inhibit the RyR2 [184, 185]. Fruen et al.(date) also reported that Ca^{2+} binding to CaM is necessary for the inhibition of both cardiac and skeletal muscle RyRs as each of the four single E to A substitutions targeting the Ca^{2+} binding sites for CaM, abolished the CaM inhibition in both isoforms. The authors concluded thatCa^{2+} binding to CaM was the main determinant for Ca^{2+} interactions with both RyR1 and RyR2s [201].

1.3.8.6 Conversion of CaM from RyR1 activator into a channel inhibitor

A few studies showed that Ca^{2+} binding to the C-domain of CaM was the switch to convert CaM from activation to inhibition [199, 201]. However, Boschek et al., proposed that Ca^{2+} binding to the C-domain of CaM caused RyR1 activation and Ca^{2+} binding to the N-domain caused inhibition [202]. These authors compared the Ca^{2+} dependence of skeletal muscle SR [^{3}H]-ryanodine binding with Ca^{2+}-induced changes in the signal from CaM that was fluorescently labelled on the N- or C-domain and bound to a putative RyR1 CaM-binding peptide [202]. The Ca^{2+} dependence conformational changes in the C-domain of CaM and the Ca^{2+} activation of SR vesicle ryanodine binding occurred in the same concentration range. Moreover, the Ca^{2+}-dependence of

conformational changes in the N-domain of CaM and the Ca^{2+} inhibition of the SR vesicle [^{3}H]-ryanodine binding occurred within the same concentration range.

Therefore, it remained a puzzle whether Ca^{2+} binding to the N–domain or C-domain was the main switch for conversion of CaM from activation to inhibition. In an attempt to solve this puzzle, Jiang et al., 2010 recently used a series of mutant CaMs which were designed to individually increase the Ca^{2+} affinity of each of CaMs's EF-hands. The authors reported that mutations in sites I or II in the N-terminal domain had no effect on the CaM-Ca^{2+} affinity and regulation of RyR1s since mutations did not change Ca^{2+} affinity of the relative domain nor alter the Ca^{2+} switch-point.[203] However, the site III mutation N97D increased the Ca^{2+} binding affinity of CaM's C-terminal domain and caused CaM to inhibit RyR1 at a lower Ca^{2+} concentration compared with wild-type CaM [203]. Conversely, the site IV mutation Q135D decreased the Ca^{2+} binding affinity of CaM's C-terminal domain causing inhibition of RyR1 receptors at a higher Ca^{2+} concentration compared with wild-type CaM[203]. These results suggested that Ca^{2+} binding to CaM's C-terminal acted as the switch converting CaM from a RyR1 activator into a channel inhibitor [203].

1.4 RyR modification

1.4.1 Phosphorylation

Many phosphorylation sites have been identified on RyR proteins [125, 204, 205] and the receptors are the target for several kinases (PKA, PKG and CaMKII) and phosphatases (PP1, PP2A and PDE4D3). RyRs bind with some of these regulatory enzymes via scaffolding proteins, allowing for specific and compartmentalized regulation [57]. The RyR1 has been found to be phosphorylated at serine 2834 by PKA, PKG and CaMKII in skeletal muscle [206-210]. Single channel recordings showed RyR1 activity enhanced by PKA or CaMKII phosphorylation [211-213]. Depolarization-induced Ca^{2+} release from skeletal muscle SR is stimulated by cAMP [214] thus suggesting endogenous PKA modulation of Ca^{2+} release via the phosphorylation of RyR1 during E-C coupling of skeletal muscle. Interestingly, PKA phosphorylation of RyR1 at serine-2834 caused the dissociation of FKBP12, thereby increasing the open probability of the channel [115].

The major PKA phosphorylation targets are Ser-2843 on skeletal ryanodine receptors but RyR2s are phosphorylated at Ser-2809 by PKA, PKG and CaMKII [125, 206, 208, 215, 216]. PKA activity in cardiac muscle cells is increased via intracellular cAMP upon beta-adrenergic stimulation [217]. Isoproterenol, a beta-adrenergic agonist, and cAMP stimulate the ATP-induced PKA phosphorylation of RyR2 in cardiac muscle cells [218] In single channel recordings, PKA increased the open probability of RyR2s [108, 109]. In cardiac muscle cells, RyR2 activation by PKA phosphorylation induces a positive inotropic action upon beta-adrenergic stimulation. A few studies reported that PKA phosphorylation of the RyR2 at serine-2809 caused the dissociation of FKBP12.6 and subsequently an increase in the channel open probability [92, 101]. It is well known that the beta-adrenergic receptor is chronically stimulated in heart failure and phosphorylation of RyR2 by PKA in failing heart is about 4-fold higher than in non-failing hearts [92]. This hyperphosphorylation of RyR2s by PKA causes a depletion of FKBP12.6 from the RyR2 [92, 103] and consequently an aberrant SR Ca^{2+} leak [104, 105]. In contrast, using single channel recordings, it was demonstrated that CaMKII phosphorylation either activates [108, 125] or inhibits [126] RyR2 activity by phosphorylating serine-2815 [106]. CaMKII phosphorylation of RyR2 was positively correlated with heart rate [106] since the time-averaged [Ca^{2+}] is increased at higher heart rates. The elevation of intracellular [Ca^{2+}] activates the CaMKII activity in cardiac muscle cells, inducing the phosphorylation of RyR2s.

1.4.2 Oxidation and nitrosylation

Oxidation has been known to affect the Ca^{2+} sensitivity of RyR2s and more interestingly it also affects their affinity for CaM [184]. TheRyR has 80 to 100 cysteines per monomer and 25 to 30 of them are in the reduced state. However, an additional 6 to 8 cysteines are hyperactive so they are very susceptible to oxidation [219]. Gating properties are affected when the RyR1 channel is oxidized and it was thought to alter the responsiveness of channel modulators such as Ca^{2+}, Mg^{2+}, ATP and caffeine. RyR activity is reduced by NADH but increased by NAD^{+} [220]. Reactive oxygen species such as superoxide, hydroxyl radicals and hydrogen peroxide are found to affect the Ca^{2+} sensitivity of RyR2s and their affinity for CaM [184, 221, 222]. Reactive oxygen

species affect SR function by affecting the activity of the RyR2 by the dissociation of endogenous CaM from the SR [223].

Nitric oxide (NO) also plays a role in E-C coupling of cardiac muscle [224, 225]. Of three NO isoforms expressed in mammalian cells, namely endothelial, neuronal and inducible NO, the endothelial isoform is the main isoform under normal conditions. Endothelial NO is localized to caveolae whilst neuronal NO is on the SR [226]. Under pathological conditions where inflammation occured, the inducible NO was stimulated by inflammatory mediators [227]. Notably, it has been reported that NO can regulate the activity of the RyR channel[219, 228, 229]. The underlying mechanism whereby NO has been found to have a role in ischaemic heart disease but remains poorly understood [230].

1.5 Catecholaminergic polymorphic ventricular tachycardia (CPVT)

CPVT is an inherited arrhythmogenic disease in which bidirectional ventricular tachycardia and sudden death are initiated by exercise or emotional stress in circumstances where there is no structural heart disease. CPVT is usually diagnosed before the age of 10 years but it can also occur at later ages [231, 232]. It is well known that the main causes of CPVT are delayed after-depolarizations (DADs) and aberrant calcium leak from the SR [233] associated with adrenergic stimulation. However, some CPVT mutations (e.g. the knock-in mice model with R4496C mutation in RyR2) can cause DADs in the absence of adrenergic stimulation [234]. Gain of RyR2 function and Ca^{2+} leakage from SR has been found in cardiac myocytes with RyR2 mutations, CASQ2 and CaM [235-238]. RyR2 carries the primary gene for the autosomal dominant type of CPVT [239] with approximately 60% of CPVT patients showing mutations in RyR2 [231]. CASQ2 mutations are linked from 1 to 2 % of CPVT patient cases [236], whereas CaM mutations have been identified in only two families. These mutations all lead to enhanced basal activity of RyR2 channels during diastole [235, 240, 241].

More than 150 RyR2 mutations linked to CPVT have been discovered [242]. Two mechanisms have been proposed to explain how the CPVT-linked mutations may

increase RyR2 activity. Firstly, binding of FKBP12.6 to RyRs causes closure of the receptor during diastole by stabilizing the channels in a closed state [101]. This prevents abnormal calcium release during the diastolic phase of the cardiac cycle [101]. CPVT mutations in RyR2s reduced the binding affinity of FKBP12.6 [101] resulting in decreased inhibition of the RyR2. Second, it is thought that RyR2 mutations interfere with inter-domain interactions that stabilize the closed-state channel [243, 244]. This idea originally came about to explain the observation that CPVT mutations of RyR2s are found frequently in two separate domains, the N-terminal domain (amino acids 1to 600) and the central domain (amino acids 2000 to 2500); mutations in either domain produced similar disease phenotype [245]. (The domain hypothesis is introduced in more detail in section 1.7.2.)

Fourteen CASQ2 mutations linked to CPVT were discovered of which four are nonsense mutations resulting in a non-functional protein [246]. CASQ2 null mice were reported to have VT induced by exercise and catecholamines similar to transgenic mice carrying the mutation in the RyR2 [141]. An aberrant calcium leak from the SR during diastole was found in CASQ2-null myocytes when exposed to catecholamines [246]. Another study showed a vast reduction in calsequestrin protein could increase the susceptibility of the heart to arrhythmias, independent of any changes in other SR proteins including triadin and junctin [247]. It has been reported that CASQ2 loss leads to increased RyR2 activity because CASQ2 both acts as a buffer and a direct modulator of SR Ca^{2+} release [248].

Two CaM mutations have been linked to CPVT. Since CaM can directly bind to the RyR2 decreasing its open probability [178], it has been suggested that an increase in the RyR2 channel open probability could result from disruption of the interaction between the RyR2 and calmodulin [238]. This suggestion was supported by several animal studies investigating the effect of abnormal CaM and RyR2 binding on arrhythmia and heart failure [178, 249, 250]. Xu et al., found that when stimulated with catecholamines, a single mutation causing disruption of RyR2 and CaM resulted in aberrant calcium leak and arrhythmia in a knock-in mouse with CPVT-type CaM mutation (R2474S) [250]. Based on the finding from these animal studies, the linkage study was done in a Swedish family with CPVT and reported that CALM1 (heterozygous missense mutation) is associated with CPVT [238]. They also discovered that another missense CPVT mutation (N98S) contributed to the defective

interaction between RyR2 and CaM, causing aberrant calcium leak [238]. The conclusion was that both CALM1 and N98S cause the development of early onset CPVT exhibiting a CPVT-like arrhythmia [238].

Recent reports show that only one type of CPVT-CaM mutant (N54I) increased open probability of the RyR2 in single channel recordings. Two different types of mutant CPVT-CaMs (N54I and N98S) were added to RyR2s devoid of endogenous CaM, using a specialized tube system during single channel recording. Interestingly, N54I-CaM significantly increased the activity of the RyR2 channel compared with either WT-CaM and N98S-CaM, whereas N98S-CaM failed to inhibit the channel [251].

1.6 Malignant hyperthermia (MH)

MH is a pharmacogenetic disorder of skeletal muscle, which is usually characterized by a life-threatening hypermetabolic crisis upon exposure to halogenated volatile anaesthetics during surgery. A rise in core body temperature, increase in aerobic and anaerobic metabolism, elevated CO_2 and lactic acid, tachycardia and skeletal muscle contractures are usually observed in an MH episode [252, 253]. MH episodes affect 1:12,000 to 1:50,000 individuals receiving general anesthesia. However, the true number of MH susceptible people is believed to be much greater as only individuals who undergo anaesthesia could be noted [254]. It was first demonstrated in pigs that MH resulted from a defect in the skeletal muscle RyR1 [255]. MH episodes may be precipitated by triggering agents such as halothane, producing a large increase in cytoplasmic [Ca^{2+}] in skeletal muscle [252, 253] leading to muscle rigidity (*i.e.*, contraction) and hyperthermia [252, 253]. The responses stem from Ca^{2+}-dependent activation of muscle contraction and aerobic and anaerobic metabolism.

Thirty-four RyR1 mutations in human families that exhibit MH have been identified [256-258]. As seen with CVPT mutations in the RyR2, the majority of the RyR1 mutations are located within an N-terminal (residues 35-614) or central domain (residues 2129-2458) of the protein whereas fewer mutations are found in the C-terminal region (residues 3916-4942) [259]. This suggests a role for inter-domain interactions in the etiology of the disease. It has been reported that up to 70% of

families susceptible to MH carry one of the thirty-four casual mutations for MH, with other potential variants yet to be identified [258].

A CASQ1 knock-out mouse study showed these mice are susceptible to heat and anaesthetic-induced mortality analogous to MH, suggesting that calsequestrin could be another potential candidate for MH [260-262]. Some *CASQ1* variants have been identified in humans [263] however, there is no clear evidence that variants in this gene can cause MH [264].

At least six genetic loci, in addition to RyR1, have been implicated in MH. However, only one other gene, *CACNA1S* that encodes the main subunit of L-type channels, is altered by an MH-linked variant [265-267]. MH has been linked with DHPR mutations in two families, suggesting that MH can stem from a defect of more than one component of E-C coupling. Central core disease (CCD) is also linked with mutations in the RyR1 and most of these individuals are also diagnosed as MH [257] but exhibit a different phenotype. CCD is a rare non-progressive myopathy which is usually characterized by hypotonia and proximal muscle weakness [268]. An interesting finding is the reduced threshold for K^+-induced contractions of MH muscle fibres suggesting that MH mutations have an effect on the sensitivity of Ca^{2+} release from the SR to the level of depolarization of the transverse tubule membrane. Moreover, SR Ca^{2+} release is activated at more negative membrane potentials in myotubes from MH than control pigs [269, 270]. Taken together, these studies indicate that MH mutations increase RyR1 sensitivity to activation by the voltage-sensing DHPR during EC coupling.

Recently, *STAC3* gene (*stac3)* has been identified as one of the candidates of MH mutations in a Native American tribe [271]. The ablation of *stac3* results in severe locomotor defects and a decrease in EC-coupling as observed in Zebra fish [272]. In addition, paralysis and perinatal lethality were found in STAC3 knock-out mice [273]. The STAC3 protein was shown to traffic together with the L-type calcium channel, supporting a role for STAC3 in EC-coupling [274].

The effects of MH mutations on channel regulation by endogenous regulators such as Ca^{2+}, Mg^{2+} and CaM and pharmacological agents such as caffeine, halothane, and dantrolene were characterized in isolated SR vesicle preparations [275-279]. The MH arg615$\rightarrow$cys mutation in the RyR1 resulted in an increase in RyR1 activation by Ca^{2+}

without affecting the Ca^{2+} threshold for activation [279, 280]. Similarly, the human MH gly2434→arg mutation within the central domain also increased RyR1 activation [275]. In addition, it was reported that the inhibitory effect of Mg^{2+} on the RyR1 is reduced in MH arg615→cys muscle [281].

CaM regulation was originally suggested to be affected in MH [282]. In relaxed muscle, CaM activates channel activity in the presence of submicromolar concentrations of Ca^{2+} and a significant increase in CaM activation was observed in the MH muscle mutation [280].

1.7 Dantrolene

1.7.1 Role of dantrolene

Dantrolene is a hydrantoin derivative that acts as a skeletal muscle relaxant [280]. It is the most effective drug for treating malignant hyperthermia [283]. It can also be administered in treating other medical conditions such as neuroleptic malignant syndrome and muscle spasticity [284]. Clinically, a concentration of ~10 μM has been used to treat this condition [285]. Dantrolene suppresses the abnormal Ca^{2+} elevation in skeletal muscle, muscle contracture and accelerated metabolism. It is a muscle relaxant that acts directly within the fibre and inhibits SR Ca^{2+} release [32]. It was demonstrated that dantrolene (~10 μM) reduced skeletal muscle contraction by 50% through changing the sensitivity of contractile activation to higher membrane potentials [286]. Dantrolene inhibits SR Ca^{2+} release and hence inhibits muscle contracture and accelerated metabolism which are the major problems [285]. Interestingly, it was demonstrated that the action of dantrolene on RyR1s is to reduce the extent of channel activation by CaM although they missed out the essential role of CaM in dantrolene inhibition [280].

A dantrolene binding site has been identified in the DP1 regions in RyR1 and RyR2 [283, 287-289]. Interestingly, dantrolene also binds to the respective amino sequence (amino acid 601-620) of the RyR2 [289, 290]. Some groups have therefore proposed that dantrolene has an effect on cardiac RyR2s [283, 291]. However, Diaz-Sylvester PL et al.(date) did not see any effect of dantrolene on the activity of RyR2 channels [292]. In our single channel recordings, CaM dissociated within a minute when SR vesicles were incorporated so CaM had been absent in the experiments. Recently, it was

reported that abnormal Ca^{2+} release in heart failure is ameliorated by dantrolene [249, 283]. Dantrolene was also found to preserve inotropy in heart failure cardiomyocytes by reducing the frequency of diastolic Ca^{2+} sparks and increasing the threshold of SR Ca^{2+} release. Thus, it prevents the loss of Ca^{2+} from cellular storage of myocytes [280]. Interestingly, it was found that dantrolene altered the binding of CaM to the RyR [250]. It is possible that the inhibitory effect of dantrolene is achieved via its interaction with CaM.

MH is an inherited muscular disorder in which the majority of identified mutations are located in the genes encoding RyR1 [293, 294] or L-type Ca^{2+} channels [265, 295-297]. Dantrolene reduced the aberrant Ca^{2+} release from the SR into the myoplasm during an MH episode [284]. Interestingly, dantrolene has been shown to reduce store-operated [298, 299] and voltage-triggered Ca^{2+} entry [300, 301] into muscle from outside the cell. One of the major routes of calcium entry is the Ca^{2+} current conducted by L-type Ca^{2+} channels [301, 302]. It was accepted that dantrolene inhibits E-C coupling without greatly affecting the ability of skeletal muscle fibres to conduct action potentials [303]. In contrast, it was recently reported that dantrolene has an inhibitory effect on skeletal muscle Ca^{2+} current and charge movement attributed to L-type Ca^{2+} channels [301, 304, 305], suggesting the dantrolene inhibition of L-type Ca^{2+} channels by altering the membrane environment. Bannister et al., 2013 investigated whether the depolarizing shift was a consequence of a dantrolene-induced depression in membrane excitability or a modification of bidirectional communication between RyR1 and L-type Ca^{2+} channels [306]. Firstly, they measured the effects of dantrolene on Na^{+} currents as an assay to gauge membrane excitability. Dantrolene did not show any effect on the average peak current density, voltage dependence of activation, voltage dependence of inactivation or recovery from inactivation of the Na^{+} current in developing myotubes [306], thus ruling out the membrane excitability as a plausible explanation for dantrolene action [306].

They further investigated the dantrolene inhibition of L-type Ca^{2+} currents from (RyR1 null) myotubes. Interestingly, the dantrolene effect was not observed on the amplitude, voltage dependence or inactivation kinetics of L-type Ca^{2+} currents in Dyspedic (RyR1 null) myotubes [306], thereby excludingdirect interaction of dantrolene with L-type Ca^{2+} channels. It could be suggested that dantrolene might selectively interact with high Po state of L-type Ca^{2+} channels that occurs with the influence of the RyR1 [24, 307]. Finally, they concluded that expression of RyR1s is necessary for dantrolene inhibition

on L-type Ca^{2+} channels with dantrolene altering the conformational coupling between the two channels.

1.7.2 Dantrolene and domain interaction theory

The majority of MH mutations are localized in the N-terminal (Cys35-Arg614), and central (Asp2129-Arg2458) domains whereas fewer mutations are found in the C-terminal region (Ile3916-Gly4942) [259]. One of the characteristics of RyR1 Ca^{2+}-release channels with MH mutations is the SR Ca^{2+} leak [259, 308]. An hypothesis of domain interaction has been proposed whereby interactions between the N-terminal and the central domain of the RyR1 are involved in Ca^{2+} regulation, serving as a "domain switch" [243, 309-311]. In the resting state, there is close contact between the N-terminal and the central domain at several as yet unidentified subdomains (domain zipping). This domain zipping stabilises and maintains the closed state of the Ca^{2+} channel. Stimulation of the RyR1 during E-C coupling and some pharmacological agents such as halothane and succinylcholine, weaken the interdomain contacts and reduce the conformational constraints (domain unzipping), lowering the energy barrier for the Ca^{2+} channel opening. MH mutations were reported to weaken the domain interactions between the N-terminal and the central domains, destabilising the closed state of the channel [312]. Kobayashi et al. used DP4 (a synthetic peptide corresponding to amino acids 2442-2477 of the RyR1) or anti-DP4 antibody to mimic the MH condition [313]. They used the *Stern-Volmer* plot of fluorescence quenching of MCA that is attached to the N-terminal domain, with different concentrations of DP4. The Stern-Volmer quenching constant (K_Q) which is equal to the slope of the plot, gives the measure of the degree of domain unzipping. Dantrolene stabilized a zipped configuration of the domain switch altered by DP4 because dantrolene reduced the K_Q that was increased by DP4 [313].

Interestingly, some RyR2 mutations in cardiac disease patients were found in the regions corresponding to the skeletal N-terminal and central domains where most of the MH mutations are found [314]. This led to the suggestion that RyR1s and RyR2s share a common intrinsic regulation of domain interactions. It was reported that channel gating is destabilized by the inter domain interaction defect of RyR2s, leading to contractile dysfunction [315]. Kobyashi et al., 2005 proved that a weakened

interdomain interaction is one of the key mechanisms underlying the pathogenesis of ARVC2, CPVT and heart failure [313]. In heart failure, an unzipped or destabilized interdomain interaction between the domains of RyR2 channels was observed which could be the result of posttranslational modifications such as phosphorylation [92, 316] or oxidation [317]. These altered interactions contribute to the defective function of the channel and aberrant cellular Ca^{2+} dynamics. It was also suggested to cause the increased diastolic Ca^{2+} leak and activation of spontaneous Ca^{2+} waves [318, 319]. The Ca^{2+} leak via the RyR2 causes the loss of Ca^{2+} from the SR with the NCX extruding these Ca^{2+} ions out of the myocyte [320]. This loss of Ca^{2+} reduces the Ca^{2+} content of the SR, weakening myocyte contraction [321, 322]. It was proposed recently that dantrolene could stabilize the interdomain interaction of RyR2 and prevent Ca^{2+} release from the SR during diastole in heart failure [141, 249, 313]. In addition, it was found that dantrolene decreased the frequency of Ca^{2+} sparks whereas it increased the SR Ca^{2+} content in HF myocytes [323].

1.7.3 Dantrolene as a potential anti-arrhythmic drug

There are a few reasons why dantrolene has been considered an antiarrhythmic drug through its action on RyR2. RyR1 and RyR2s are both likely regulated by similar interactions between the N-terminal and central domains. Disruptions in these interactions are believed to lead to MH in skeletal muscle, CPVT and heart failure in cardiac muscle. The ability of dantrolene to restore failing interdomain interactions in RyR1s and RyR2s [283], provides a mechanism for its therapeutic action for MH and therefore may also be therapeutic in CPVT and heart failure in cardiac muscle. They reported that dantrolene inhibited Ca^{2+} leak and improved the cardio myocyte function in the failing heart. This finding has opened the doors for the development of new therapeutic drugs against heart failure, arrhythmia and CPVT [283].

1.7.4 Dantrolene effects on the RyR affinity for divalent ions

Dantrolene inhibition was shown to depend on the cytosolic [Ca^{2+}]. Ca^{2+} release experiments in skinned fibres of mouse skeletal muscle showed that dantrolene reduced

the rates of Ca^{2+} release (~50%) but it exhibited very little effect on Ca^{2+} release at higher Ca^{2+} concentrations. Similarly, dantrolene inhibition of RyR2 also depends on the cytosolic [Ca^{2+}]. Dantrolene inhibits the frequency of Ca^{2+} sparks but does not inhibit the amplitude of Ca^{2+} transients [323, 324]. Thus, dantrolene was a diastolic inhibitor of Ca^{2+} release in rabbit failing heart [323] and it reduced diastolic SR Ca^{2+} leak after ventricular fibrillation [324]. Dantrolene inhibition was also observed on the ryanodine binding to MH-susceptible (MH) and normal vesicles activated by Ca^{2+} and CaM, highlighting the importance of Ca^{2+} and CaM in dantrolene inhibition [280].

The dantrolene effect on skinned muscle fibres was reported to be more pronounced when ATP was present in the medium [325]. It was supported by another finding that adenine nucleotides enhanced the binding of [^{3}H]-dantrolene to SR vesicles [326]. Zhao et al. (2001) further reported that dantrolene inhibition was dependent on adenine nucleotide as they found dantrolene inhibition of [^{3}H]ryanodine binding only in the presence of ATP [291].

A physiological Mg^{2+} concentration (~1mM) fully blocks RyR1 activation by Ca^{2+} [20, 327], effectively preventing SR Ca^{2+} release in resting skeletal muscle [327, 328]. RyR1 activation during E-C coupling is dependent on L-type Ca^{2+} channels causing a reduced Mg^{2+} affinity for the RyR1 [329]. Dantrolene inhibition of SR vesicle [^{3}H]-ryanodine binding was not associated with an altered IC_{50} for Mg^{2+} [291]. They further indicated that the effects of dantrolene on the apparent Ca^{2+} affinity of RyR1 activation sites [280] were not associated with changes in the affinity of these same sites for Mg^{2+}.

1.7.5 Dantrolene reduces RyR1 sensitivity to caffeine

Dantrolene reduces the sensitivity of the isolated RyR1 to Ca^{2+} activation and it was suggested that a reduced affinity of Ca^{2+} binding to RyR1 activation sites might be the basis of dantrolene inhibition of Ca^{2+} release in skeletal muscle [280]. Caffeine activates the RyR by increasing the Ca^{2+} sensitivity of the channel [328]. A reduction in the threshold for caffeine activation is characterized in MH RyR1 mutations[330]. To show this was possible, Zhao et al., 2001 examined the effect of dantrolene on the RyR1's sensitivity to caffeine [291]. They reported that dantrolene (10μM) shifted the caffeine threshold for activation of [^{3}H]ryanodine binding to higher caffeine concentrations, and also increased the EC_{50} activation of both MH and normal SR

vesicles more than two-fold[291]. They concluded that dantrolene reduced the apparent caffeine sensitivity of the RyR1 and opposed the effects of MH mutations on caffeine activation of RyR1s.

1.8 Hypotheses and objectives

Hypothesis 1:

CaM regulates the function of the RyR1 by altering its calcium and magnesium regulation.

The first objective was to fully understand how CaM regulation of RyR1s is modulated by Ca^{2+} and Mg^{2+} ions (**Chapter 3**).

Hypothesis 2:

CaM is essential for dantrolene inhibition of cardiac RyR (RyR2) and skeletal RyR (RyR1).

The second and main objective was to investigate the inhibition of RyR1 and RyR2 by dantrolene in the presence and absence of exogenous CaM. This study presents the first measurement of dantrolene inhibition in single channel recordings. (**Chapter 4**).

Hypothesis 3:

Dantrolene inhibits the RyR2 even in the presence of mutant CaM (N54I and N98S).

The third objective was to test whether dantrolene inhibition could be observed in the presence of mutant CaMs that can alter the channel function. Dantrolene inhibition of RyR2s was therefore measured following the addition of mutant CaM to the bath solution during single channel recordings. (**Chapter 4**)

Hypothesis 4:

Dantrolene inhibition of RyR1 is modulated by cytosolic and luminal [Ca^{2+}] and cytosolic [Mg^{2+}].

The fourth objective was to investigate how Ca^{2+} and Mg^{2+} modulate dantrolene inhibition of the skeletal RyR1 from both the luminal and cytosolic sides of the channel. (**Chapter 5**)

Hypothesis 5:

Dantrolene inhibits RyR1 activity altered by ATP, halothane and DP4.

The fifth objective was to test whether dantrolene could inhibit the channel activity altered by ATP, halothane and DP4 (**Chapter 5**).

Hypothesis 6:

Dantrolene inhibition of RyR2 depends on cytosolic [Ca^{2+}]

The final objective was to understand the cytosolic [Ca^{2+}]-dependent effect of dantrolene inhibition by measuring the effects on RyR2 receptors at different cytosolic [Ca^{2+}] (**Chapter 6**).

Chapter 2 Methods

2.1 Source of tissues

SR vesicles containing cardiac ryanodine receptors (RyR2) for this study were obtained from sheep and human hearts. Skeletal muscle ryanodine receptors (RyR1) were isolated from rabbit skeletal muscle. Animal tissues were obtained with approval from the Animal Care and Ethics Committee of the University of Newcastle, Australia (Approval number A-2009-153). Human tissues were obtained with an approval from the human research ethics committees of University of Newcastle (approval number H-2009-0369) and the University of Sydney (approval numbers 09-2009-12146 and 2012/2814). Human left ventricular tissues were obtained from explanted 'unused' donor hearts of four non-myopathic (healthy) patients and a failing heart tissue was obtained from explanted hearts from patients with terminal heart failure undergoing heart transplantation. The characteristics of donor hearts (failing and non-failing human hearts) are summarized in **Table 2.1**. Hearts were flushed with an ice-cold cardioplegia package under sterile conditions and were then transported by the Australian Red Cross Blood Service and delivered to the Bosch Institute. Liquid nitrogen (-196° C) was used to snap freeze the transmural sections of the left ventricle free wall (~1 g) within three to four hours of delivery.

Sample		Sex	Age	Cause of death/ aetiology	Source
6.048	RV	F	54	Subarachnoid haemorrhage	University of Sydney
7.060	LV	M	40	Stroke	University of Sydney
ICM	LV	M	58	Ischemic Cardio Myopathy	Queensland University of Technology

Table 2.1: Characteristics of hearts from the Human Heart tissue repository; (University of Sydney and the Queensland University of Technology. Failing heart tissue (ICM) was obtained from explanted hearts of patients with terminal heart failure undergoing heart transplantation. LV: left ventricle, RV: right ventricle.

2.2 Preparation of SR Vesicles

Isolation of SR vesicles was based on previous methods [331, 332]. Muscle tissues were minced and homogenized in a Waring blender (4 x 15 sec bursts at high speed) in homogenizing buffer containing 0.3 M sucrose, 10 mM imidazole, 0.5 mM dithiothreitol (DTT), 3 mM sodium azide, and 20 mM NaF; pH 6.9, and the protease inhibitors, 0.5 mM phenylmethylsulfonylfluoride (PMSF), 1 ug/ml leupeptin, 1 ug/ml pepstatin and 1 mM benzamidine. , About 1-2 g of tissue in 10 ml of buffer was used for human preparations and about 100 g of tissue in 500 ml of buffer was used for sheep preparations. NaF was used to stop the action of phosphatases during the RyR isolation procedure. The homogenate was further homogenised by 10 manual strokes of a loose glass/glass Dounce homogenizer. The homogenate was then centrifuged at 8,000 g for 20 minutes using a Beckman Optima L-100XP ultracentrifuge so as to sediment cell debris and connective tissue. The supernatant was centrifuged at 170,000 g for 30 minutes to collect the cell microsomes. The resultant pellet was resuspended with a glass/glass Dounce homogenizer in homogenizing buffer containing 0.65 M KCL, incubated for 30 minutes on ice before centrifuging at 8,000 g for 15 minutes to sediment the myosin. The supernatant was centrifuged at 170,000 g for 1 hour. The pellet containing SR vesicles was resuspended in storage buffer (homogenizing buffer + 0.65 KCl), snap frozen in liquid nitrogen and stored at -80°C. For the majority of the experiments, about 1-2 µl of preparation was used to obtain the channel fusion.

2.3 Single Channel recording

2.3.1 Overall lipid bilayer set-up

The bilayer rig generally consists of an apparatus to support the lipid membrane, high gain, amplification of signals, shielding from electromagnetic interference and mechanical vibration, mechanisms for stirring and changing solutions, signal filtering, data acquisition hardware and software, data analysis software, and a means to archive acquired data. A schematic representation of the bilayer setup and current recording system is shown in **Figure 2.1**.

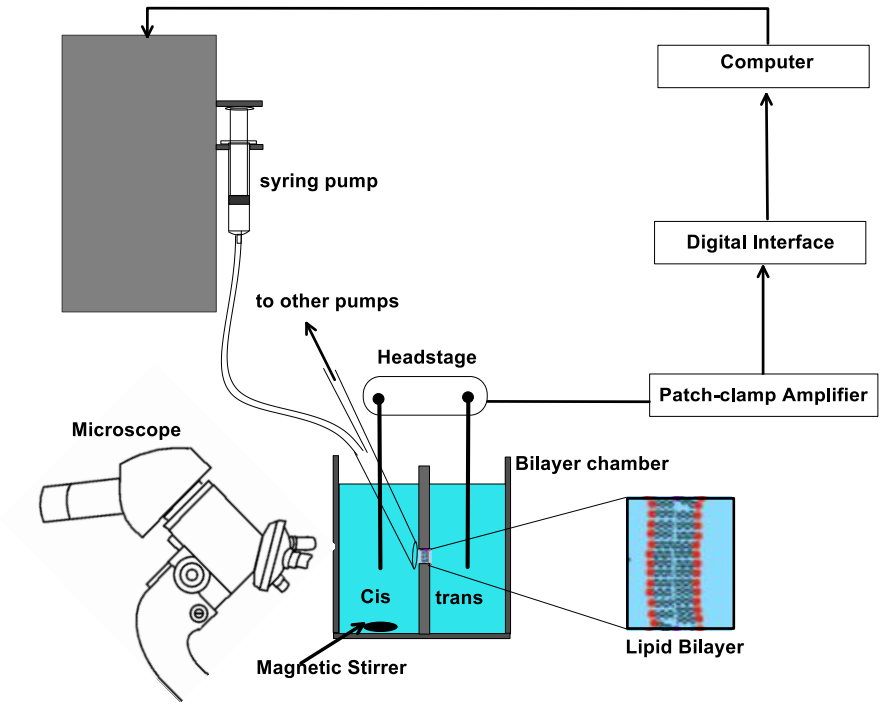

Figure 2.1: Schematic diagram of single channel recording system. The bilayer chamber consisted of *cis* and *trans* baths separated by a partition on which the bilayer was formed. A Delrin cup containing the *trans* bath is inserted into the chamber holder, forming the *cis* bath. A hole formed by spark discharge was punched into the side of the inner chamber to produce the support for the artificial lipid bilayer. The bevelled PVC nozzle of the perfusion tube was positioned over the bilayer using a micromanipulator connecting with 8 plastic syringes pressed by Teflon pistons. A large portion of the lateral wall of the bath partition near the bilayer aperture was machined away, allowing adequate access for the perfusion tube and flow solution. The bilayer membrane and perfusion tube were viewed under a 10–40× binocular microscope. Electrical connection with the bath was made using a silver chloride coated silver wire. The *cis* chamber was electrically grounded to prevent the tubing leading to the flow nozzle, the reservoir and the solution from becoming a source of electrical interference. Voltage was controlled and current was recorded with an Axopatch 200B amplifier (Axon Instruments). During the experiments, the bilayer current and voltage were recorded at a bandwidth of 5 kHz (Modified from Laver DR (2009a)) [333].

2.3.2 Membrane formation and vesicle fusion

Millar and Racker [334] discovered that SR vesicles isolated from muscle could be incorporated into an artificial lipid bilayer in the presence of high [Ca^{2+}] (1-5 mM) and an osmotic difference across the bilayer. Artificial lipid bilayers were composed of a lipid mixture of phosphatidylethanolamine and phosphatidylcholine (8:2 wt/wt) in n-decane (a hydrophobic solvent, 50 mg/ml). A film drainage method was used to form bilayers across the hole in a Delrin cup [335]. A flamed polished glass rod (1-2 mm) was used to apply lipid to the surface of the aperture in a Delrin cup, providing a thick lipid film separating the two baths. The lipids form two monolayers across the hole (diameter 150-200 μm) with the *n*-decane between them. The n-decane drains under buoyancy so the final thin bilayer forms due to compressive forces of Van der Waals attraction between molecules in solution and either side of the bilayer membranes. In most cases, the bilayers become thin spontaneously, but it can also be facilitated by gentle touching of the film with the glass rod or by rapid changes of the voltage applied across the lipid/*n*-decane film. The bilayer was observed either visually under the microscope (Figure 2.2) or electrically by measuring the bilayer capacitance. The geometry of the aperture is critical for the stability of the painted membrane. If the diameter of the hole is small then the membrane formed will be mechanically robust and the electrical noise reduced, whereas, a larger hole diameter increases electrical noise and is mechanically more fragile. Notably, the probability of vesicle fusion to the membrane is inversely proportional to the membrane size.

Silver chloride-coated silver electrodes were used to make electrical connections to each chamber, transducing ionic currents in the electrolyte solution to an electron current within the wire. This was done by utilizing a reversible oxidation/reduction reaction between the silver in the electrode and Cl- ions in the bath. The chemical reaction is given below:

$$Cl^- + Ag^+ \longrightarrow AgCl + e^-$$

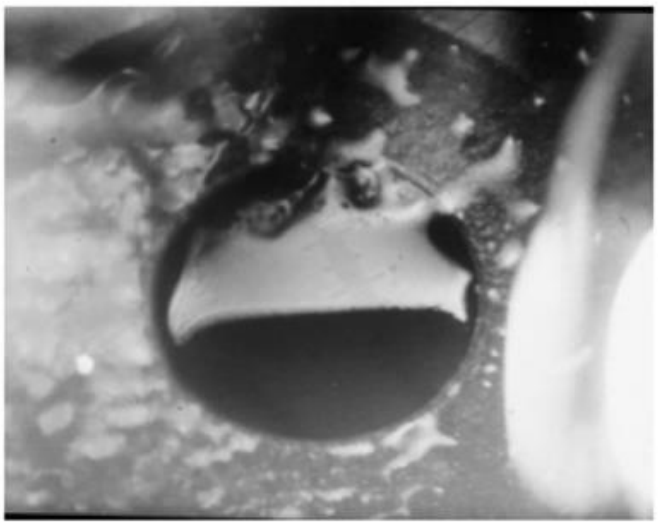

Figure 2.2: A photograph of a lipid bilayer (bottom half of aperture) formation from a thick lipid film (top half). Lipid film is seen (reflecting light) in the upper half circle due to the strong reflection of the incident light whereas the dark lipid bilayer is seenin the lower half circle due to vanished reflection of the light. The bilayer portion of the film spreads across the entire aperture in a few seconds, leaving a region of thick film at the periphery. Photograph obtained from DR Laver (2001) [336].

This chemical reaction is associated with a voltage difference between the silver and the electrolyte that depends on the Cl- concentration. Differences in these potentials at each electrode produced an offset voltage on the lipid bilayer. This offset voltage was nulled in the signal detection amplifier.

The bilayer chambers were mounted above a magnetic stirrer to provide stirring of the *cis* bath to facilitate fusion of SR vesicles. The bilayer apparatus was enclosed in a copper mesh Faraday cage to isolate the high impedance electronics from external electrical noise. The bilayer apparatus was mounted on a vibration isolation table to provide long-term mechanical stability for the lipid bilayer.

RyRs (from human and sheep hearts and skeletal muscle) were incorporated into the artificial lipid bilayer simply by adding SR vesicles containing ion channel proteins (1-10 μg/ml) to the cis bath and stirring (using magnetic stirrer) until channel activity indicated vesicle fusion with the bilayer (detected by conductance changes in the bilayer membrane). The side of the bilayer to which the vesicles were added is defined as the *cis* side and vesicles always fuse such that the *cis* bath faces the cytoplasmic side of the membrane and the *trans* bath faces the SR luminal side. Conditions t used to promote vesicle fusion are gradient in osmotic potential across the membrane (*cis* high) and *cis* [Ca^{2+}] at mmol/L concentrations, plus vigorous stirring of the *cis* bath. [332].

2.3.3 Amplification and filtering

Experiments were carried out at room temperature (23 ± 2^{o} C). Electric potentials are expressed using standard physiological conventions (*i.e.* cytoplasm relative to SR lumen at virtual ground). Control of the bilayer potential and recording of unitary currents was done using an Axopatch 200B amplifier (Axon Instruments Pty Ltd, Foster City, CA USA) or a Bilayer clamp -525C (Warner Instruments Corp). The current signal was digitized at 5 kHz and low pass-filtered at 1 kHz. The recordings were stored on computer disk using a data interface (either Data Translation DT301 or DT3001) under the control of in-house software written in Visual Basic by DR Laver (University of Newcastle, Australia).

2.3.4 Chemicals and solutions

Lipids were obtained in chloroform from Avanti Polar Lipids (Alabama USA). Caesium salt used in both *cis* and *trans* chambers was obtained from Aldrich Chemical Company. $CaCl_2$ and $MgCl_2$, were from BDH Chemicals, and TES and ATP were obtained from Sigma (St Louis, USA). Calmodulin (CaM) was obtained from either Sigma (St Louis, USA; prepared from bovine testes) or Enzo Life Sciences (New York USA; prepared from pig brain). Dantrolene (powder) was obtained from Sigma (St Louis, USA). Dantrolene was prepared as stock solutions in DMSO and calmodulin was prepared in milliQ water. Halothane was obtained from ICI Pharmaceuticals. The

stock solution of halothane in the liquid form was used straight away after dilution tothe required concentration (5mM). The concentration of halothane in the *cis* solution was adjusted by adding liquid anaesthetic and sealing the solution in glass-teflon syringes before the experiments were performed. The peptide DP4 (^{2442} LIQAGKGEALRIRAILRSLVPLDDLVGIISLPLQIP ^{2477}) was obtained from Noriaki Ikemoto (Boston Biomedical Research Institute, Watertown, Massachusetts 02472 USA).

In this study, 150 mM Cs^+ was used for all experiments since 250 mM Cs^+ could affect the dissociation rate of CaM. During vesicle fusion the *cis* solution contained 150 mM Cs^+ (130 mM caesium methane sulfonate ($CsCH_3O_3S$), 20 mM CsCl), 1.0 mM $CaCl_2$ and 500 mM mannitol, whilst the *trans* solution contained 50 mM Cs^+ (30 mM $CsCH_3O_3S$, 20 mM $CsCl_2$) and 0.1 mM $CaCl_2$. These solutions provided the necessary Ca^{2+} and trans bilayer osmotic difference necessary for SR vesicle fusion with the bilayer. Caesium methane sulfonate was used as the principal salt in the bathing solution to prevent current signals from other ion channels interfering with ryanodine receptor recordings. After vesicle fusion and prior to single channel recording, the [$CsCH_3O_3S$] in the *trans* solution was increased to 130 mM by adding an aliquot of 4M $CsCH_3O_3S$ to the *trans* bath (*i.e*., producing 150 mM Cs^+ in both *cis* and *trans* baths).

All solutions were pH buffered using 10 mM TES (N-tris[hydroxymethyl] methyl-2-aminoethanesulfonic acid; ICN Biomedicals), and titrated to pH 7.4 using CsOH (ICN Biomedicals). Solutions were buffered to a redox potential of -232 mV (cytoplasmic level) using a combination of oxidized and reduced glutathione disulfide (GSSG (0.2 mM) and GSH (4 mM)). GSH and GSSG are the main intracellular redox buffers [337]. The ratio of redox buffer was calculated [338, 339] using the Nernst equation to eliminate experimental variations in RyR2 activity.

In this study, Cs^+ was used as the principal current carrier because it has a higher conductance (500 ± 12 pS) in the RyR than Ca^{2+} (110 ± 10 pS) [340, 341] and therefore increases both the current signal and the signal to noise ratio in the recordings. RyRs are highly permeable to K^+ [342]. Therefore, K^+ will carry most of the current *in vivo* given the high [K^+] in the cell. Cs^+ was used as a surrogate for K^+ because it relieves the constraints on the Ca^{2+} concentrations used in the studies of Ca^{2+} regulation of RyR2s. In addition, CsMS salt also reduces interfering signals from K^+ and Cl^- channels (Cs^+ blocks K^+ channels [343]) located in SR vesicles. Cs^+ is likely to be a good surrogate for

K^+ because the Ca^{2+}-dependence of [^{3}H]ryanodine binding indicated that Ca^{2+} regulation of RyRs is the same in both K^+ and Cs^+ solutions [19]. The use of Cl^- in both *cis* and *trans* solutions stabilised junction potentials between the solutions and the AgCl-coated silver electrodes. Cl^- concentrations were set at 20 mM which is similar to levels present in the cell. The concentration of Cl^- in the solutions was not sufficient to induce interfering unitary currents from the Cl^- channels present in SR vesicles.

Several Ca^{2+} chelators were used to buffer free Ca^{2+}. Free Ca^{2+} was buffered using 4.5 mM BAPTA (1,2-bis(o-aminophenoxy) ethane- *N*,*N*,*N*',*N*'-tetraacetic acid obtained from Invitrogen; free [Ca^{2+}] < 1 μM), dibromo BAPTA (up to 2 mM; free [Ca^{2+}] between 1-10 μM) [344] or sodium citrate (up to 6 mM; free [Ca^{2+}] between 10-50 μM in the absence of Mg^{2+}). Free Ca^{2+} was titrated with $CaCl_2$. Because all solutions applied in the *cis* bath contained 2 mM ATP (ATP chelates Ca^{2+} and Mg^{2+}), free levels of Mg^{2+} (added as $MgCl_2$) were calculated using estimates of ATP purity and effective Mg^{2+} binding constants that were determined previously under our experimental conditions [60]. Under given concentrations of ATP (mM), BAPTA (mM), ionic strength, pH and temperature, free [Mg^{2+}] in the *cis* solution was calculated using *Bound And Determined* software [345],based on the equations established by Marks PW and Maxfield FR [346].

Solution	Component	Final concentration
Homogenizing buffer	Sucrose Imidazole DTT Sodium azide	300 mM 10 mM 0.5 mM 3 mM pH 6.7 with HCl
Re-suspension or storage buffer	KCl PMSF Homogenising buffer	650 mM 0.5 mM pH 6.7 with HCl <100 μl
Protease inhibitors	Leupeptin Pepstatin A Benzamidine PMSF	1 μg/ml 1 μg/ml 1 mM 0.5 mM

Table 2.2: Solutions used in SR vesicle preparation from skeletal and cardiac muscles

2.3.5 Data Analyses

Single channel recordings of open probability (P_o), mean open time (T_o) and mean closed time (T_c) were measured using a threshold discriminator at 50% of channel amplitude (Channel3 software by NW Laver) as shown in **Figure 2.3.** Recordings of 30s duration or longer were used to analyse the data.

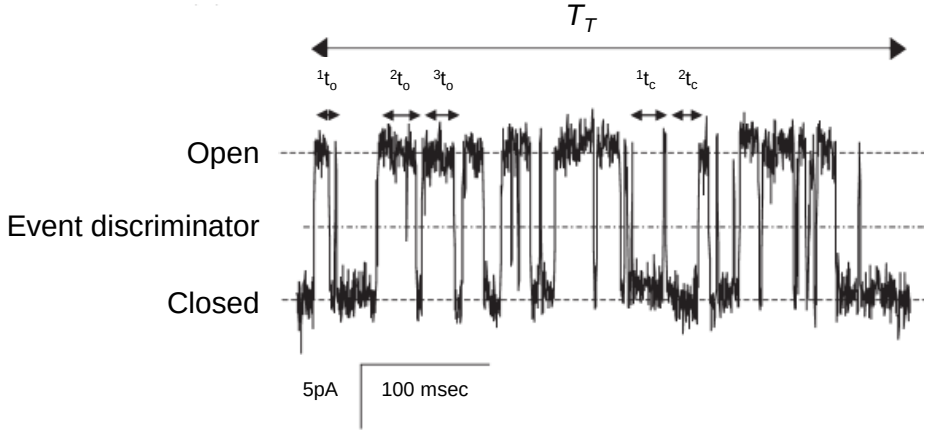

Open probability (P_o) = ($^1t_o + {}^2t_o + {}^3t_o \ldots + {}^nt_o$)/$T_{total}$

Mean open time (T_o) = ($^1t_o + {}^2t_o + {}^3t_o \ldots + {}^nt_o$)/n

Mean closed time (T_c) = ($^1t_c + {}^2t_c + {}^3t_c \ldots + {}^nt_c$)/n

Figure 2.3: Analysis of a single channel recording data. At + 40 mV, the upward current signals show the channel opening and the baseline is regarded as channel closure. The dashed line in the middle shows the current threshold and defines opening and closing events of the channels. Open and closed dwell times are denoted by t_o and t_c respectively. T_{total} is the total time of the data and n is the number of events. The above equations show how (P_o), (T_o) and (T_c) are calculated using the above four parameters. Figure adapted from Laver et al. (2001) [347] .

2.3.6 Calibration of Ca^{2+} electrode

A Ca^{2+} electrode (radiometer) was used in our experiments to determine the purity of Ca^{2+} buffers and Ca^{2+} stock solutions as well as free [Ca^{2+}] when [Ca^{2+}] was >100 nM.

A radiometer electrode was used to calibrate the Ca^{2+} meter and buffer stock solutions. The calibration of the Ca^{2+} electrode and BAPTA stock solutions was done by titrating $CaCl_2$ standard solutions with BAPTA solutions (a highly selective Ca^{2+} buffer and less sensitive to changes in pH, developed by Tsien in 1980 [348]). The titration was monitored by the Ca^{2+} electrode (**Figure 2.3A**) and the equivalence point, where the concentration of BAPTA is equal to the concentration of Ca^2, indicates a precise estimate of the concentration of the BAPTA stock. The titration curve was also used to calculate the calibration curve for the Ca^{2+} electrode (**Figure 2.3B**). A subsequent titration using the calibrated BAPTA solution, was used to calibrate an experimental Ca^{2+}- stock solution.

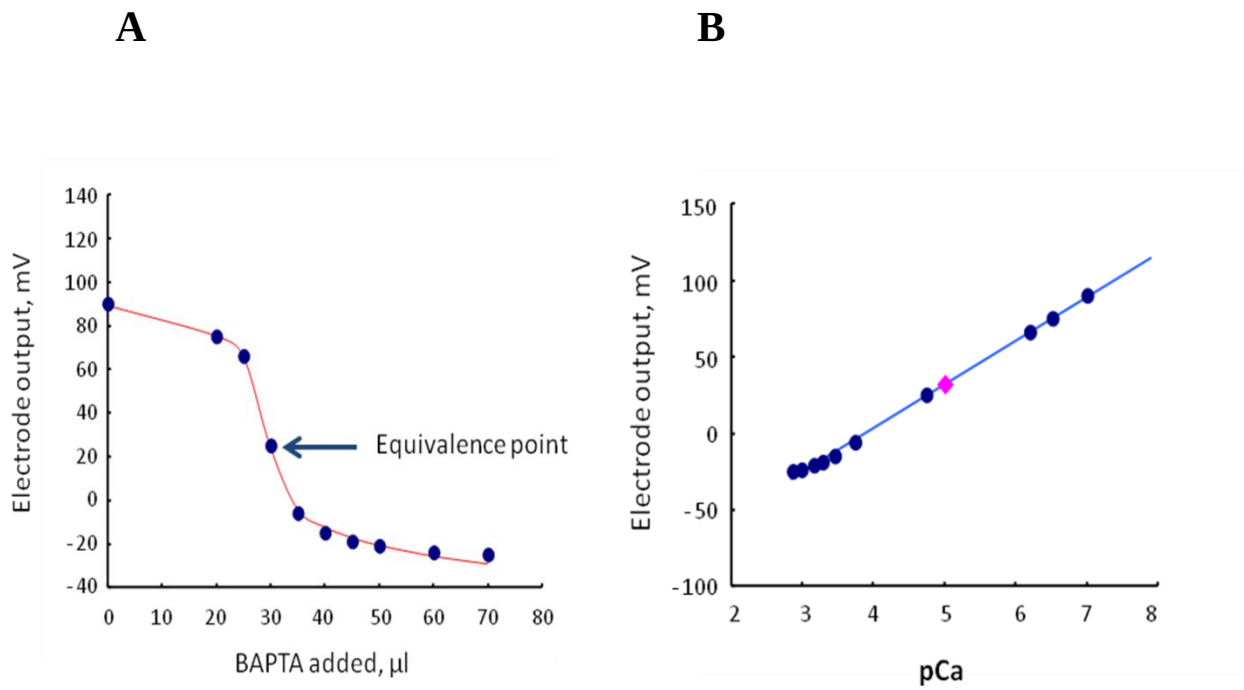

Figure 2.4: Ca^{2+} electrode calibration. (A) The measured electrode potential (blue circles) was plotted against the amount of BAPTA (~100 mM) added into the *cis* solution (70 ml) initially containing a 1 mM Ca^{2+} standard. The theoretical red line shows the electrode potential calculated from the electrode calibration and the dependence of free Ca^{2+} on [$BAPTA_{total}$] and [$Ca^{2+}{}_{total}$]. The concentration of free Ca^{2+} was calculated using the following quadratic equation:

$$[X^{2+}] = \frac{-([Anion]_T + K_{app} - [X]_T) + \sqrt{([Anion]_T + K_{app} - [X]_T)^2 + 4K_{app}[X]_T}}{2}$$

Where X is Ca^{2+} and the anion is BAPTA in our titration, K_{app} is the apparent equilibrium constant and T is the total concentration of ligand. **(B)** The blue line shows the linear relationship between the electrode potential (blue circles) and Ca^{2+} standards (pCa (–log[Ca^{2+}], M)).

2.3.7 Statistics

Unless otherwise stated, all data are presented as arithmetic mean ± standard error of the mean (SEM). The statistical significance of difference was determined using Student's *t* test on normal distributions. The test was performed as two sided for all paired data. Asterisks indicate being significantly different to 100% where (*) $p<0.05$ was considered significant and (**) $p<0.01$ was considered highly significant. One way ANOVA was used to determine whether there are any significant differences between the means of three groups. Optimization of theoretical curves to data was achieved using Microsoft Excel Solver and least square criteria for best fit.

2.3.8 Advanced perfusion methods

A perfusion system was established to allow solution exchanges in the *cis* chamber and applied to single channel recordings. The perfusion apparatus consisted of 8 plastic micro-syringes (1 ml-volume) driven by syringe pumps using computer control (**Figure 2.4**). These syringes were connected with PVC and quartz tubes to a nozzle positioned over the lipid bilayer. Pressure-driven syringe injections were used to flow the solution over the bilayer, allowing solution exchanges at the nozzle. The advantage of this system was that it provided flexibility in manipulating the different experimental conditions. Thus, the response of channels to a variety of substances in the cytosolic bath could readily be examined when solutions were rapidly and transiently altered. This design permitted quite sophisticated experimental protocols to obtain detailed information about mechanisms determining channel conductance and gating. The concentrations of calmodulin, dantrolene, ATP, Ca^{2+}, Mg^{2+}, halothane and DP4 in the cytoplasmic solution were altered by a local perfusion system [349] which allowed exposure of a single channel to multiple bathing conditions applied in any chosen sequence with an exchange time of ~3s.

Figure 2.5: Bilayer perfusion system. The apparatus consisted of 8 separate plastic syringes connected via PVC and quartz tubing to a micro manifold (2 µl dead space, made in-house). Each syringe was loaded with a specific solution. Once the syringe was selected via the computer, the piston pressed down on the syringe enabling the solution to flow through the tube and micro manifold thus perfusing the lipid bilayer.

Chapter 3

CaM Regulation of skeletal ryanodine receptors

3.1 Introduction

The skeletal ryanodine receptor (RyR1) is the calcium release channel located in the sarcoplasmic reticulum of muscle cells that is essential for excitation-contraction coupling (ECC) in a skeletal muscle [30]. Several endogenous ligands including Ca^{2+}, Mg^{2+}, ATP and the calcium binding protein calmodulin physiologically modulate the gating properties of the channels [185, 350-353]. CaM, the major regulatory protein, has been reported to bind tightly to RyRs regardless of whether it is in the Ca^{2+}-CaM or apo-CaM state [156, 354]. Regardless of whether CaM is Ca^{2+} bound, CaM binding is 1 molecule of CaM per RyR subunit [180, 184]. The amino acid sequence 3614-3643 of the RyR1 has been involved in binding for both apo-CaM and Ca^{2+}-CaM [180, 181]. Fluorescence anisotropy measurements show that, in native skeletal muscle SR vesicles, CaM binded to the RyR1 with high affinity (K_d = 5-25 nM) both in the absence and presence of micromolar Ca^{2+} [179, 180, 355]. Using electron microscopy techniques, it was suggested the CaM binding site was on the RyR surface facing the cytoplasm (at least 10 nM from the transmembrane channel of the skeletal rabbit ryanodine receptor) [356]. In single channel recordings, CaM inhibition of the SR Ca^{2+} release channel was observed as a reduction in the channel open time with no observable effect on single-channel conductance. In addition, CaM inhibition was observed in single channel measurements even in the absence of ATP, highlighting again a direct inhibition of CaM [64, 357-359].

ApoCaM is a weak activator of RyR1s whilst Ca^{2+}-CaM is an inhibitor of the channel activity [179, 360-362]. Bilayer studies demonstrated that micromolar concentrations of cytoplasmic Ca^{2+} activates the RyR1 channel whereas millimolar concentrations inhibit the channel. This biphasic regulation is characterized by the typical bell-shaped Ca^{2+} concentration dependence [19, 72]. On the other hand, SR calcium stores also play an important role in the regulation of Ca^{2+} release in skeletal muscle [363]. Increased luminal Ca^{2+} concentration enhanced the RyR1 opening when activated by ATP [60, 67, 69]. ATP activates the rabbit skeletal RyR1 in single channel recordings with a K_a

of ~0.36 mM [62]. Binding of ATP to a low-affinity site (K_a ~ 1 mM) stimulates the RyR1 channel opening even in the absence of cytoplasmic [Ca^{2+}] [17]. Using ^{3}[H]-ryanodine binding assays, it was found that the adenine nucleotide is the absolute requirement for CaM activation of RyR1s, suggesting an interaction between CaM and ATP activation of the RyR1 [177]. On the other hand, Mg^{2+} has a powerful inhibitory effect on skeletal ryanodine receptors under resting conditions. Mg^{2+} can inhibit RyRs as it competes with Ca^{2+} for the activation and inhibition sites as an antagonist [18, 364]. The affinity of the activation site (A-site) for Mg^{2+} is approximately more than 50-fold lower than for Ca^{2+}, and Mg^{2+} binding does not activate the channel [20]. According to the dual inhibition model, it is predicted that competition between Ca^{2+} and Mg^{2+} at the A-site results in significant Mg^{2+} inhibition when muscle is at rest (the cytoplasmic Ca^{2+} level is less than 100 nM)[20]. However, I-sites produce Mg^{2+} inhibition (K_i= 200 µM) over the entire physiological range of the [Ca^{2+}] [20, 281]. In skeletal muscle, Ca^{2+} activation is mainly regulated by the presence of Mg^{2+} in the cytoplasm and lowering the free [Mg^{2+}] below its physiological level of 1 mM to approximately 0.05 mM causes spontaneous RyR1 opening so that all the Ca^{2+} is lost from the SR [82, 83].

It is not fully understood how CaM regulation of RyR1s is affected by Ca^{2+}, Mg^{2+} and ATP. Moreover, although regulation of RyR1s by Ca^{2+}, Mg^{2+} and ATP is well characterised, there is little data on these regulation processes in the presence of CaM [179]. Therefore, in this thesis the single channel recording was used to investigate the effects of CaM on Ca^{2+} activation and inhibition of RyR1s as well as its regulation by luminal Ca^{2+} and inhibition by cytoplasmic Mg^{2+} in the single channel recording.

There is also a wide range of exogenous effectors of RyR1s [352, 353]. Two of these relevant to this study are halothane and the RyR1 domain peptide DP4. Halothane is known to trigger malignant hyperthermia in individuals carrying mutations in RyR1 [365, 366]. Louis et al. (1992) suggested SR calcium release as the primary site of volatile anesthetics in skeletal muscle [367]. It has since been found that halothane at mM concentrations less than 1 mM, is a strong activator of the RyR1 channel [292, 368, 369].

DP4 is a synthetic domain peptide which induces SR calcium release [309] and increases the gating activity of RyR1 in the single channel recording [370]. DP4 is believed to do this by competitively displacing the corresponding region of RyR1 in domain-domain interactions between amino acids Leu-2442-Pro-2477 [310]. In doing so, DP4 mimics the domain-disrupting effects of MH mutations in RyR1s. Again, there have been no studies of how these substances alter RyR1 activity in the presence of CaM and this study will address this gap.

3.2 Materials and Methods

3.2.1 Single channel recording

In all experiments in this chapter, SR vesicles containing RyR1s were isolated from rabbit skeletal muscle [371] and incorporated in artificial bilayer membranes as described in **Chapter 2** (2.3.2). Control of the bilayer potential and recording of unitary currents were made using an Axopatch 200B amplifier (Axon Instruments Pty, Ltd). Single channel recordings of open probability, mean open time and mean closed time were measured using a threshold discriminator at 50% of channel amplitude (Channel3 software by NW Laver). See **Chapter 2** (2.3.5) for details.

3.2.2 Statistics

Unless otherwise stated, all data were presented as arithmetic mean ± standard error of the mean (SEM). The statistical significance of difference was determined using Student's *t* test on normal distributions. Asterisks indicate being significantly different to 100%. (*) $p<0.05$ was considered significant and (**) $p<0.01$ was considered highly significant. One way ANOVA was used to determine whether there are any significant differences between the means of three groups.

3.3 Results

3.3.1 CaM regulation of RyR1s depends on the cytoplasmic Ca^{2+} concentration

The effects of 100 nM exogenous cytoplasmic CaM were measured to determine the open probability of the RyR1 over a range of cytoplasmic [Ca^{2+}]; Anexample recording is shown in **Figure 3.1** and grouped data in **Figures 3.2-3.4**. Consistent with the previous findings [179, 372, 373], CaM had a biphasic effect on RyR1, by increasing the open probability of the RyR1 to ~150 % of control (*i.e.* vehicle alone) at cytoplasmic [Ca^{2+}] of 0.1 μM but it reduced the open probability of the RyR1 to ~50 % of control (*i.e.* vehicle alone) at 1 μM and also at concentrations above 500 μM (**Figure 3.2**). Notably, CaM had no significant effect on RyR1 at intermediate cytoplasmic [Ca^{2+}] of 10-100 μM. The effects of CaM were mediated by changes in both the mean open time (T_o) and opening rate ($1/T_c$) of the RyR1 (**Figures 3.3 and 3.4**). CaM reduced the mean open time of the RyR1 at 1 μM and also at concentrations above 500 μM but had no effect at 0.1 μM and intermediate cytoplasmic [Ca^{2+}] between 10 and 100 μM (**Figure 3.3**). CaM increased the opening rate of theRyR1 to ~130 % of control (*i.e.* vehicle alone) at cytoplasmic [Ca^{2+}] of 0.1 μM but it reduced the opening rate of RyR1s to ~69 % of control at 1 μM and also to 60-76 % at concentrations above 500 μM (**Figure 3.4**). Again, CaM failed to have any impact on the opening rate of RyR1s at intermediate cytoplasmic [Ca^{2+}] of 10-100 μM, following a similar pattern of CaM effects on open probability. Therefore, it could be concluded from the data that CaM regulation of RyR1 depended on cytoplasmic Ca^{2+} concentrations and these changes could be due to effects of CaM on mean open time and the opening rate of the RyR1.

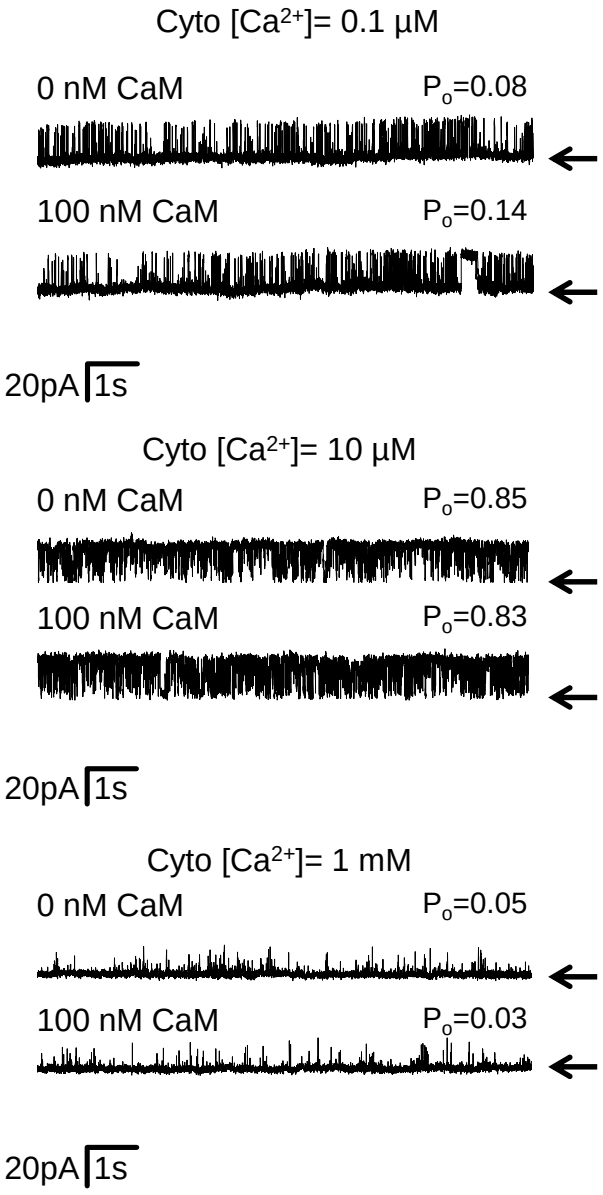

Figure 3.1: CaM regulation of RyR1s depends on cytoplasmic calcium concentration. Single channel recordings for CaM regulation of RyR1s at 0.1 µM, 10 µM and 1 mM cytosolic Ca^{2+}. The luminal bath contained 0.1 mM Ca^{2+}. Experiments were carried out at +40 mV and the upward current jumps represent the channel openings. The arrows show the recording baseline.

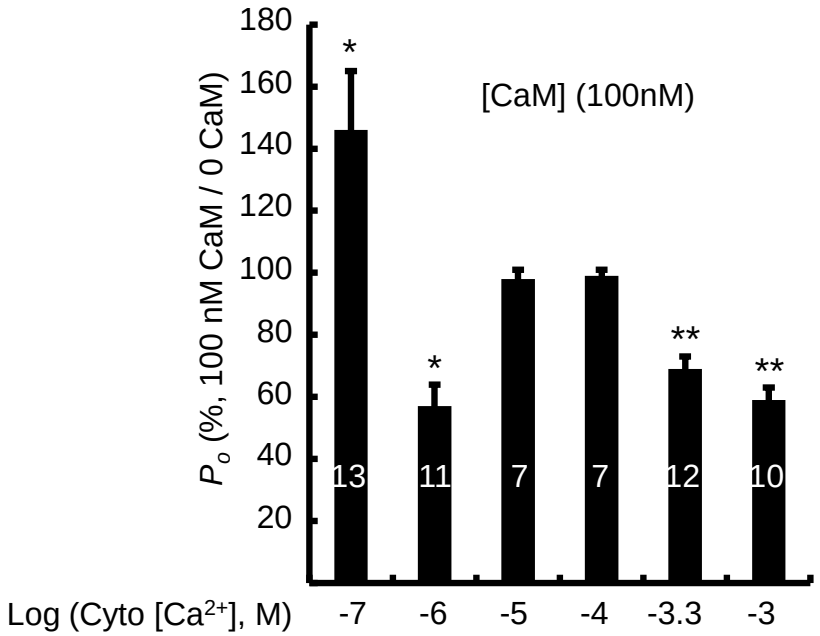

Figure 3.2: Relative changes in open probability induced by 100nM CaM over a range of cytoplasmic [Ca^{2+}] from 0.1μM to 1mM. The luminal bath contained 0.1 mM Ca^{2+} and experiments were carried out at +40 mV. Numbers of measurements for each bar are given in the figure label. The asterisks show values significantly different to 100% (* $p<0.05$, ** $p<0.01$, mean ± SEM).

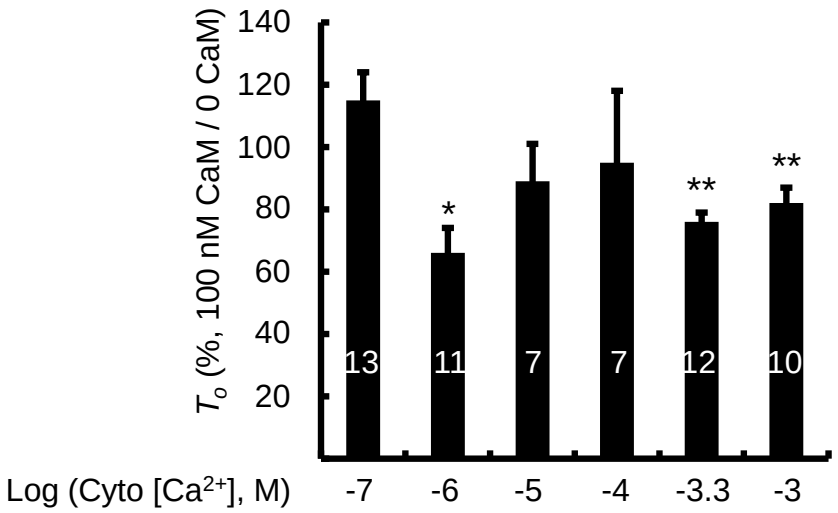

Figure 3.3: Relative changes in open time (T_o) induced by 100 nM CaM over the range of cytoplasmic [Ca^{2+}] from 0.1 μM to 1 mM. The luminal bath contained 0.1 mM Ca^{2+} and experiments were carried out at +40 mV. Numbers of measurements for each bar are given in the figure labels. The asterisks show values significantly different to 100% (* $p<0.05$, ** $p<0.01$, mean ± SEM).

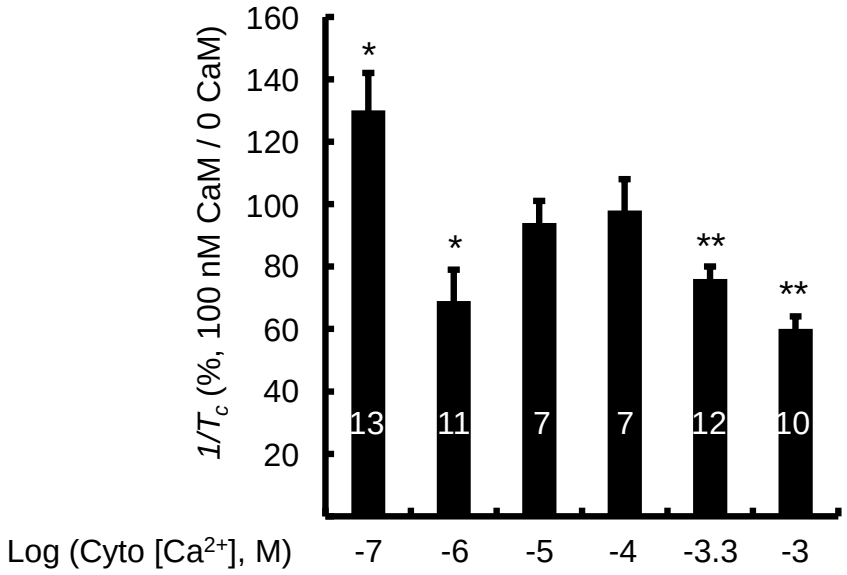

Figure 3.4: Relative changes in opening rate ($1/T_c$) induced by 100 nM CaM over the range of cytoplasmic [Ca^{2+}] from 0.1 μM to 1 mM. The luminal bath contained 0.1 mM Ca^{2+} and experiments were carried out at +40 mV. Numbers of measurements for each bar are shown in figure labels. The asterisks show values significantly different to 100% (* $p<0.05$, ** $p<0.01$, mean ± SEM).

3.3.2 Effects of luminal [Ca^{2+}] on CaM regulation of RyR1s at positive and negative voltages

Figure 3.5 shows the CaM regulation of RyR1s at different luminal [Ca^{2+}] in the presence of 100 nM cytoplasmic Ca^{2+} and cytoplasmic ATP (2mM), and absolute values for the vehicle (control) group are shown in **Table 3.1**. CaM significantly increased the open probability of the RyR1 by ~140% at both 0 and 100 µM luminal [Ca^{2+}] whereas it was inhibited by 25-35% at 1000 µM luminal [Ca^{2+}]. Also tested at various voltages,was the CaM effects on RyR1s at different luminal [Ca^{2+}] as this could give an indication whether CaM senses the flow of Ca^{2+} through the pore. However, CaM effects did not depend on the voltage difference at any luminal [Ca^{2+}] tested. It was further investigated how CaM regulated the activity of the RyR1 by measuring the effects of CaM on mean open time and opening rate. The effects of CaM on the mean open time were barely observed at any luminal [Ca^{2+}] at both positive and negative voltages, except at 100 µM luminal Ca^{2+} at positive voltage where a slight effect on the mean open time reached statistical significance (**Figure 3.5B**). In contrast, CaM increased the opening rate of RyR1s by 130-160% at 0 and 100 µM luminal Ca^{2+} but reduced it by 30-40% at 1000 µM luminal Ca^{2+} at both positive and negative voltages (**Figure 3.5C**). This result agreed withd the pattern of regulation on the open probability (**Figure 3.5A**). Therefore, it could be concluded that CaM regulation depends on the luminal [Ca^{2+}] and it works mainly through the modulation of the opening rate of the channel regardless of the voltage.

Luminal [Ca^{2+}], µM	**Voltage**	***n***	***P_o***	***T_o (ms)***	***$1/T_c$ (1/s)***
0	(+)	8	0.3 ± 0.1	1.2 ± 0.3	0.4 ± 0.1
	(-)	11	0.1 ± 0.1	1.9 ± 0.6	0.08 ± 0.02
100	(+)	14	0.1 ± 0.1	1.3 ± 0.6	0.15 ± 0.04
	(-)	8	0.06 ± 0.03	0.8 ± 0.2	0.07 ± 0.02
1000	(+)	10	0.5 ± 0.1	4.4 ±1.2	0.4 ± 0.1
	(-)	8	0.6 ± 0.1	2.2 ± 0.4	0.8 ± 0.1

Table 3.1: Absolute values of open probability (P_o), mean open time (T_o) and opening rate (the inverse of mean closed time, T_c) for vehicle (control) groups.

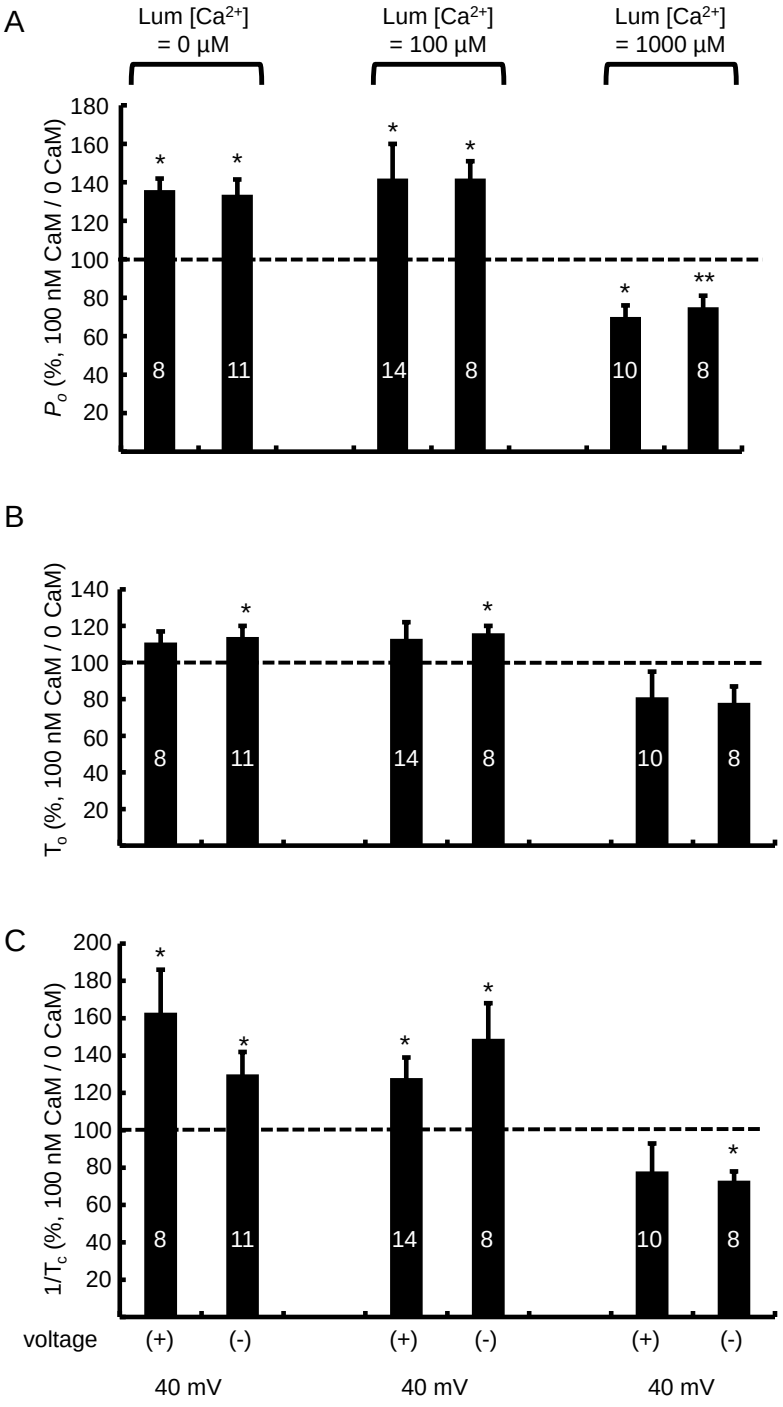

Figure 3.5: The effects of luminal [Ca^{2+}] on CaM regulation of RyR1s. Relative activation and inhibition of the RyR1 (A) open probability (P_o) (B) mean open time (T_o),, and (C) opening rate (the inverse of mean closed time, T_c) by 100 nM CaM at three different luminal Ca^{2+} concentrations and at positive and negative 40 mV. (Numbers of measurements for each bar are given in figure label.) The cytoplasmic bath contained 100 nM Ca^{2+} and 2 mM ATP. The asterisks show values that are significantly different to 100% (* $p<0.05$, **$p<0.01$, mean ± SEM).

3.3.3 Role of cytoplasmic Mg^{2+} in dantrolene inhibition of skeletal ryanodine receptors

The effects of CaM on RyR1 at 100 nM cytosolic [Ca^{2+}] in the absence and presence of 20 and 50 µM cytosolic [Mg^{2+}] were measured (**Figure 3.6**). CaM equally increased the open probability of the RyR1 to approximately 150-200% in all cases at 100 nM cytoplasmic [Ca^{2+}] (with 2 mM ATP) and these changes were associated with an increase in the open time and the opening rate of the receptors (**Figure 3.6**). In addition, there were no statistically significant differences between average values at any [Mg^{2+}] as determined by one-way ANOVA ($p = 0.25$). One can also interpret these data to mean CaM activation of the RyR1 had little impact on the potency of RyR1 inhibition by cytosolic [Mg^{2+}]. It is noted that the absolute P_o values for all control groups **(Table 3.2)** do not seem to follow the Mg^{2+} inhibition. This was mainly due to the fact that channel activity of the skeletal muscle ryanodine receptor greatly varies from one experiment to another. In fact, at concentrations of 20 and 50 µM, Mg^{2+} had a strong inhibitory effect on RyR1s as shown in **Figure 5.11**.

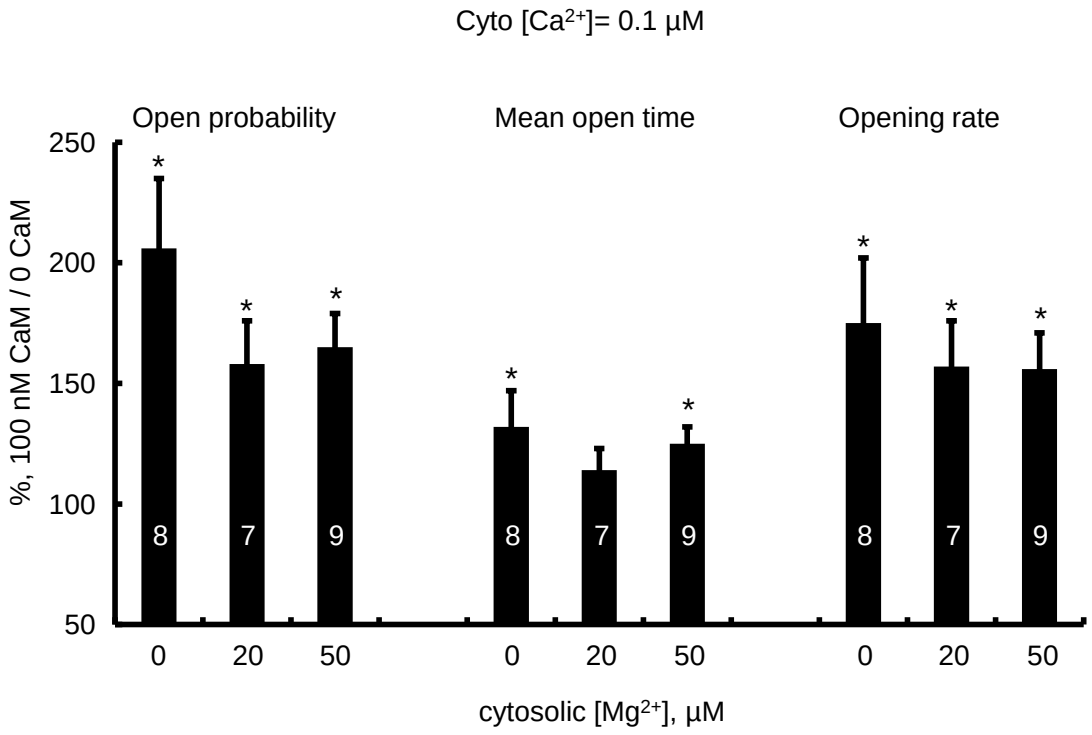

Figure 3.6: Relative activation of RyR1 open probability (P_o), mean open time (T_o) and opening rate (the inverse of mean closed time, T_c) induced by 100 nM CaM in the presence of low cytoplasmic [Ca^{2+}], ATP (2 mM) and various Mg^{2+} concentrations. The luminal bath contained 0.1 mM [Ca^{2+}]. Experiments were carried out at +40 mV. The numbers of measurements for each bar are given in the figure label. The asterisks show values that are significantly different to 100% (* $p<0.05$, **$p<0.01$, mean ± SEM).

Cytosolic [Mg^{2+}], µM	***n***	***P_o***	***T_o (ms)***	***$1/T_c$ (1/s)***
0 µM	8	0.05 ± 0.03	0.6 ± 0.1	0.07 ± 0.03
20 µM	9	0.06 ± 0.01	0.8 ± 0.1	0.08 ± 0.02
50 µM	12	0.13 ± 0.03	1.0 ± 0.1	0.14 ± 0.04

Table 3.2: Absolute values of open probability (P_o), mean open time (T_o) and opening rate (the inverse of mean closed time, T_c) for vehicle (control) in the absence and presence of different concentrations of cytoplasmic Mg^{2+}.

3.3.4 CaM regulates RyR1s activated by ATP, halothane and DP4

ATP, halothane and DP4 were all found to activate the channel gating of RyR1s (**Table 3.3-3.5**). The first investigations of CaM regulation of RyR1s were carried out in the absence and presence of 2 mM ATP at 100 nM cytoplasmic Ca^{2+} (**Figure 3.7**). As noted in the previous section, CaM similarly increased the open probability of the RyR1 by about 140-200% due to the activation in open time and the opening rate of the RyR1s. It is noted that there was no difference between the two groups (T-test, $p = 0.4$), suggesting that CaM activation was not altered by ATP at low cytoplasmic [Ca^{2+}]. It was then considered whether CaM regulation of RyR1s would be altered when they were activated by both ATP and Ca^{2+} (*e.g.* 100 μM cytoplasmic Ca^{2+}). Interestingly, under these conditions, CaM exhibited a substantially reduced inhibition of RyR1activity only in the absence of ATP with no effect observed in the presence of ATP. It could be suggested that ATP, or enhanced channel activity in the presence of higher cytoplasmic [Ca^{2+}], could abolish the CaM effect.CaM regulation of RyR1s activated by halothane and DP4 in the presence of 100 nM cytoplasmic Ca^{2+} was also investigated. CaM increased the channel opening of RyR1s similarly in both the absence and presence of DP4 by increasing both the mean open time and opening rate (**Figure 3.9**). Likewise, CaM increased the open probability of RyR1s in the absence and presence of halothane and these changes were also associated with the increase in the open time and the opening rate (**Figure 3.10**).

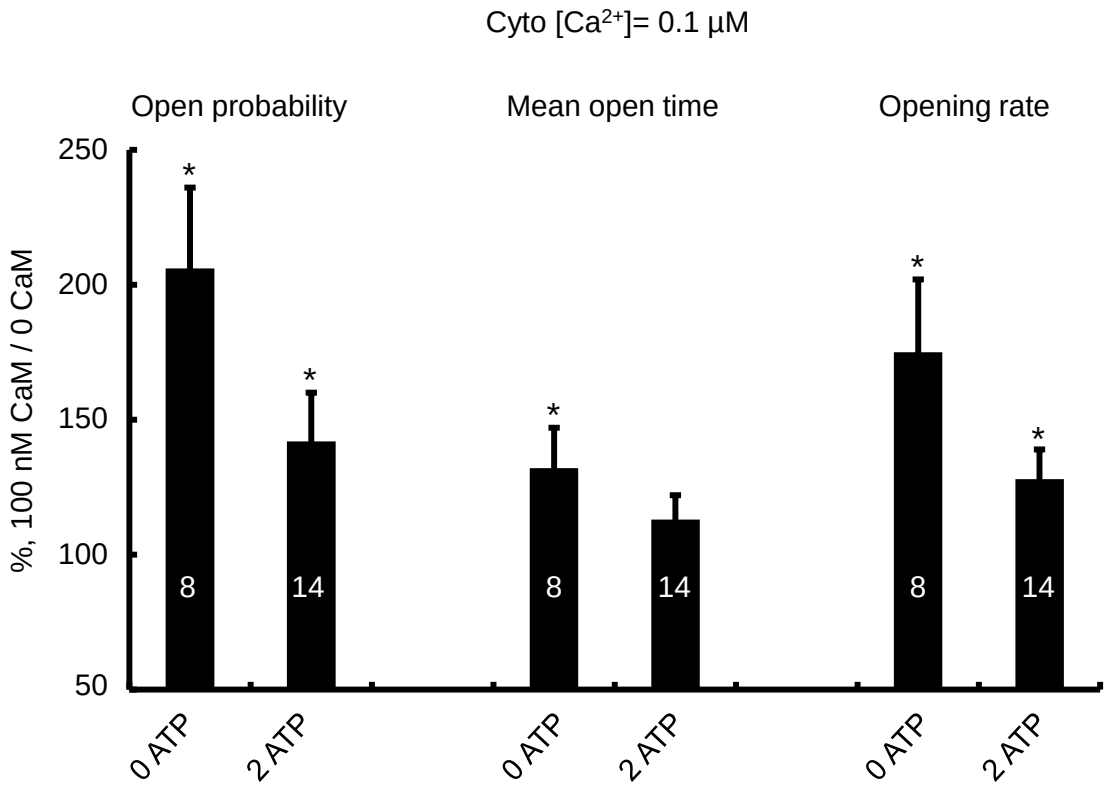

Figure 3.7: Relative activation of open probability (P_o), mean open time (T_o) and opening rate (the inverse of mean closed time, T_c) by 100 nM CaM in the absence and presence of ATP at low (100 nM) cytoplasmic [Ca^{2+}]. The luminal [Ca^{2+}] is 0.1 mM. Experiments were carried out at +40 mV. Numbers of measurements for each bar are given in the figure label. The asterisks show values that were significantly different to 100% (* $p<0.05$, **$p<0.01$, mean ± SEM).

ATP	n	P_o	T_o (ms)	$1/T_c$ (1/s)
0 mM	8	0.05 ± 0.03	0.6 ± 0.1	0.10 ± 0.03
2 mM	14	0.13 ± 0.10	1.3 ± 0.6	0.20 ± 0.04

Table 3.3: Absolute values of open probability (P_o), mean open time (T_o) and opening rate (the inverse of mean closed time, T_c) for vehicle (control) in the absence and presence of 2 mM ATP at 100 nM cytosolic [Ca^{2+}].

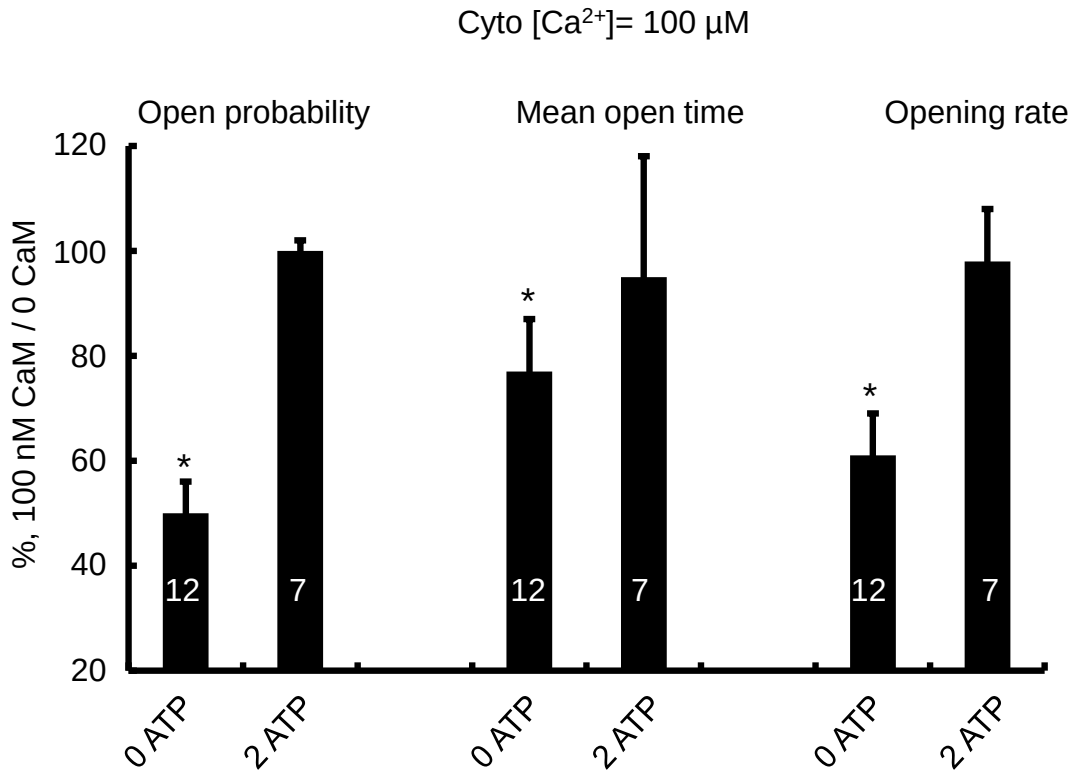

Figure 3.8: Relative inhibition of open probability (P_o), mean open time (T_o) and opening rate (the inverse of mean closed time, T_c) by 100 nM CaM in the absence and presence of ATP at high (100 µM) cytoplasmic [Ca^{2+}]. The luminal [Ca^{2+}] is 0.1 mM. Experiments were carried out at +40 mV. Numbers of measurements for each bar are given in the figure label. The asterisks show values that are significantly different to 100% (* $p<0.05$, **$p<0.01$, mean ± SEM).

ATP	**n**	***Po***	***To (ms)***	***1/Tc (1/s)***
0 mM	12	0.2 ± 0.1	1.9 ± 0.3	0.2 ± 0.1
2 mM	7	0.92 ± 0.02	5.2 ± 2.5	0.8 ± 0.2

Table 3.4: Absolute values of open probability (P_o), mean open time (T_o) and opening rate (the inverse of mean closed time, T_c) for vehicle (control) in the absence and presence of 2 mM ATP at 100 µM cytosolic [Ca^{2+}].

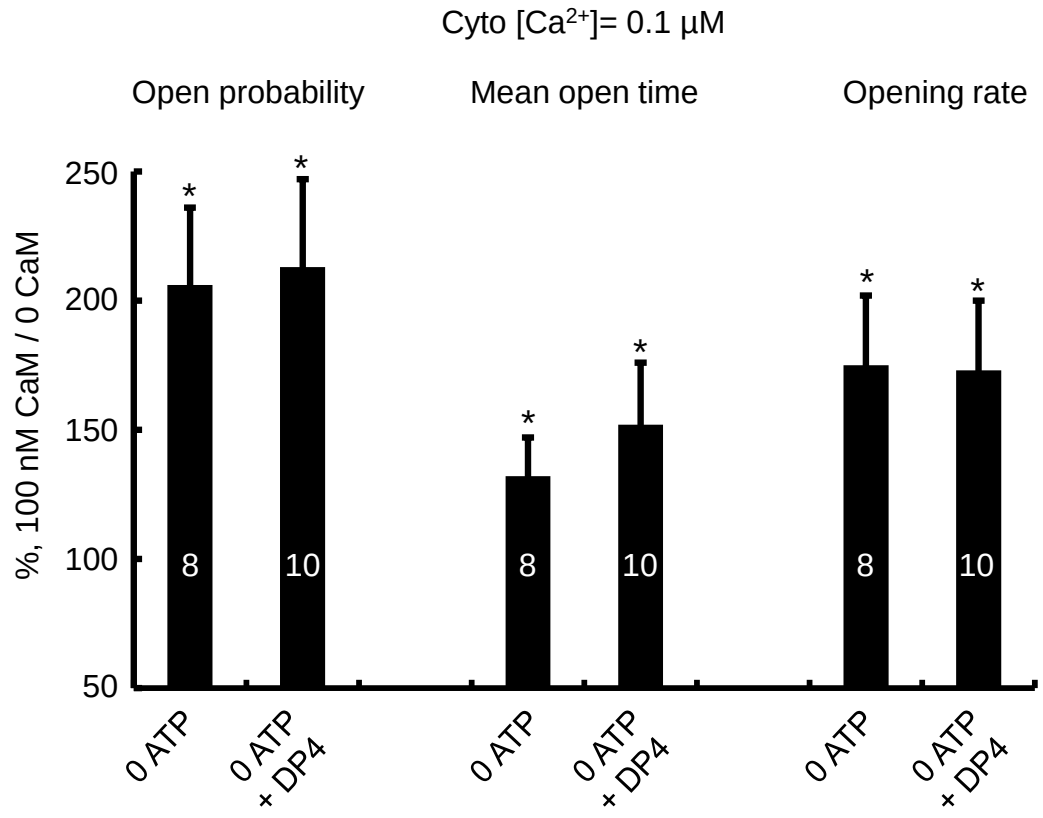

Figure 3.9: Relative activation of open probability (*Po*), mean open time (*To*) and opening rate (the inverse of mean closed time, *Tc*) by 100 nM CaM in the absence and presence of DP4 at low (100 nM) cytoplasmic [Ca^{2+}]. The luminal [Ca^{2+}] is 0.1 mM. Experiments were carried out at +40 mV. Numbers of measurements for each bar are given in the figure labels. The asterisks show values that are significantly different to 100% (* $p<0.05$, **$p<0.01$, mean ± SEM)

Activator	**n**	P_o	T_o *(ms)*	$1/T_c$ *(1/s)*
0 ATP	8	0.05 ± 0.03	0.6 ± 0.1	0.07 ± 0.03
0 ATP + DP4	10	0.11 ± 0.05	0.8 ± 0.1	0.16 ± 0.07

Table 3.5: Absolute values of open probability (P_o), mean open time (T_o) and opening rate (the inverse of mean closed time, T_c) for vehicle (control) in the absence and presence of DP4 at 100 µM cytosolic Ca^{2+}.

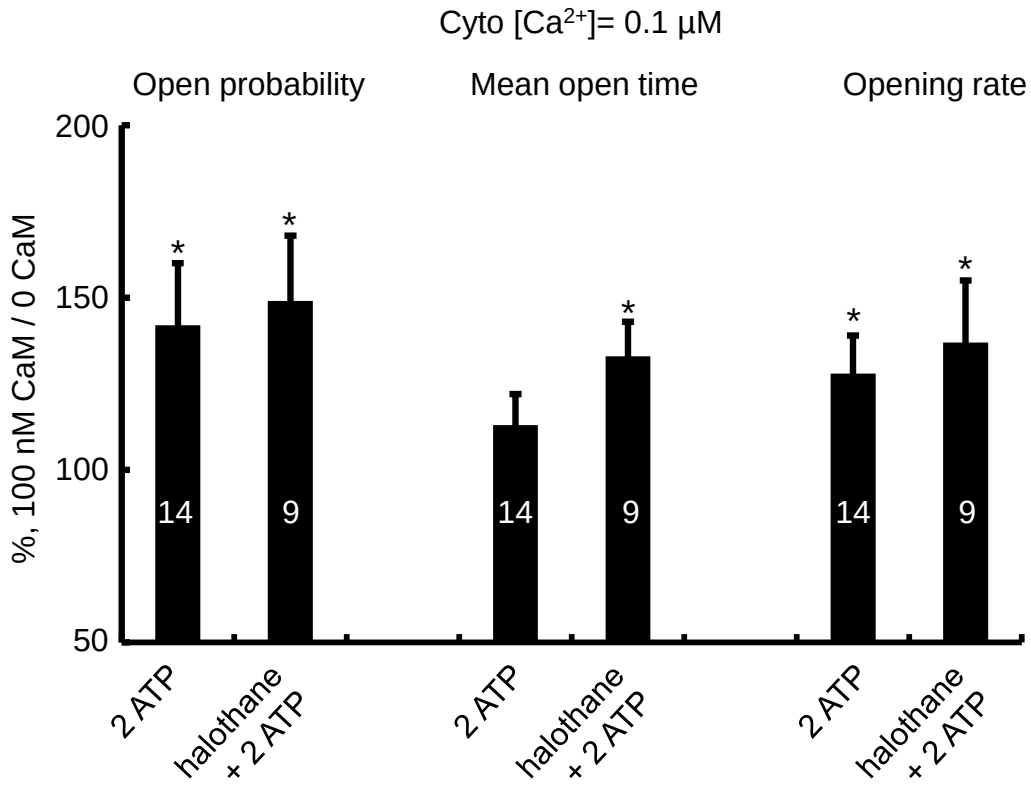

Figure 3.10: Relative activation of open probability (P_o), mean open time (To) and opening rate (the inverse of mean closed time, T_c) by 100 nM CaM in presence of 2 mM ATP and halothane plus 2 mM ATP at low (100 nM) cytoplasmic [Ca^{2+}]. The luminal [Ca^{2+}] is 0.1 mM. Experiments were carried out at +40 mV. Numbers of measurements for each bar are given in the figure label. Theasterisks show values that are significantly different to 100% (* $p<0.05$, mean ± SEM)

Activators	**n**	***P_o***	***T_o (ms)***	***$1/T_c$ (1/ms)***
2 mM ATP	14	0.13 ± 0.1	1.3 ± 0.6	0.2 ± 0.04
2 mM ATP + Halothane	9	0.2 ± 0.04	1.6 ± 0.2	0.1 ± 0.03

Table 3.6: Absolute values of open probability (P_o), mean open time (T_o) and opening rate (the inverse of mean closed time, T_c) for vehicle (control) in the absence and presence of halothane and 100 µM cytosolic Ca^{2+}.

3.4 Discussion

This study presents a detailed, single channel characterisation of CaM regulation of the skeletal ryanodine receptor showing the first investigation of CaM effects on RyR1 regulation by cytoplasmic ATP, luminal Ca^{2+} and cytosolic Mg^{2+} modulation, as well as how CaM interacts with RyR1 activation by halothane and DP4.

The data showed that CaM activated the RyR1 in the presence of 100 nM cytoplasmic [Ca^{2+}] whereas it inhibited the activity when the calcium concentration was increased above 100 nM (**Figure 3.2**). This was consistent with previous findings that conversion of the wt-CaM from an activator (apoCaM) to an inhibitor (Ca^{2+}CaM) required [Ca^{2+}] greater than or equal to 1μM [201]. It was also consistent with the CaM inhibition of RyR1 at nanomolar concentrations of Ca^{2+} seen in single channel recordings [179]. However, their finding that CaM inhibited RyR1 at 56 and 100 μM [179] is not consistent with results here that failed to see any effect of CaM on RyR1s at 10 and 100 μM cytoplasmic Ca^{2+} where the calcium release channel was fully active (**Figure 3.2**). One possible explanation could be due to differences in experimental condition where they used 2mM MgATP instead of 2mM ATP to activate the channel. It is noted that the channel activity in their study is lower than that of this study (open probability of 0.33 compared with 0.92 in this study). Therefore, it is possible that the higher channel activity at 10 and 100 μM cytoplasmic [Ca^{2+}] in my study masked the effects of CaM on the RyR1s.

Increased SR calcium load enhanced the sensitivity of Ca^{2+} release in skeletal muscle to cytosolic calcium [374], and luminal Ca^{2+} increased the activity of RyRs in the presence of cytoplasmic ATP [60, 67, 69]. Luminal Ca^{2+} activation of RyR1s is enhanced at negative membrane voltage allowing the flow of Ca^{2+} ions from the lumen to the cytosolic side of the RyR; this Ca^{2+} flux binds to the cytoplasmic Ca^{2+} activation sites, activating the channel by the so-called *feedthrough mechanism* [60], a mechanism that is strongly voltage sensitive. Findings here showed that CaM effects depended on the luminal [Ca^{2+}] since CaM significantly activated the open probability of the RyR1s at 0 and 100 μM luminal [Ca^{2+}], whereas it inhibited it at 1000 μM luminal [Ca^{2+}] (**Figure 3.5**). The findings that effects of CaM on open time of the channel vary with

cytoplasmic [Ca^{2+}] and show an inhibition in the low µM range (**Figure 3.3**), beggar the question of whether the Ca^{2+} flux from the lumen affects the CaM regulation. Such a mechanism would be expected to produce voltage-dependent CaM effects on luminal regulation of RyR1s, effects that are clearly absent in the data (**Figure 3.5**). However, given the widely spaced samples of luminal Ca^{2+} and membrane voltage, it is possible that the Ca^{2+} feedthrough did not produce local cytoplasmic Ca^{2+} in the low µM range where it would alter CaM regulation relative to low luminal Ca^{2+}. CaM activation was inhibited by physiological concentrations of Mg^{2+} in [^{3}H]-ryanodine binding (ref). However, findings here indicate that CaM does not alter Mg^{2+} sensitivity of RyR1s at 100 nM cytosolic [Ca^{2+}]. Since CaM activates RyR1s under resting condition, it might be suggested from these data that CaM still activates the channel even in the presence of strong Mg^{2+} inhibition in skeletal myocytes.

Fruen et al. (2000) reported the extent of CaM activation was dependent on adenine nucleotide [177]. When AMP-PCP was absent, CaM activation of normal skeletal muscle SR vesicle [^{3}H]-ryanodine binding was less than 5% of maximum [177]. However, CaM activated [^{3}H]-ryanodine binding by 150% of maximal activation when 3mM AMP-PCP was added [177]. In contrast, this study demonstrated that CaM activation of RyR1 is independent of ATP concentration since CaM equally activated the channels in the absence and presence of 2 mM ATP (**Figure 3.7**). This discrepancy might be explained by the very low level of [^{3}H]-ryanodine binding levels in the absence of AMPCP in their experiments since it might not have been possible to detect the accurate CaM activation from background [^{3}H]-ryanodine-binding levels under those conditions.

A domain interaction hypothesis proposes that the interactions between the RyR1 N-terminal and the central domain are involved in Ca^{2+} regulation, serving as a "domain switch" to turn the channel on or off [243, 309-311]. In the resting state, it is a thought there is a close contact between the N-terminal and the central domain at several subdomains (domain zipping) for stabilising and maintaining the closed state of Ca^{2+} channels. T-tubule depolarization or chemical agonists stimulate and open the RyR channel by causing unzipping of the domain switch. In cardiac muscle, CaM binding to RyR2s enhanced the zipped state and inhibited RyR2 leak by suppressing DPc10 access

[375]. However, to date nothing is known about the CaM effect on the zipped sate of RyR1s in skeletal muscle. This study showed that CaM equally activated the channel both in the absence and presence of DP4. Therefore, it could be suggested that CaM activation of the RyR1 is independent of the unzipping effect of DP4. Similarly, it could be argued from the data presented here, that the effects of CaM also work independently from channel activation by halothane .

In summary, the data demonstrated that CaM regulates the gating of the RyR1 by altering the sensitivity of cytosolic and luminal [Ca^{2+}] without changing the sensitivity of cytosolic [Mg^{2+}] and ATP. In addition, CaM activation of the RyR1 was independent of the channel unzipping effect of DP4 and the activation by halothane.

Chapter 4
The essential role of calmodulin in RyR inhibition (RyR1 and RyR2) by dantrolene

4.1 Introduction

Dantrolene is a well-known inhibitor of Ca^{2+} release in skeletal muscle [376] that has been used clinically as a treatment for malignant hyperthermia (MH). MH is a potentially fatal, inherited disorder of skeletal muscle in which mutations in the proteins involved in excitation-contraction coupling (e.g. RyR1 and L-type Ca^{2+} Channel) [295, 377, 378] causes uncontrolled SR calcium release and muscle contracture in the presence of volatile anesthetics. Notably, mutations in the cardiac RyR isoform (RyR2) that correspond to the MH mutations in RyR1 cause catecholaminergic, polymorphic ventricular tachycardia (CPVT) [259]. Recent *in vitro* and animal studies suggest that dantrolene has antiarrhythmic effects on CPVT and possibly also on heart failure [283, 323, 378, 379].

Dantrolene acts on skeletal and cardiac muscle by inhibiting Ca^{2+} release from the SR [244, 313, 376]. Assays of Ca^{2+} release in intact myocytes and cell homogenates containing SR vesicles [280] suggest that dantrolene inhibits the SR Ca^{2+} release channel with a half-inhibiting concentration (IC_{50}) of 0.3 μM [283]. Even though a dantrolene binding site has been identified in the DP1 regions in RyR1 and RyR2s [283, 287-289], there has been only one direct observation of RyR inhibition by dantrolene in bilayer-based single channel recordings [380]. Studies since then have not found any effect by dantrolene in single channel recordings of RyR2s [292, 300, 304, 381]. Hence, it is not clear if dantrolene acts directly on the RyR2 or some other proteins, such as the DHPR, become involved in the excitation-contraction coupling [382, 383].

Calmodulin (CaM) is known to regulate the activity of RyR1 and RyR2 [384, 385]. CaM inhibits RyR2 directly by binding to residues 3583-3603 of each RyR2 subunit [386] with high affinity (K_d = 30-100 nM) [387]. By contrast, mutant CaMs (CPVT-CaMs) are implicated in channel regulation of the RyR2 and Hwang et al. (2014) recently reported that the (CPVT-CaM) N98S mutant failed to inhibit RyR2 channels like wild-type CaM and the (CPVT-CaM) N54I mutant even caused their activation [251]. In RyR1, wild-type CaM may either increase channel activity at resting cytoplasmic [Ca^{2+}] or decrease activity at higher [Ca^{2+}] [385]. Fruen and colleagues

[280, 291] found that dantrolene reduced the effect of RyR1 activators (but interestingly, not in RyR2) including CaM, suggesting that CaM might augment dantrolene inhibition of RyR1s. During the process of RyR2 isolation from the heart and their incorporation into artificial lipid bilayers, the RyR macromolecular complex stays mostly intact [36] with the exception of CaM which is reported to dissociate from the RyR complex with a time constant of less than 1 min [387]. Hence, bilayer-based channel studies would generally have been made devoid of this important regulatory molecule in the RyR complex, whereas CaM is abundant in intact cells and cell homogenates. Therefore, it was hypothesized here that the absence of CaM in bilayer experiments provided an explanation as to why dantrolene inhibition has not been observed in most single channel RyR recording experiments. This hypothesis was tested here by examining the effects of dantrolene, in the absence and presence of exogenous CaM, on the gating of RyR1 and RyR2s incorporated into artificial lipid bilayers. These results were compared with whole cell studies from the Knollmann group (collaborators at Vanderbilt University) who measured the frequency and amplitude of Ca^{2+} waves in permeablized cardiomyocytes. This chapter is transformed from my paper, Oo et al., published in Molecular Pharmacology Journal in 2015 [388].

4.2 Materials and Methods

4.2.1 Single channelrecordings

SR vesicles containing RyR1s were isolated from rabbit skeletal muscle and RyR2s were isolated from sheep hearts [371] and from healthy and failing human hearts [389]. Individual readings of dantrolene inhibition were derived from recordings of control RyR activity measured for 1 minute, followed by 1 minute exposure to dantrolene followed by 1 minute washout - all done in the absence and presence of exogenous 100 nM CaM. CaM regulation was also measured in a similar way. At -40 mV, the channel activities are higher compared with the correspondent activities measured at + 40 mV. Therefore, low-activity RyR2 sheep channels were measured at -40 mV whereas, high-activity RyR1 skeletal channels were measured at + 40 mV in order to obtain reasonable expanses of channel activity for accurate analysis. Further details of single channel recording methods are given in **Chapter 2**.

4.2.2 Ca^{2+} wave experiments in ventricular myocytes

Single ventricular myocytes from 12-16-week-old C57Bl/6 mice were isolated using an enzymatic digestion method as previously described [246]. Myocytes were first exposed to a Ca^{2+}-free relaxing solution and then permeabilized with saponin (40 μg/mL) for 60 s and placed in an internal solution composed (in mM) of: 120 K-aspartate, 15 KCl, 5 KH_2PO_4, 0.75 $MgCl_2$, 4% dextran (40,000), 10 HEPES, 5 Mg_2ATP, 10 glutathione (reduced), 0.025 Fluo-4 and 10 phosphocreatine (di-Na). The solutions also contained 10 U/ml creatine phosphokinase [251] and had free [Ca^{2+}] = 120 nM. To allow a complete removal of CaM binding to the RyR2 in permeabilized myocytes [390], all Ca^{2+} wave recordings were done after a 30 minute incubation with dantrolene alone or dantrolene plus CaM. Free CaM was kept at the physiological concentration of 100 nM. Ca^{2+} waves in myocytes were imaged with a confocal microscope (LSM 510 Zeiss) in line scan mode. Ca^{2+} wave analysis was performed as described [251]. Given the variability between different experimental days, the Ca^{2+} wave frequency and amplitude data were normalised to the mean of vehicle group obtained on the same day.

4.2.3 Statistics

Average data are presented as the arithmetic mean standard error of the mean (SEM). The statistical significance of difference was tested using Student's *t* test on normal distributions.

4.3 Results

4.3.1 The essential role of CaM on RyR1 and RyR2 inhibition by dantrolene

To investigate whether CaM binding to RyR1s and RyR2s is a prerequisite for their inhibition by dantrolene, RyR activity was measured in the presence of 100 nM cytoplasmic Ca^{2+} plus 2 mM ATP (vehicle) for periods of 1 minute and then during 1 minute exposure to added dantrolene, and again after dantrolene washout. This sequence was repeated in the absence and presence of exogenous 100 nM CaM as shown in **fFigure 4.1** for rabbit RyR1 (left panel) and for sheep RyR2 (right panel). In the absence of CaM, dantrolene had no observable effect on the channel open probability (P_o) of either RyR1 or RyR2 receptors. However, when CaM was present in the experimental solutions, dantrolene reduced the P_o of both RyR isoforms. This effect of dantrolene on RyR1 and RyR2 was reversible upon dantrolene washout and inhibition could be seen during multiple applications (**Figure 4.2**). The data summary from application-washout experiments in **Figure 4.3** shows that dantrolene at 10 - 50 μM inhibited RyR1 and RyR2 activity by ~ 50% compared to vehicle alone. When CaM was subsequently washed out by perfusion with CaM-free solutions for 1 minute, dantrolene inhibition was abolished (RyR2 open probability 95 ± 9 % of vehicle, p = 0.24 and RyR1 open probability 94 ± 6 % of vehicle, p = 0.63). These data clearly indicate that dantrolene inhibition of RyR1 and RyR2 required the presence of CaM.

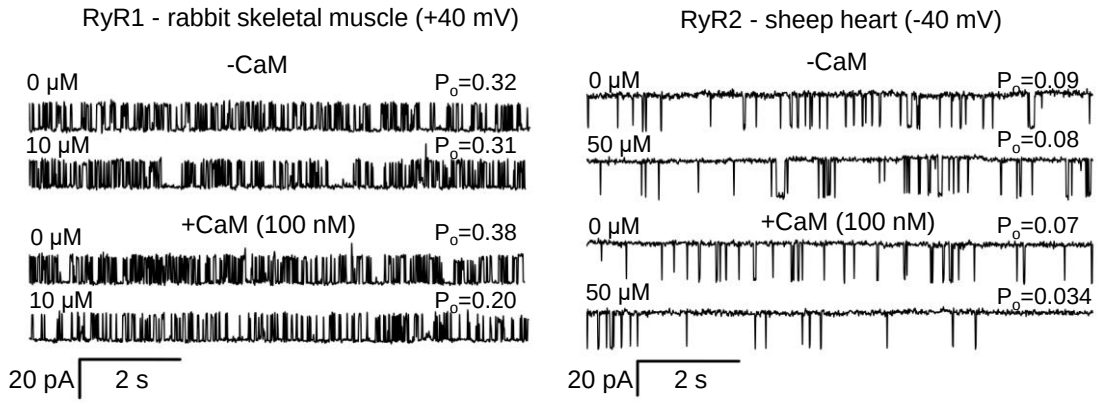

Figure 4.1: Dantrolene inhibited RyR1 and RyR2 only in the presence of CaM.

Left panel: Representative 10 s segments of RyR1 activity from rabbit skeletal muscle illustrating the inhibitory effect of 10 µM dantrolene in the absence (-CaM) and presence (+CaM) of 100 nM CaM. Experiments were recorded at +40 mV where upward current jumps represent channel openings.

Right panel: Corresponding activity of RyR2s showing inhibition by 50 µM dantrolene. Experiments were recorded at -40 mV where downward current jumps represent channel openings. The luminal [Ca^{2+}] was 0.1 mM and the cytoplasmic bath contained 2 mM ATP and 100 nM Ca^{2+}.

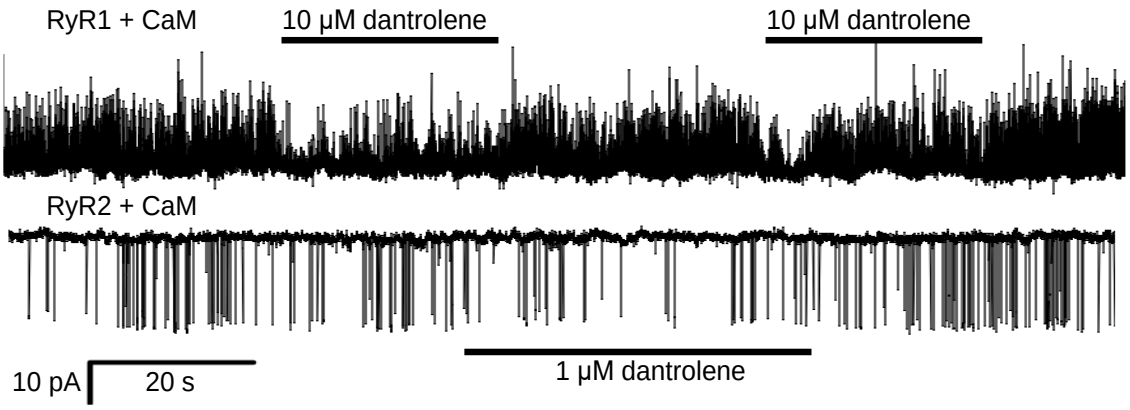

Figure 4.2: Dantrolene inhibition of RyR1 and RyR2 in the presence of CaM. Recordings of 140 s periods of RyR1 and RyR2 activity during dantrolene application (bars) and washout. Upper trace: RyR1 activity showing inhibition by 10 µM dantrolene . Experiments were recorded at +40 mV where upward current jumps represent the channel openings. Lower trace: corresponding activity of RyR2 showing inhibition by 1 µM dantrolene. Experiments were recordedat -40 mV where downward current jumps represent channel openings. The luminal [Ca^{2+}] was 0.1 mM and the cytoplasmic bath contained 2 mM ATP and 100 nM Ca^{2+}.

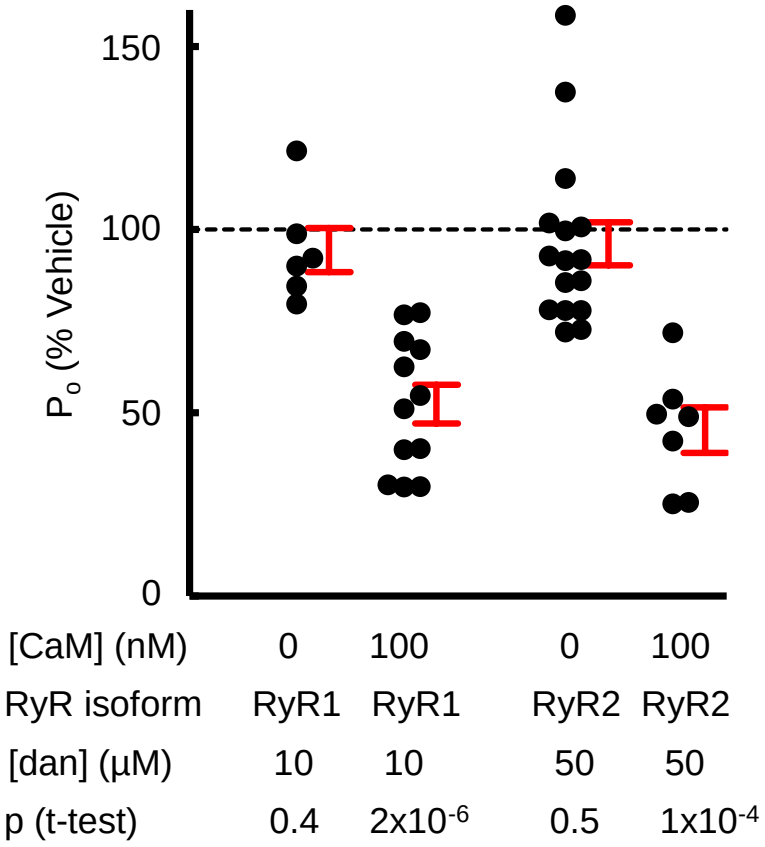

Figure 4.3: Relative inhibition of RyR1s by 10 μM dantrolene and RyR2s by 50 μM dantrolene. Each sample represents the RyR P_o in the presence of dantrolene relative to the mean P_o bracketing periods in the absence of dantrolene. Experiments were recorded at +40 mV for RyR1s and -40 mV for RyR2s. The luminal [Ca^{2+}] was 0.1 mM and the cytoplasmic bath contained 2 mM ATP and 100 nM Ca^{2+}. SEM is indicated by the vertical bars; *p*-values indicate significant difference of the mean from 100%.

4.3.2 Effect of dantrolene on Ca^{2+} waves in mouse cardiomyocytes

The amplitude and frequency of spontaneous Ca^{2+} waves -two parameters that have been implicated as independent predictors of arrhythmogenicity [391] - were measured in mouse ventricular myocytes. Examples of the effect of 30 minutes exposure to dantrolene (3, 10, 50 µM) on Ca^{2+} waves recorded in the presence or absence of CaM are presented in **Figure 4.4**. Dantrolene reduced Ca^{2+} wave amplitude (**Figure 4.5**) and frequency (**Figure 4.6**) in the presence of CaM but had no effect in the absence of CaM [388].

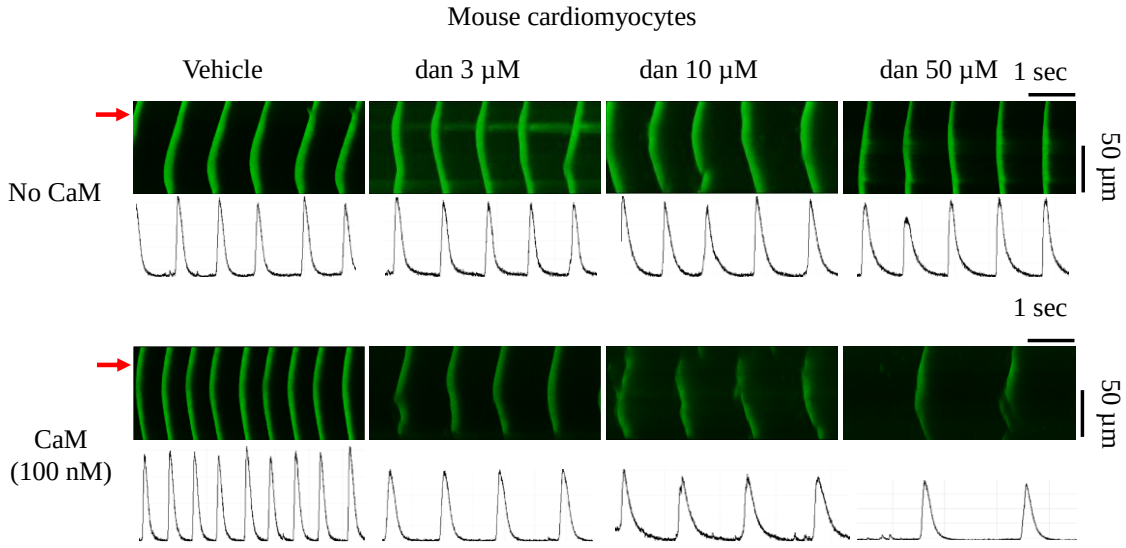

Figure 4.4: Dantrolene reduced spontaneous Ca^{2+} wave frequency and amplitude only in the presence of CaM [388]. The presence of CaM is required for dantrolene action on arrhythmogenic Ca^{2+} waves in cardiomyocytes. The images show representative confocal microscope line scans from permeabilised mouse ventricular myocytes after a 30minute incubation with either dantrolene alone or dantrolene + CaM (100 nM). The red arrows indicate the location of the line-scans plotted below each confocal image.

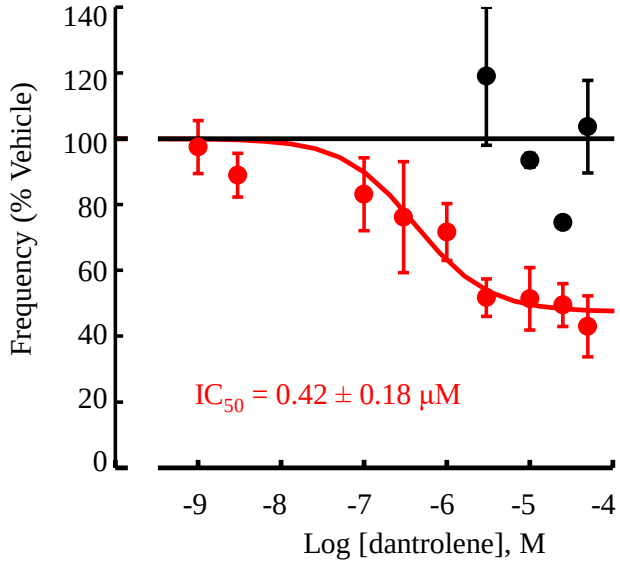

Figure 4.5: Concentration response curves for Ca^{2+} wave frequency relative to vehicle in the absence (black ●) or presence (red ●) of CaM 100 nM. The solid curves show the Hill fit to the data using the equation in the caption to **Figure 6.1**. IC_{50} = 0.42 ± 0.18 µM and E_{max} = 47 ± 4%.

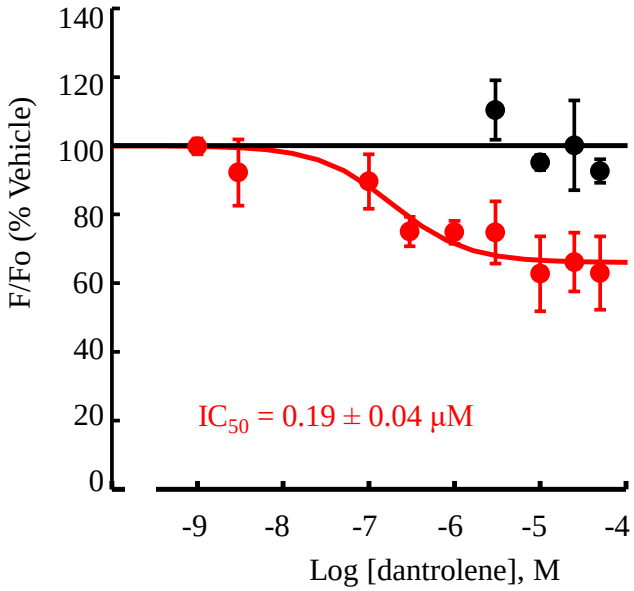

Figure 4.6: Concentration response curves for Ca^{2+} wave amplitude relative to vehicle in the absence (black ●) or presence (red ●) of CaM 100 nM. The solid curves show the Hill fit to the data using the equation in the caption to **Figure 3.4**. IC_{50} = 0.19 ± 0.04 µM and E_{max} = 66 ± 2%.

4.3.3 Dantrolene inhibition can be mediated by CaM mutants

Since both dantrolene and CaM are RyR2 inhibitors, the possibility that dantrolene acts by amplifying CaM inhibitory action on RyR2 was investigated. To test this possibility, dantrolene inhibition of sheep RyR2 in the presence of 100 nM wt-, N54I- and N98S-CaM and skeletal RyR1 in the presence of 100 nM wt-CaM were measured. As shown in **fFigure 4.7**, N54I increased RyR2 P_o (the opposite effect to wt-CaM) whereas N98S-CaM has no inhibitory effect on RyR2 [251]. It is also shown in **Figure 4.7** that the addition of wt-CaM to RyR1s caused channel activation in accordance with previous findings [385]. If dantrolene merely amplifies the action of CaM, then one would expect dantrolene to be an activator in the presence of N54I-CaM for RyR2s and in the presence of wt-CaM for RyR1s. This was not the case. Dantrolene had the same inhibitory action in the presence of wt-CaM, N54I- and N98S-CaM for both the RyR1 and the RyR2 (**Figure 4.8**).

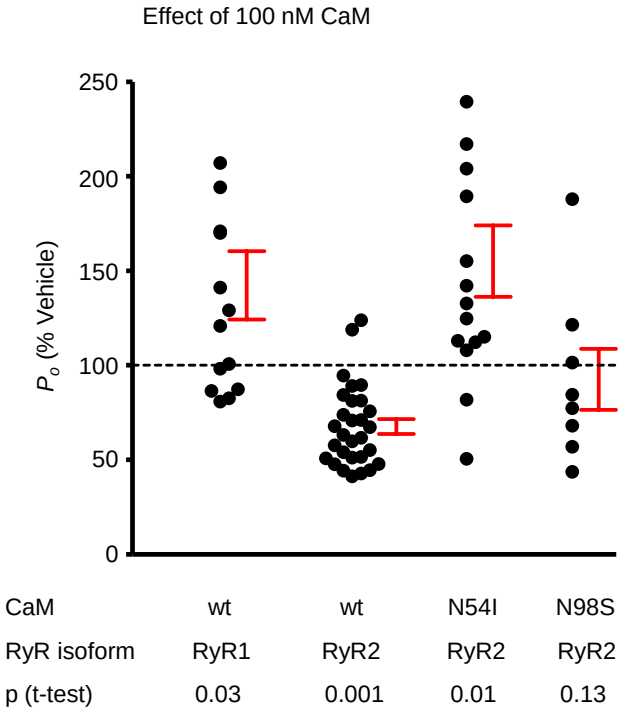

Figure 4.7: Relative effect of wt-CaM (100 nM) on the open probability of RyR1s and RyR2s, plus N54I- and N98S-CaM on RyR2s. Each sample represents the RyR P_o in the presence of CaM relative to the mean P_o in the absence of CaM. Experiments were recorded at +40 mV for RyR1s and -40 mV for RyR2s. The luminal [Ca^{2+}] was 0.1 mM and the cytoplasmic bath contained 2 mM ATP and 100 nM Ca^{2+}. The vertical bars indicate SEM.

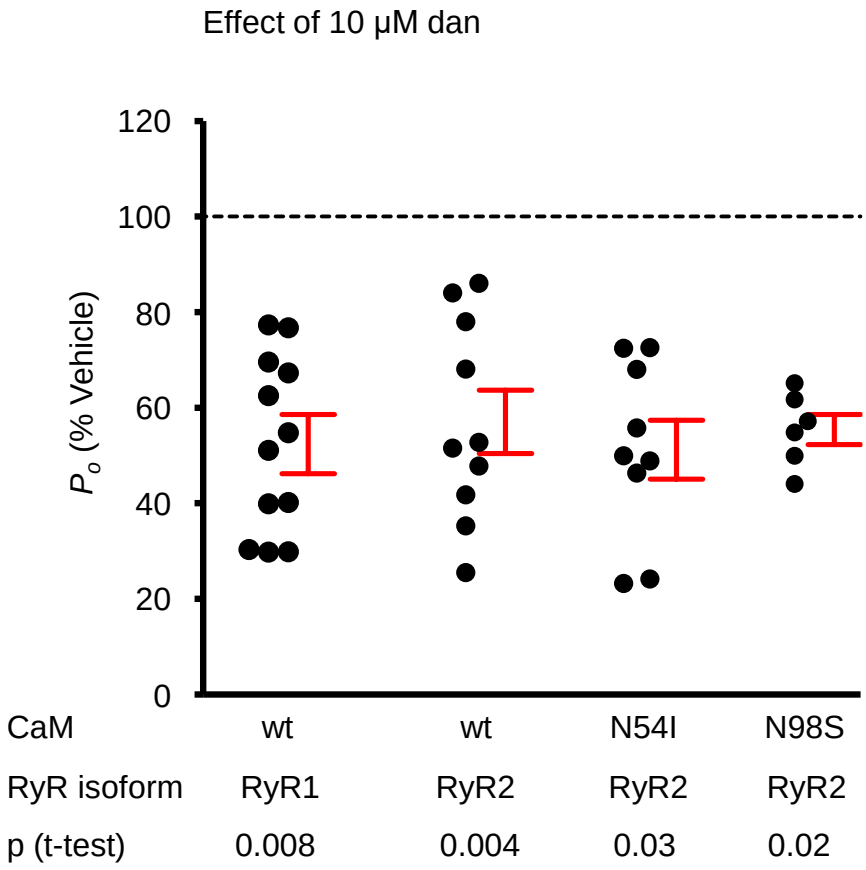

Figure 4.8: Relative effect of 10 µM dantrolene on open probability of RyRs1 and RyR2s in the presence of wt and mutant CaMs. Each sample represents the RyR P_o in the presence of dantrolene relative to the mean P_o in the absence of dantrolene. Experiments were recorded at +40 mV for RyR1s and -40 mV for RyR2s. The luminal [Ca^{2+}] was 0.1 mM and the cytoplasmic bath contained 2 mM ATP and 100 nM Ca^{2+}. SEM is indicated by the vertical bars.

4.3.4 Effect of Dantrolene on RyR2 from healthy and failing human heart

It was found here that RyR2s from apparently healthy sheep hearts were significantly inhibited by dantrolene. However, previous studies have reported that dantrolene restores normal Ca^{2+} handling in cardiomyocytes in pathological states (e.g. heart failure and congenital arrhythmias) but has no significant effect on Ca^{2+} release under physiological conditions in human, rabbit and mouse hearts [283, 323, 378, 379]. To explore this possible inconsistency the effect of dantrolene on RyR2 from healthy and failing human hearts in the presence of 100 nM CaM was measured (**Figure 4.9**). Dantrolene (10 µM) had no effect on RyR2s isolated from two healthy hearts but it caused a significant reduction in P_o of RyR2 from a human heart with ischemic cardiomyopathy. This indicated that the effect of dantrolene depended both on species (human *vs.* sheep) and on the pathological state of the heart (healthy *vs.* failing).

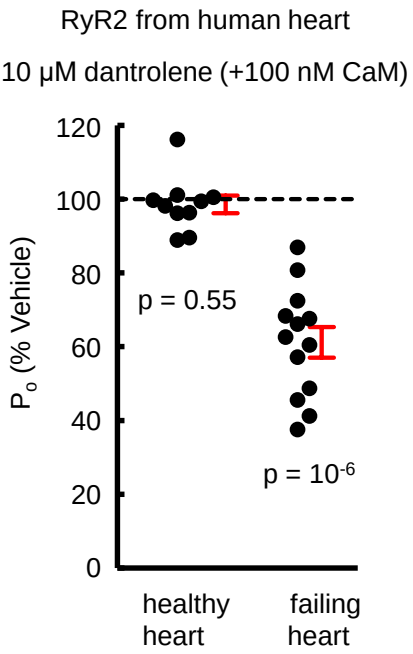

Figure 4.9: Dantrolene inhibition of human RyR2 differs in human and failing hearts;. the relative inhibition of human RyR2 by 10 µM dantrolene. Samples were taken from two healthy hearts and one failing heart with ischemic cardiomyopathy. Details of each heart are given in **Table 2.1** (page ??). The luminal [Ca^{2+}] was 0.1 mM and the cytoplasmic bath contained 2 mM ATP and 100 nM Ca^{2+}. Mean values and SEM are indicated by the red bars; *p*-values indicate significant difference of the mean from 100%.

4.4 Discussion

This study presents the first demonstration of dantrolene inhibition of mammalian RyR1 and RyR2 single channel recordings along with experiments using permeabilised cardiomyocytes showing that CaM was essential for dantrolene inhibition. The finding that a physiological concentration of CaM (100 nM) is required for dantrolene inhibition of RyRs provided an answer to the long-standing question of why dantrolene, an inhibitor of SR Ca^{2+} release, had no effect on the activity of mammalian RyR1 and RyR2 in previous single channel studies [292, 304, 381]. Since CaM readily dissociates from the RyR complex [387], CaM would have been absent during those experiments.

^{3}[H]-ryanodine binding assays have demonstrated a reduction of CaM activation of purified pig RyR1 by dantrolene [280], consistent with CaM mediated dantrolene inhibition of these channels. However, a single channel bilayer study [300] using similar experimental conditions (100 nM cytoplasmic Ca^{2+} at 35ºC), reported no inhibition by dantrolene (20 μM) of purified rabbit RyR1 channels in the presence of exogenous FKBP12 and CaM. These results suggest that the inhibitory effect of dantrolene on RyRs seen here not only requires CaM, but also other RyR-associated proteins that are present in native preparations but presumably absent in some purified RyR preparations.

The means by which CaM facilitates dantrolene inhibition is not yet clear. By measuring dantrolene inhibition in the presence of CaM mutants that activate RyR2s, it was shown here that dantrolene does not merely increase the efficacy of CaM, but is an inhibitor in its own right (**Figures 4.7 and 4.8**). Also, given the redox buffering of our experimental solutions (4mM GSH in bilayer experiments and 10 mM GSH in myocyte experiments), it is unlikely that the reducing properties of dantrolene underlie its inhibition. An alternative possibility is that CaM is a part of the pathway that transduces dantrolene binding into RyR inhibition. Several studies presented evidence that dantrolene modulated inter-domain interactions in RyR1s [313] and RyR2s [244, 283, 323, 392] between the N-terminal (residues 1-619), central (residues 2000-2500) and C-terminal domains (3900-end). Our data are consistent with both these possibilities.

The finding here was that dantrolene inhibition, in the presence of CaM, is species dependent. The data clearly demonstrated Dantrolene inhibition in RyR2 from healthy hearts from sheep (**Figures 4.1-4.3**), mouse (**Figures 4.4-4.6**) but not from human

(**Figure 4.9**). Our finding that dantrolene inhibited RyR2 from failing human heart but had no effect on RyR2 from healthy human heart (**Figure 4.9**), indicated that RyR2 inhibition by dantrolene depended on properties of the RyR macromolecular complex that are yet to be identified.

In conclusion, the data show that CaM binding to the RyR is required in order to produce dantrolene inhibition in both RyR1s and RyR2s. It is likely that other as yet undefined factors, also play a similar role in facilitating dantrolene inhibition.

Chapter 5

Inhibitory effects of dantrolene on skeletal ryanodine receptor

5.1 Introduction

Dantrolene is a muscle relaxant that has been used clinically in the treatment of malignant hyperthermia (MH) for several decades [308]. Dantrolene inhibits SR Ca^{2+} release but the precise molecular mechanism of dantrolene for this has been difficult to define because dantrolene inhibition of the SR Ca^{2+} release channel (RyR1) has not been detected in single channel recordings. **Chapter 3** showed that dantrolene inhibition of RyR1 requires the co-protein, calmodulin (CaM) to be bound to the RyR which was usually absent in single channel recording experiments on isolated channels because it readily dissociates from RyRs [388]. Here, single channel recordings of RyR1 isolated from rabbit skeletal muscle and incorporated into artificial lipid bilayers were made in the presence of exogenous CaM, demonstrating the first characterization of dantrolene inhibition of RyR1.

The ion transport properties of RyR1 are physiologically regulated by endogenous ligands such as Ca^{2+}, Mg^{2+} and ATP in both the cytoplasm and SR lumen [353]. The RyR1 is activated by cytoplasmic Ca^{2+} at ~1 μM and inhibited at ~1 mM [72]. It is also activated by Ca^{2+} in the SR lumen [363] and this activation is markedly increased by the MH mutation R615C in RyR1s when expressed in HEK cells [369]. Cytoplasmic Mg^{2+} inhibits the RyR1 by competing with Ca^{2+} for cytoplasmic activation sites [18, 364] and by binding to the Ca^{2+} inhibition sites [20]. Single channel recordings show the R615C mutation shifts the Mg^{2+} inhibition response to higher concentrations [281], thus reducing RyR1 sensitivity to Mg^{2+}. This is consistent with a loss of Mg^{2+} sensitivity of

SR calcium release in MH-susceptible muscle fibres [393]. Although dantrolene has been seen to restore normal Mg^{2+} sensitivity to MH-susceptible muscle fibres for SR Ca^{2+} release, single channel experiments have not yet been performed to confirm that this is due to a restoration of Mg sensitivity in RyR1 [22, 393]. ATP activates RyR1 with a K_a of ~0.36 mM [62] and it has been shown to enhance the inhibitory effect of dantrolene on skinned muscle fibres [325]. As yet, it is not known how dantrolene affects RyR1 activity in the presence of various physiological ligands. In this study,the effects of Ca^{2+}, Mg^{2+} and ATP on dantrolene inhibition of RyR1 were investigated.

RyR1 can be activated by exogenous substances such as volatile anaesthetics [369] or by peptides that disrupt inter-domain interactions in the RyR1 molecule. Volatile anesthetics such as halothane can trigger MH in susceptible individuals [365, 366] by activating SR calcium release [279] and by increasing store operated Ca^{2+} entry (SOCE) in skeletal muscle [394]. Many MH mutations in the RyR1 are thought to act by destablising domain-domain interactions in the RyR1 molecule. The synthetic peptide, DP4, corresponds to amino acids 2442-2477 of the RyR1 and it is thought to destabilise inter-domain interactions within RyR1s by displacing the corresponding RyR1 domain, thus producing an MH-like condition [309, 311]. DP4 induces SR calcium release in skinned muscle fibres [309] and increases the RyR1 activity in single channel recordings [370]. However, the mechanisms for the beneficial action of dantrolene on RyR1s with destablised domains, or RyR1s activated by halothane, have not been investigated using single channel recordings. This chapter describes investigations into the effects of dantrolene on RyR1 activity in the presence of halothane and DP4.

5.2 Materials and Methods

5.2.1 Single Channel Recordings

RyRs were isolated from a rabbit skeletal muscle [371] and incorporated in artificial bilayer membranes and channel gating was measured at 40 mV by single channel recordings. Single channel recordings of open probability, mean open time and mean closed time were measured using a threshold discriminator at 50% of channel amplitude (Channel3 software by NW Laver). Dantrolene was added and removed from the RyR1s by using a local perfusion method (**fFigure 2.4)**. Measurements were carried out with the *cis* solution voltage-clamped at +40 mV unless otherwise specified.

5.2.2 Statistics

Average data were presented as arithmetic mean standard error of the mean (SEM). The statistical significance of difference was tested using Student's *t* test on normal distributions. Asterisks indicate significantly different to 100% (* $p<0.05$, **$p<0.01$). One way ANOVA was used to determine whether there are any significant differences between the means of three groups.

5.3 Results

5.3.1 Dantrolene dose response curve of skeletal ryanodine receptors in the presence of exogenous CaM

Measurements of the relative dantrolene inhibition of RyR1s in cytoplasmic (vehicle) solutions containing 100 nM Ca^{2+}, 2 mM ATP and 100 nM CaM as shown in **Figure 5.1**. RyR1 activity was measured during 1 minute exposure to vehicle solutions, then during 1 minute exposure to solutions containing dantrolene and again for 1 minute to vehicle. Dantrolene inhibition was determined from the P_o during dantrolene exposure relative to the mean RyR1 activity during bracketing exposures to vehicle only. Dantrolene inhibition was readily observed at concentrations as low as 0.2 μM but not detectable at 0.03 μM (**Figure 5.2**). The dantrolene concentration-dependence RyR1 P_o is shown in **Figure 5.3**. Dantrolene inhibition of RyR1s exhibited a hyperbolic dependence on concentration (sigmoidal on the log-concentration plot). Hill fits to the data gave an IC_{50} of 0.20 ± 0.02 μM, a Hill coefficient of ~1.0 ± 0.2 and a maximal inhibition (E_{max}) of 50 ± 2%.

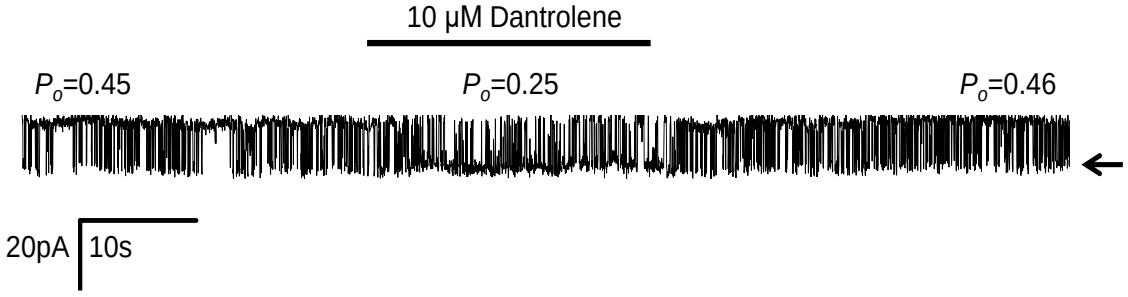

Figure 5.1: Representative 90 s segment of RyR1 activity from a rabbit skeletal muscle in the presence of 100 nM CaM showing the inhibitory effect of 10 μM dantrolene (horizontal bar). The luminal [Ca^{2+}] was 0.1 mM and the cytoplasmic bath contained 2 mM ATP and 100 nM Ca^{2+}. Experiments were recorded at +40 mV and upward current jumps represent the channel openings. The rrow shows the recording baseline.

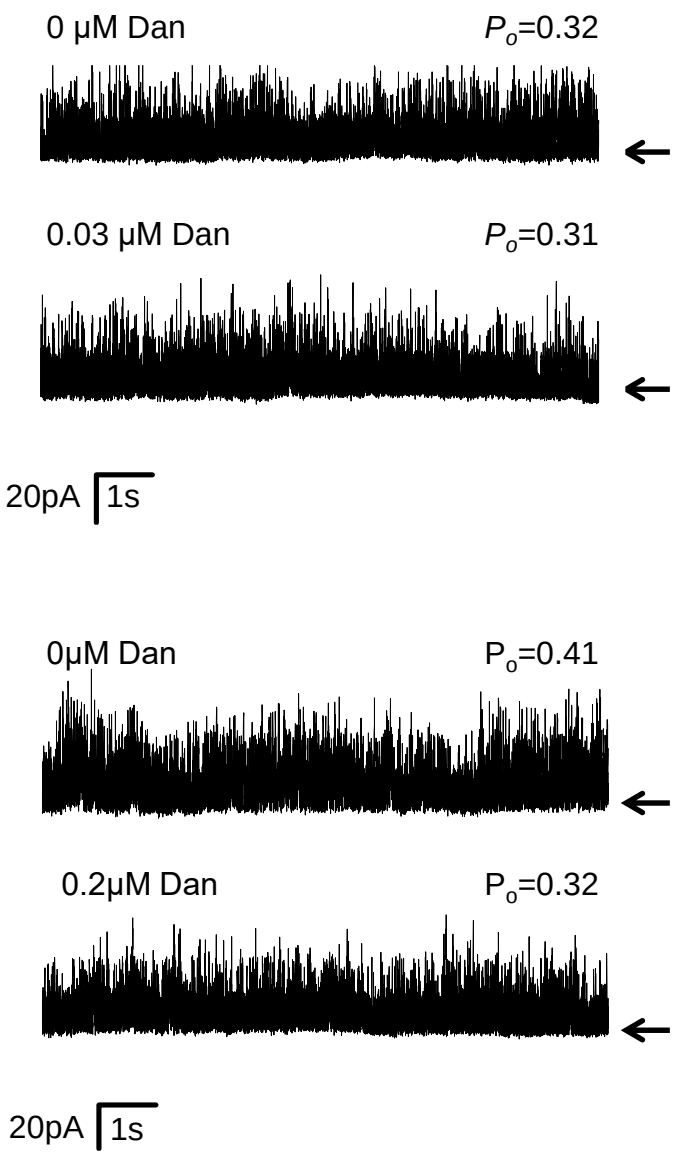

Figure 5.2: Representative 10 s segments of RyR1 activity showing the inhibitory action of two different concentrations of dantrolene (Dan). Experiments were recorded at +40 mV and upward current jumps represent the channel openings. The luminal [Ca^{2+}] was 0.1 mM and the cytoplasmic bath contained 2 mM ATP and 100 nM Ca^{2+}. The arrows show the baseline of the recordings.

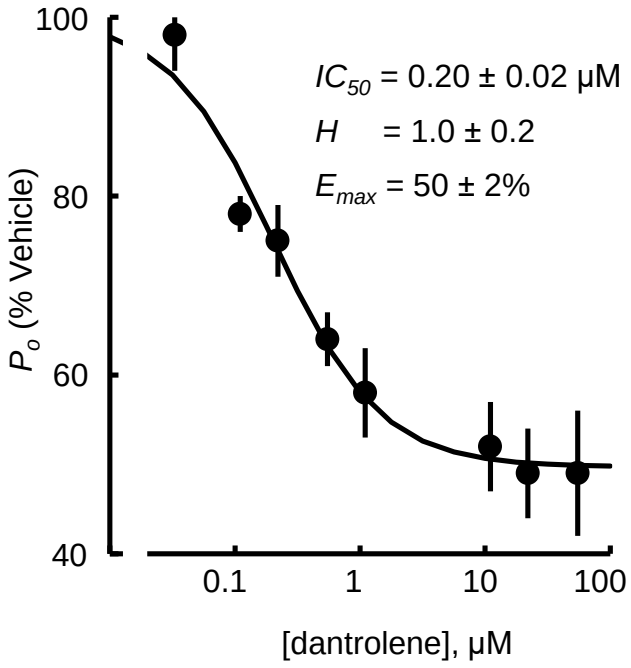

Figure 5.3: Concentration-dependence of dantrolene inhibition of RyR1 in presence of 100 nM CaM (mean ± SEM, n= 7 to 20). The luminal [Ca^{2+}] was 0.1 mM and the cytoplasmic bath contained 2 mM ATP and 100 nM Ca^{2+}. The curve shows the Hill fit to the data using the equation:

$$Po = \{1 + E_{max}\,([dantrolene]/IC_{50})^{H}\}/\{1 + ([dantrolene]/IC_{50})^{H}\}$$

5.3.2 Dantrolene inhibition of RyR1 depends on cytoplasmic Ca^{2+} concentration

The RyR1 exhibited a characteristic bell-shaped dependence on cytoplasmic Ca^{2+} which is shown in the presence of 2 mM ATP without exogenous CaM in **Figure 5.4**. The data were fitted with Hill curves with an activation EC_{50} of 1.7 ± 0.4 μM (H_a= 1.3 ± 0.2) and an inactivation IC_{50} of 0.22 ± 0.01 mM (H_i= 2.7 ± 0.5). At intermediate concentrations of 10-100 μM, the RyR1 P_o attained a maximal activation of 0.93 ± 0.04. At sub μM Ca^{2+}, the RyR1 did not fully deactivate and had a mean P_o (P_{min}) of 0.04 ± 0.03. The maximal dantrolene inhibition over a range of cytoplasmic [Ca^{2+}] using 10 μM dantrolene is shown in **Figures 5.4** and **5.6,** with example recordings shown in **Figure 5.5**. Dantrolene reduced the open probability of the RyR1s to ~50 % of control (*i.e.* vehicle alone) at cytoplasmic [Ca^{2+}] ≤1 μM and >0.2 mM but had no significant effect at intermediate [Ca^{2+}] of 10-100 μM, similar to that of CaM (**Figure 5.6**).

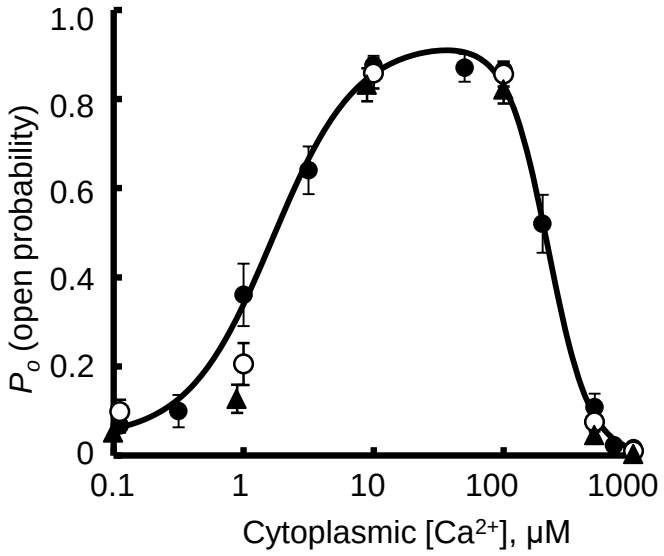

Figure 5.4: Cytoplasmic [Ca^{2+}] dependence of the RyR1 P_o in the presence of 0.1 mM luminal Ca^{2+} and cytoplasmic ATP (2 mM) (●, n= 7 to 18), and in the presence of 100 nM CaM (○, n= 7 to 13), and CaM plus 10 μM dantrolene (▲, n= 8 to 16).

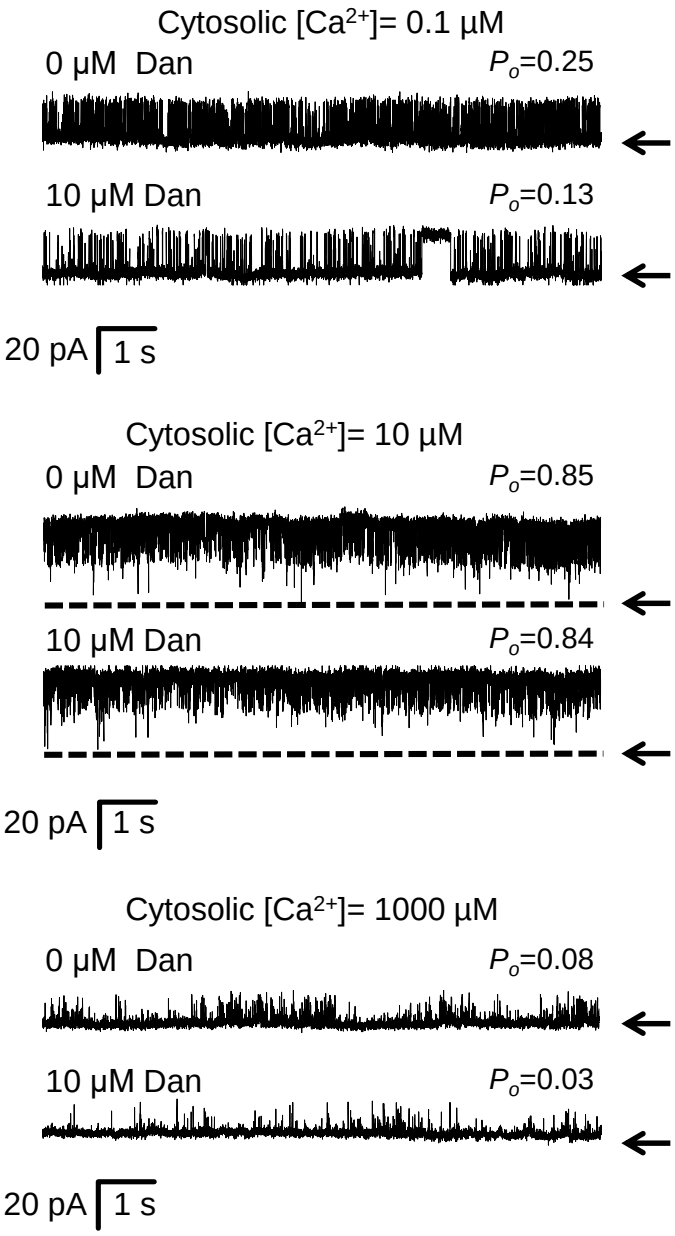

Figure 5.5: Single channel recordings for dantrolene inhibition of the RyR1 in the presence of 100 nM CaM with cytosolic [Ca^{2+}] of 0.1 µM, 10 µM and 1000 µM. The luminal [Ca^{2+}] is 0.1 mM. Experiments were recorded at +40 mV and upward current jumps represent the channel openings. The arrows indicate the baseline.

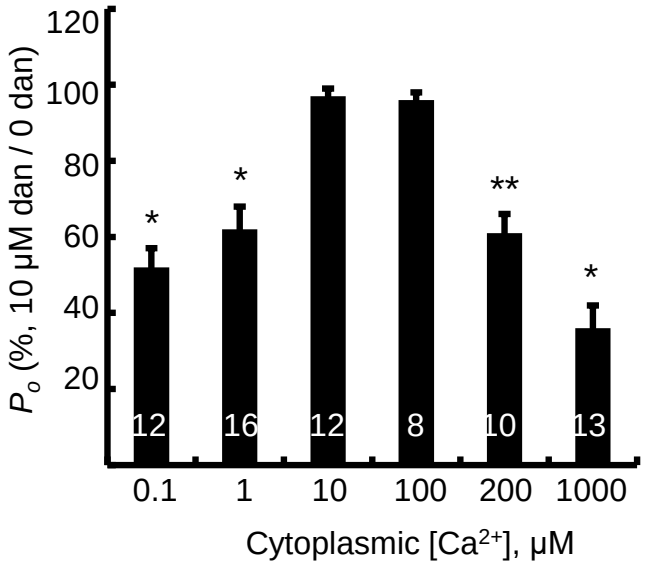

Figure 5.6: Dantrolene inhibition of the RyR1 depends on the cytoplasmic calcium concentration**.** The histogram shows the relative reduction in RyR1 open probability induced by 10 µM dantrolene in the presence of 100 nM CaM. The luminal [Ca^{2+}] was 0.1 mM. Experiments were recorded at +40 mV. The numbers of measurements for each bar are specified in the figure labels. The asterisks denote the significant difference to 100% (* $p<0.05$, **$p<0.01$, mean ± SEM).

5.3.3 Luminal [Ca^{2+}] does not alter dantrolene inhibition of RyR1s regardless of the voltage

Figure 5.7 shows the dantrolene inhibition of RyR1s at luminal [Ca^{2+}] of 0, 100 μM and 1000 μM in the presence of 100 nM cytoplasmic (*cis*) [Ca^{2+}], 2 mM ATP and 100 nM CaM; the absolute values for all controls are given in **Table 5.1**. Dantrolene significantly reduced the open probability of the RyR1 at all luminal [Ca^{2+}] tested at both positive and negative voltages (**Figure 5.7A**) and these changes were associated primarily with a reduction in the opening rate of the RyR1 (**Figure 5.7C**). The effect of dantrolene on the mean open time of the RyR1 depended on luminal [Ca^{2+}] and bilayer voltage (**Figure 5.7B**). In the absence of luminal Ca^{2+}, dantrolene did not alter the mean open time. However, at 100 μM luminal Ca^{2+} dantrolene decreased the mean open time at +40 mV, and at 1000 μM luminal Ca^{2+} it also decreased the mean open time at -40 mV. **Table 5.1** shows the absolute values for all control groups.

Luminal [Ca^{2+}] μM	Voltage	n	P_o	T_o (ms)	$1/T_c$ (1/s)
0	(+)	10	0.28 ± 0.04	1.0 ± 0.1	0.4 ± 0.1
	(-)	11	0.3 ± 0.1	2.2 ± 0.4	0.3 ± 0.1
100	(+)	12	0.3 ± 0.1	6.2 ± 1.8	0.14 ± 0.02
	(-)	10	0.4 ± 0.1	1.9 ± 0.7	0.5 ± 0.1
1000	(+)	10	0.3 ± 0.1	2.6 ± 0.8	0.2 ± 0.1
	(-)	10	0.5 ± 0.1	2.8 ± 0.9	0.7 ± 0.2

Table 5.1: Effects of luminal [Ca^{2+}] on dantrolene regulation of RyR1s were shown in **Figure 5.7**. The absolute values of RyR1 open probability (P_o), mean open time (T_o), and opening rate (the inverse of mean closed time, T_c) for all control groups at three different luminal Ca^{2+} concentrations at positive and negative 40 mV are shown in this table. The cytoplasmic bath contained 100 nM Ca^{2+}, 100 nM CaM and 2 mM ATP.

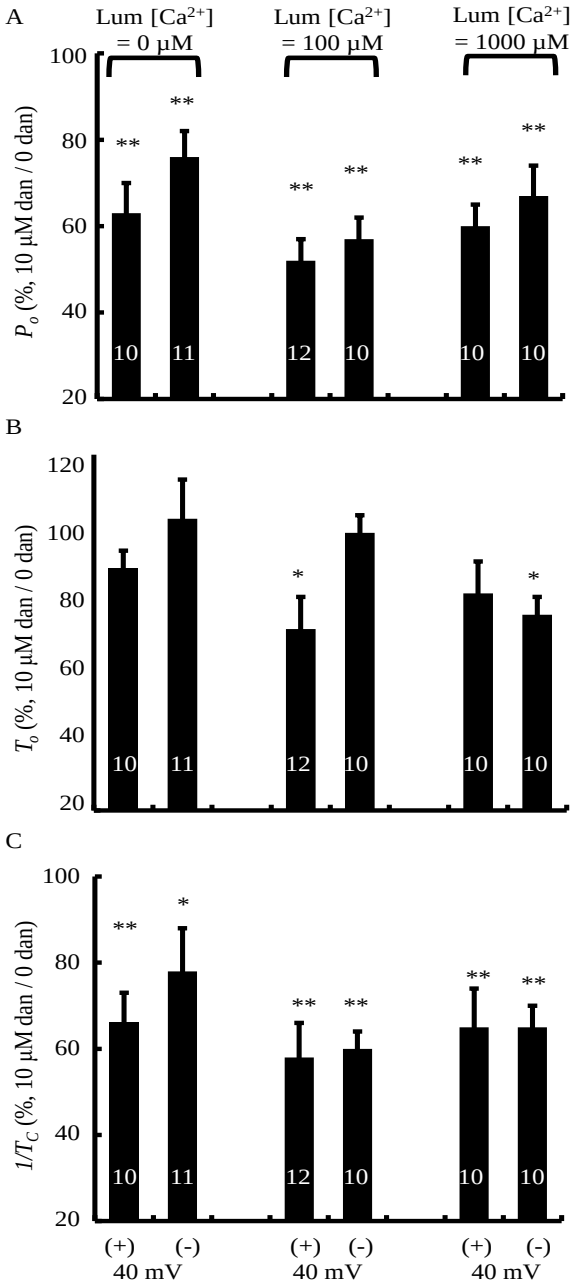

Figure 5.7: Effects of luminal (Lum) [Ca^{2+}] on dantrolene (dan) regulation of RyR1s. (A) Relative inhibition of RyR1 open probability (P_o); (B) mean open time (T_o); and (C) opening rate (the inverse of mean closed time, T_c) by 10 µM dantrolene at three different luminal Ca^{2+} concentrations at positive and negative 40 mV (Numbers of measurements (*n*) for each bar are given in figure label.). The cytoplasmic bath contained 100 nM [Ca^{2+}], 100 nM CaM and 2 mM ATP. The asterisks denote significant difference to 100% (* $p<0.05$, ** $p<0.01$, mean ± SEM).

5.3.4 Dantrolene inhibits RyR1 activated by ATP, halothane and DP4

The activation of RyR1 gating is known to be increased by intrinsic and extrinsic regulators such as ATP, halothane and the DP4 peptide [62, 370]. Here it is investigated whether dantrolene inhibition of the RyR1 would also be altered by these regulators (**Figures 5.8–5.10**). Dantrolene inhibition was first investigated here in the absence and presence of ATP concentrations that produce maximal RyR1 activation (2 mM). At 100 nM cytoplasmic [Ca^{2+}], dantrolene produced similar reductions in RyR1 open probability in the absence and presence of 2 mM ATP and its inhibition was mainly due to the reduction in the opening frequency of the receptors (**Figure 5.8**). However, at the higher cytoplasmic [Ca^{2+}] of 100 μM, dantrolene reduced the open probability of the RyR1 in the absence of ATP but not in the presence of 2 mM ATP (**Figure 5.9**), suggesting that the ATP or enhanced channel activity could probably suppress the dantrolene inhibition.

Dantrolene inhibition of RyR1s that were activated by halothane (5 mM) and the domain peptide DP4 (10 μM), in the presence of 100 nM cytoplasmic [Ca^{2+}] and 100 nM CaM was also investigated (**Figure 5.10**). Dantrolene equally reduced the channel open probability of all the RyR1sby about 50%, primarily through the reduction of opening frequency. The result showed that they were significantly different to 100%. However, it was not addressed whether there was any difference to dantrolene inhibition of RyR1s activated by halothane, ATP and DP4. It could be concluded from the data that the mechanism of dantrolene inhibition of RyR1s is independent of halothane and DP4. **Tables 5.2-5.4** show the absolute values for all control groups.

.

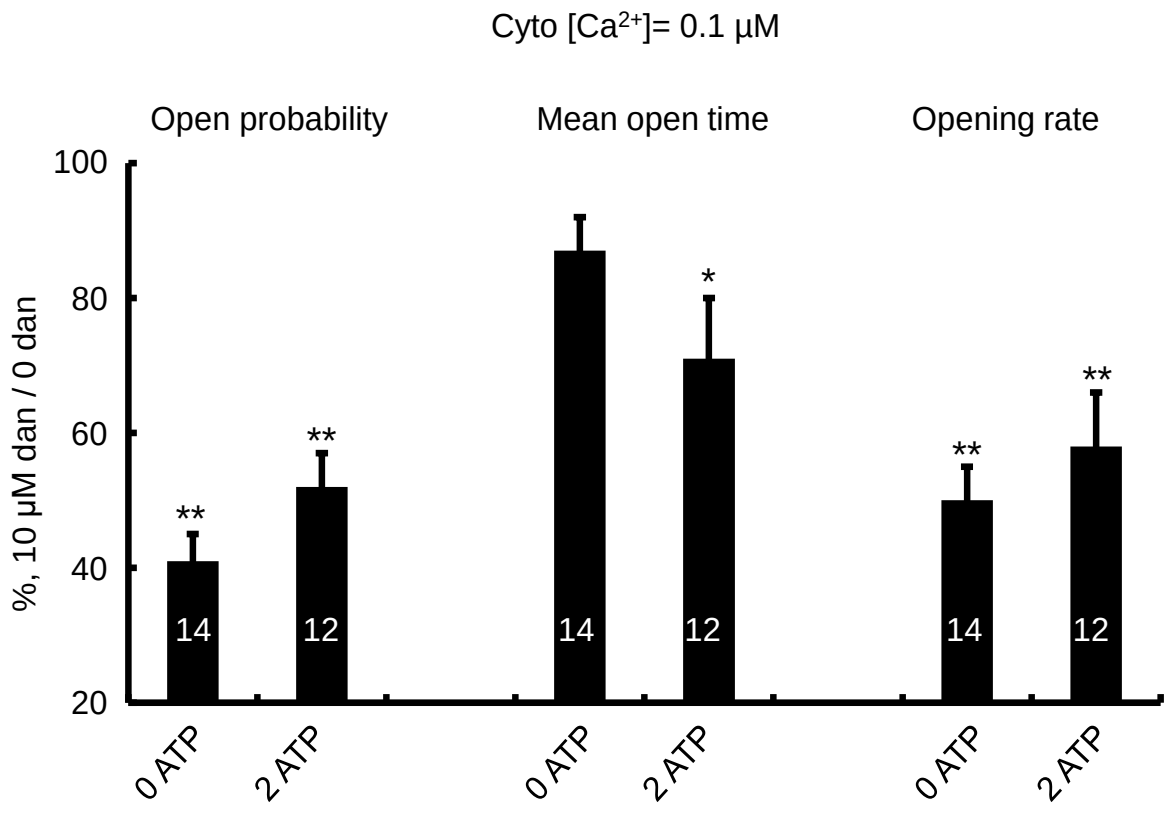

Figure 5.8: Dantrolene inhibition of RyRs1 activated by ATP showing relative inhibition of RyR1 open probability (P_o), mean open time (T_o) and opening rate (the inverse of mean closed time, T_c) by 10 µM dantrolene in the absence and presence of 2 mM ATP. The luminal [Ca^{2+}] was 0.1 mM. The asterisks show the significant difference to 100% (* $p<0.05$, ** $p<0.01$, mean ± SEM).

ATP	**n**	P_o	T_o *(ms)*	$1/T_c$ *(1/s)*
0 mM	14	0.04 ± 0.01	0.7 ± 0.1	0.06 ± 0.01
2 mM	12	0.3 ± 0.1	6.2 ± 1.8	0.14 ± 0.02

Table 5.2: Absolute values of open probability (P_o), mean open time (T_o) and opening rate (the inverse of mean closed time, T_c) for vehicle (control) in the presence of 100 nM cytoplasmic [Ca^{2+}].

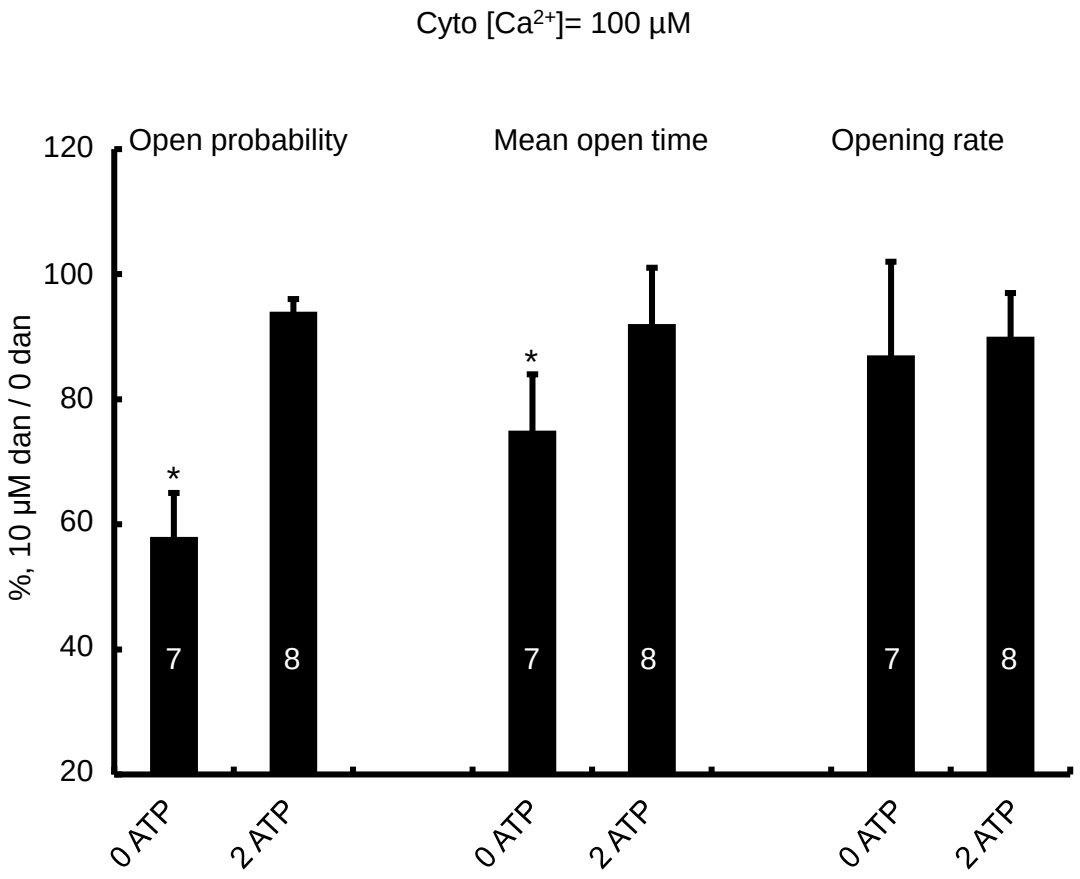

Figure 5.9: Dantrolene inhibition of RyR1s activated by ATP showing the relative inhibition of RyR1 open probability (P_o), mean open time (T_o) and opening rate (the inverse of mean closed time, T_c) by 10 µM dantrolene in the absence and presence of 2 mM ATP. The luminal [Ca^{2+}] was 0.1 mM. The asterisks show the significant difference to 100% (* $p<0.05$, mean ± SEM).

ATP	***n***	***P_o***	***T_o (ms)***	***$1/T_c$ (1/s)***
0 mM	8	0.3 ± 0.1	2.8 ± 0.9	0.1 ± 0.03
2 mM	7	0.7 ± 0.1	3.7 ± 0.8	0.9 ± 0.1

Table 5.3: Absolute values of open probability (P_o), mean open time (T_o) and opening rate (the inverse of mean closed time, T_c) for vehicle (control) in the presence of 100 µM cytoplasmic Ca^{2+}.

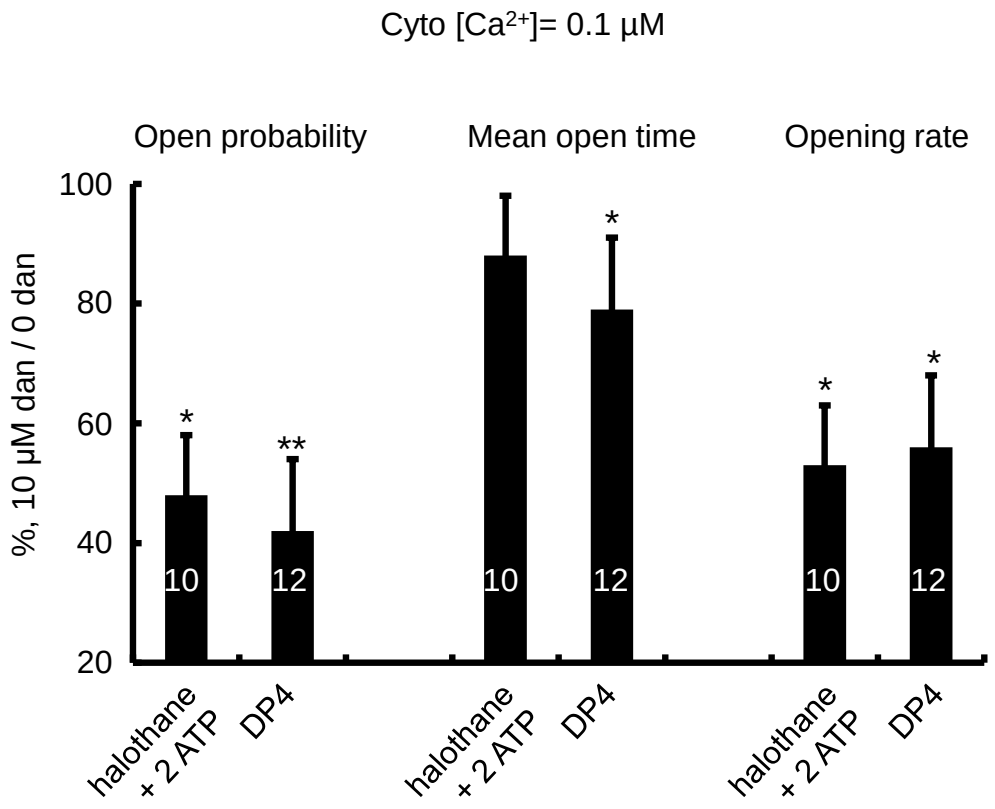

Figure 5.10: Dantrolene inhibition of RyR1s activated by halothane or DP4 showing the relative inhibition of RyR1 open probability (*Po*), mean open time (*To*) and opening rate (the inverse of mean closed time, *Tc*) by 10 µM dantrolene in the absence and presence of halothane and DP4. The luminal [Ca^{2+}] was 0.1 mM. The asterisks show the significant difference to 100% (* $p<0.05$, ** $p<0.01$, mean ± SEM).

Activators	**n**	***Po***	***T_o (ms)***	***$1/T_c$ (1/s)***
Halothane	10	0.2 ± 0.1	2.2 ± 0.8	0.12 ± 0.03
DP4	12	0.07 ± 0.04	1.0 ± 0.1	0.10 ± 0.06

Table 5.4: Absolute values of open probability (P_o), mean open time (T_o) and opening rate (the inverse of mean closed time, T_c) for vehicle (control) in the presence of halothane and DP4.

5.3.5 Role of cytoplasmic Mg^{2+} in dantrolene inhibition of skeletal ryanodine receptors

Cytoplasmic Mg^{2+} is a strong inhibitor of RyR1 activity which is known to act via two independent mechanisms [20] that lead to different channel sensitivities to cytoplasmic [Mg^{2+}] in the presence of 100 nM cytoplasmic Ca^{2+} (**Figure 5.11**). In the presence of 100 nM cytoplasmic Ca^{2+} (with 2 mM ATP, **Figure 5.11** open circles), cytoplasmic Mg^{2+} inhibited RyR1 with half maximal inhibition (IC_{50}) of 28 ± 2 μM (a Hill coefficient of 1.6 ± 0.3). The maximal inhibition of 10 μM dantrolene in the absence of cytosolic Mg^{2+} at concentrations that produced ~50% and ~80-90% inhibition were measured (**Figure 5.12**). Dantrolene equally reduced the open probability of the RyR1 to approximately 50-60%, changes that were mainly due to a reduction in the opening frequency of the RyR1. Moreover, there were no statistically significant differences among the group means at different [Mg^{2+}] as determined by one-way ANOVA ($p = 0.35$). Therefore, it could be concluded that cytosolic [Mg^{2+}] had no impact on dantrolene inhibition at 100 nM cytosolic Ca^{2+}. The absolute P_o values for all control groups as shown in **Table 5.5** do not seem to follow the Mg^{2+} inhibition because the channel activities of skeletal muscle ryanodine receptors vary from one to another. In fact, Mg^{2+} clearly inhibits as shown in **Figure 5.11**.

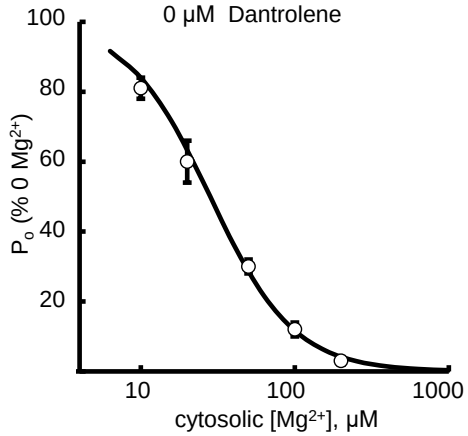

Figure 5.11: Cytoplasmic Mg^{2+} inhibition dose-response of RyR1 activity in the presence of 100 nM cytoplasmic [Ca^{2+}] (with 2 mM ATP, n= 5 to 12). The luminal bath contained 0.1 mM Ca^{2+}.

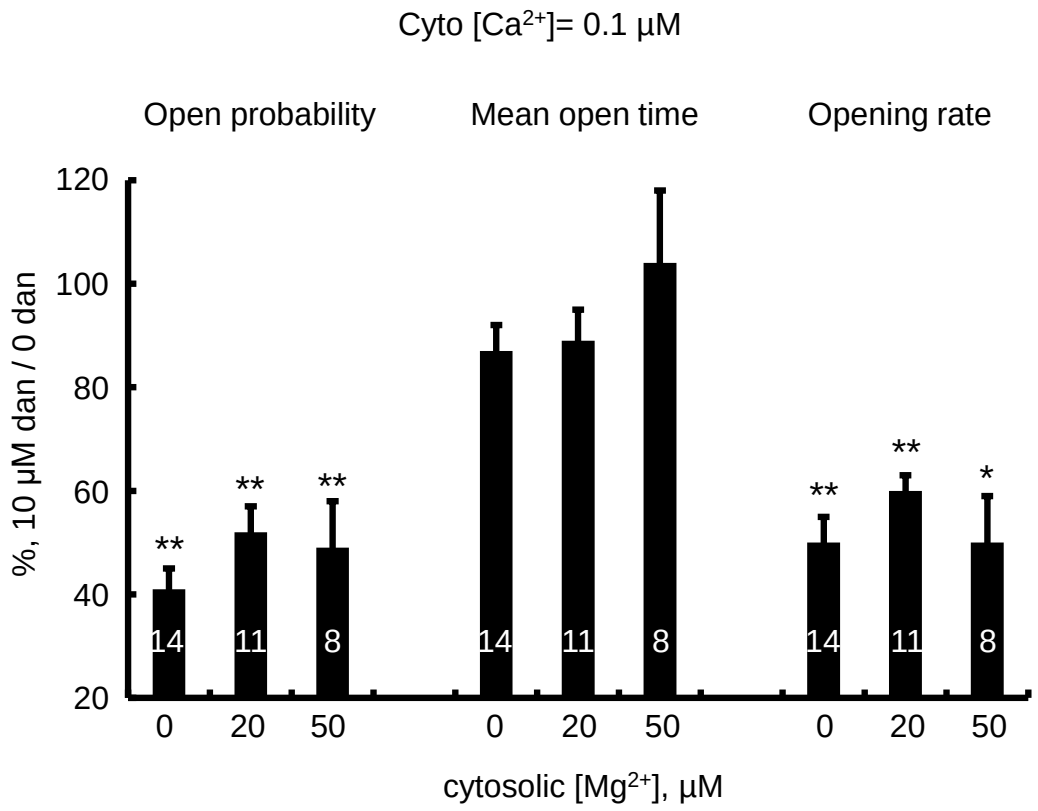

Figure 5.12: The effect of dantrolene on RyR1 regulation by cytoplasmic Mg^{2+}. The figure shows relative inhibition of the RyR1 open probability (P_o), mean open time (T_o) and opening rate (the inverse of mean closed time, T_c) by 10 µM dantrolene in the presence of nil, 20 and 50 µM cytoplasmic Mg^{2+}. The luminal $[Ca^{2+}]$ was 0.1 mM. The asterisks show significant difference to 100% (* $p<0.05$, **$p<0.01$, mean ± SEM.

Cytosolic $[Mg^{2+}]$ µM	**n**	***P_o***	***T_o (ms)***	***$1/T_c$ (1/s)***
0 µM	14	0.04 ± 0.01	0.7 ± 0.1	0.06 ± 0.01
20 µM	11	0.10 ± 0.01	1.12 ± 0.09	0.10 ± 0.02
50 µM	8	0.15± 0.03	1.34 ± 0.11	0.13 ± 0.03

Table 5.5: Absolute values of open probability (P_o), mean open time (T_o) and opening rate (the inverse of mean closed time, T_c) for vehicle (control) in the absence and presence of different concentrations of cytoplasmic Mg^{2+}.

5.4 Discussion

The first part of this study established anIC_{50} concentration for dantrolene inhibition of RyR1s in single channel recordings of 0.20 ± 0.02 μM. This value agrees well with IC_{50} values obtained using indirect assays of RyR activity: (1) the activity of purified RyR1s in ^{3}[H]-ryanodine binding assays (0.15 ± 0.02 μM) [280], and (2) the binding affinity of dantrolene to skeletal muscle SR vesicles (0.277 ± 0.025 μM) [288].

RyRs are modulated by Ca^{2+} and Mg^{2+} in the cytoplasm and SR lumen as well as by other compounds such as ATP and halothane. It was found that dantrolene inhibition of RyR1s depends on the RyR1 activation state. RyR1 with high levels of activation (e.g. P_o > 0.8) were not inhibited by dantrolene. This property of dantrolene inhibition was also noted in our previous study on the cardiac RyR2 isoform from sheep (**Chapter 4**). For example, in the presence of ATP and cytoplasmic [Ca^{2+}] between 10 and 100 μM, dantrolene failed to inhibit RyR1 activity whereas outside of this range, dantrolene was inhibitory.

That the data showing uniform dantrolene inhibition in RyR1s was subjected to a wide range of [Mg^{2+}] inhibition (**Figure 5.115.12**), suggested that dantrolene inhibition of RyR1 did not affect the sensitivity of RyR1 inhibition by cytoplasmic [Mg^{2+}]. This was the case in the presence of low cytoplasmic [Ca^{2+}] where Mg^{2+} inhibition is mainly due to its binding to the cytoplasmic Ca^{2+} activation site [20]. The findings in low [Ca^{2+}] agree with [^{3}H]-ryanodine binding assays showing that dantrolene did not significantly alter the IC_{50} for Mg^{2+} inhibition of [^{3}H] binding to either MH or normal SR vesicles [291].

My finding that dantrolene inhibition does not depend on the presence of ATP conflicts with a previous report using [^{3}H]-ryanodine binding assays [291] where it was shown that dantrolene decreased by one-third the extent of CaM-activated ryanodine binding to MH SR vesicles in the presence of a non-hydrolysable ATP analogue (AMPPCP), but it had no effect when AMPPCP was removed from the binding media. A small difference between this experiment and our study is that the media in their study contained 120 mM potassium propionate instead of 150 mM caesium methanesulfonate. It is unlikely this variation accounted for the vast difference in dantrolene inhibition. One possible explanation is that it might not have been technically possible to resolve dantrolene

inhibition from background [^{3}H]-ryanodine binding levels under those conditions because binding levels in the absence of AMPPCP were very low.

The dantrolene plasma level [395] required for 50% inhibition of skeletal contractility in an awake man was ~10 μM and this is similar to the concentrations needed to inhibit contraction of isolated skeletal muscle fibres [396]. These concentrations of dantrolene are 100-fold higher than the levels required for the inhibition of isolated RyR1s seen here and in many other studies [280, 291, 306, 313]. This has lead others to consider the possibility of alternative therapeutic mechanisms for dantrolene such as modulating store-operated Ca^{2+} entry [300] or by protecting against oxidation [397, 398]. In addition, our finding that dantrolene has no inhibitory effect on RyR1s at high [Ca^{2+}] indicates that during Ca^{2+} release, where cytoplasmic Ca^{2+} concentration in the triadic space rises to ~100 μM [399], dantrolene should not be a significant inhibitor of RyR1 activity. Thus, in order to explain any inhibitory action of dantrolene on Ca^{2+} release in skeletal muscle, there must be alternative mechanisms in action (this issue is discussed more in the General Discussion).

Two other observations in our study suggested that the actions of dantrolene in skeletal muscle may not be due to dantrolene inhibition of RyR1s. Firstly, Mg^{2+} is a potent inhibitor of RyR1 activity in skeletal muscle and MH mutations in RyR1s reduced Mg^{2+} inhibition [281] making MH-susceptible muscle fibres less sensitive to the normal inhibitory effect of cytoplasmic Mg^{2+} on the SR Ca^{2+} release [22, 393]. Dantrolene has been shown to restore the normal Mg^{2+} sensitivity to MH-susceptible muscle fibres [393]. However, the results presented here (**Figure 5.11-5.12**) suggested that dantrolene does not alter Mg^{2+} inhibition of healthy rabbit skeletal RyRs although we are not sure whether dantrolene alters Mg^{2+} inhibition of MH RyR1s. Secondly, dantrolene inhibition of Ca^{2+} release in skinned muscle fibres was only detected when ATP was present in the media [325] whereas these data show that dantrolene inhibition of RyR1 is not sensitive ATP.

One important aspect of this study is that dantrolene inhibits the RyR1 activity induced by DP4. This finding is consistent with the finding that dantrolene stabilizes the zipped configuration of the domain switch in the presence of the domain-unzipping agent, DP4 [313]. DP4 is known to induce the unzipped state of the channel/channel dysfunction that could be caused by MH mutations. Data here demonstrated that dantrolene inhibits

the same way on both zipped and unzipped channels, suggesting a different mechanism of dantrolene inhibition other than by stablisation of the zipped conformation of the RyR. Halothane stimulates RyR1-mediated Ca^{2+} release from SR vesicles isolated from wild type rabbit skeletal muscle [400]. Dantrolene has shown to prevent the effects of halothane in MH-susceptible individuals and also in animal models [284, 401, 402]. However, to date the direct inhibition of RyR1 channel by dantrolene has not been shown [280, 292]. This study showed that dantrolene inhibition was observed both in the absence and in the presence of halothane. Nevertheless, it is possible that the RyR1 will not be the target of dantrolene inhibition in the case of halothane activation of muscle fibres.

To conclude, the data presented here indicated that dantrolene inhibits RyR1s by reducing the sensitivity to activation by cytoplasmic [Ca^{2+}] without affecting RyR1 regulation by luminal [Ca^{2+}], cytosolic [Mg^{2+}] or [ATP]. Given that the properties of dantrolene inhibition of SR Ca^{2+} release in skeletal muscle are different to dantrolene inhibition of RyR1 reported here, it is suggested that the RyR1 is not the therapeutic target of dantrolene and that alternative mechanisms should be considered for the therapeutic actions of dantrolene in skeletal muscle. In addition, it has been recently suggested that dantrolene inhibits L-type Ca^{2+} channel activity [301, 304, 305]. Bannister et al. (2012) reported that dantrolene inhibition of L-type Ca^{2+} channels requires the expression of RyR1 [306]. This chapter only addressed the dantrolene inhibition of healthy RyR1s. Dantrolene has been clinically used in MH and so its mechanism of action on MH RyR1s may be different to healthy RyR1s. The limitation of this study is that - the dantrolene inhibition of MH RyR1s was not tested and investigation of dantrolene action on MH RyR1 samples could potentially provide the detailed understanding of the therapeutics action of dantrolene.

Chapter 6

Dantrolene inhibition of RyR2 in the presence of CaM

6.1 Introduction

Chapter 4 showed that CaM is the essential requirement for dantrolene inhibition of RyRs in single channel recordings. Since it is the first demonstration of dantrolene inhibition in single channel recordings, the detailed mechanism of this inhibition in RyR2s is still unknown; hence, two major issues addressed in this chapter may gain more insight into those mechanisms. The first is the concentration-dependence of dantrolene inhibition and the second is the cytoplasmic [Ca^{2+}] dependent effect. Kobayashi et al. (2009) reported the dose-dependence of dantrolene inhibition using measurements of SR Ca^{2+} sparks in normal (IC_{50} = 0.3 ± 0.09 μM) and failing dog heart (IC_{50} = 0.3 ± 0.07 μM) [283]. This chapter will demonstrate the first dose-response effect of dantrolene inhibition using single channel recordings in the presence of 100 nM exogenous CaM. In addition, the study will explore the CaM facilitation of dantrolene inhibition using (CPVT-CaM) N-98S that has no effect on RyR2 channel gating.

Several modulators such as Ca^{2+}, ATP, and Mg^{2+} have been reported to regulate RyRs. Ca^{2+} regulates RyR2 on both cytoplasmic and luminal sides of the SR as one of the most important modulators [20, 58-61]. Bilayer studies show that the RyR2 is activated at micromolar concentrations of cytoplasmic [Ca^{2+}] but it is inhibited at millimolar concentrations [61]. In cardiac muscle, Ca^{2+} entering from outside the cell and from within the SR plays a very important role in activation of RyR2s since the activation by Ca^{2+} influx and the subsequent activation of other RyR2s by Ca^{2+} release from RyR2s, could enforce Ca^{2+}-induced Ca^{2+} release (CICR),one of the major steps in EC-coupling of cardiac muscle [1, 17].

Interestingly, dantrolene was proposed as a diastolic blocker since dantrolene suppressed spontaneous Ca^{2+} release in cardiomyocytes of aged mice [403]. It was reported that dantrolene inhibited the frequency of Ca^{2+} sparks and SR leak, whereas it failed to inhibit the amplitude of Ca^{2+} transients [323, 324]. Thus, these findings support the fact that dantrolene is a diastolic inhibitor of Ca^{2+} release in failing heart

[323]. However, whether dantrolene inhibition depends on cytoplasmic [Ca^{2+}] has not been explored. (This chapter was transformed from my paper, Oo et al., Molecular Pharmacology Journal, 2015 [388].

6.2 Materials and Methods

6.2.1 Single channel recordings

SR vesicles containing RyR2s were isolated from sheep hearts and incorporated into the artificial lipid bilayers [371]. During experiments the concentrations of calmodulin, dantrolene and Ca^{2+} in the cytoplasmic solution were altered by a local perfusion system [349]. Single channel dwell-time histograms of open and closed time, open probability, mean open time and mean closed time were measured using a threshold discriminator at 50% of channel amplitude (Channel 3 software by NW Laver). Hill equations were fitted by the method of least squares to the dose-responses of the ratios of P_o in the presence and absence of dantrolene. Likewise, Hill equations were also fitted to the Ca^{2+} activation and inhibition of the ratios of P_o in the presence and absence of dantrolene. Please see details in **Chapter 2**.

6.2.2 Statistics

Average data are presented as the arithmetic mean standard error of the mean (SEM). The statistical significance of difference was tested using Student's *t* test on normal distributions. Asterisks indicate being significantly different to 100% (* $p<0.05$, **$p<0.01$).

6.3 Results

6.3.1 Concentration-dependence of dantrolene inhibition of RyR2s in the presence of CaM

The concentration-dependence of dantrolene inhibition of RyR2s is shown in **Figure 6.1**. In the presence of 100 nM CaM (●), dantrolene inhibition exhibited a sigmoidal dependence on log-concentration with an IC_{50} of 0.16 ± 0.03 µM, a Hill coefficient of ~1 and with a saturating RyR2 open probability (E_{max}) of 52 ± 4 % when compared with data obtained in the absence of dantrolene. Reducing the CaM concentration to 10 nM approximately halved the magnitude of dantrolene inhibition (E_{max} = 80 ± 5 %, **Figure 6.1**, ○).

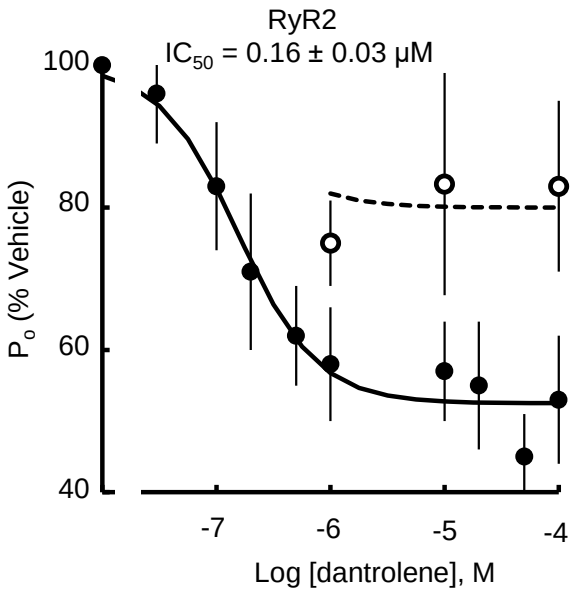

Figure 6.1: Concentration-dependence of RyR2 activity inhibition by dantrolene in the presence of 10 nM CaM (○), (mean ± SEM, n= 3 to 4) and 100 nM CaM (●), (mean ± SEM, n= 7 to 20). The luminal [Ca^{2+}] was 0.1 mM and cytoplasmic [Ca^{2+}] was 100 nM. The solid curve shows the Hill fit to the data using the equation:

$$Po = \{1 + E_{max}\,([dantrolene]/IC_{50})^{H}\}/\{1 + ([dantrolene]/IC_{50})^{H}\}$$

where IC_{50} = 0.16 ± 0.03 µM, H = 1.3 ± 0.3 and E_{max} = 52 ± 4%.

The dashed curve uses the same parameter values except E_{max} = 80 ± 5%.

6.3.2 The effect of dantrolene on RyR dwell-times and their dependencies on cytoplasmic Ca^{2+}

In order to gain more insight into the mechanism of dantrolene inhibition, dwell-time histograms of channel open and closed events of sheep RyR2s were compiled (**Figure 6.2**). Histograms are displayed using the log-bin method of Sigworth and Sine [404] where individual exponential components appear as peaks centered on their time constant value. In the absence of dantrolene, open and closed dwell times in 1 μM cytoplasmic Ca^{2+} exhibited peaked distributions that were fitted by two exponential components (exponential parameters are given in **Table 6.1**). Addition of dantrolene (10 μM) shifted the peak of the open distributions to shorter times and closed distribution to longer times. Dantrolene had a similar effect in 0.1 μM cytoplasmic Ca^{2+} but had no effect at 100 μM cytoplasmic Ca^{2+}. Dantrolene altered the time constants of the exponential fits but did not introduce additional time constants into the closed dwell-time distribution that would indicate a dantrolene-blocked state of the RyR.

The effect of dantrolene on dwell times is summarized in **Figure 6.3** showing the relative changes in RyR2 mean open and closed durations at four cytoplasmic [Ca^{2+}] ranging from 0.1 μM (end-diastolic) to 100 μM (systolic). In 0.1 μM cytoplasmic Ca^{2+}, dantrolene reduced RyR2 P_o via a decrease in mean channel open duration and an increase in mean closed duration. At 1 μM cytoplasmic Ca^{2+}, the effect of dantrolene was diminished and there was no significant inhibition occurring at higher [Ca^{2+}]. Since the inhibition of dantrolene required CaM, further investigations as to whether CaM effects also depend on cytoplasmic [Ca^{2+}] were devised to include measurements of CaM (100 nM) inhibition at several cytoplasmic [Ca^{2+}], ranging from 0.1 μM (diastolic) to 100 μM (systolic) (**Figure 6.4**). Similarly, CaM reduced the open probability of RyR2s to ~50 % of control (*i.e.* vehicle alone) at cytoplasmic 0. 1 μM Ca^{2+} and the inhibitory effect of CaM was reduced as the cytoplasmic [Ca^{2+}] was increased. Notably, CaM had no significant effect at intermediate [Ca^{2+}] of 10-100 μM where the channels are fully activated. Therefore, it is possible to conclude that regulation of CaM is also dependent on cytoplasmic [Ca^{2+}] in a similar way to dantrolene.

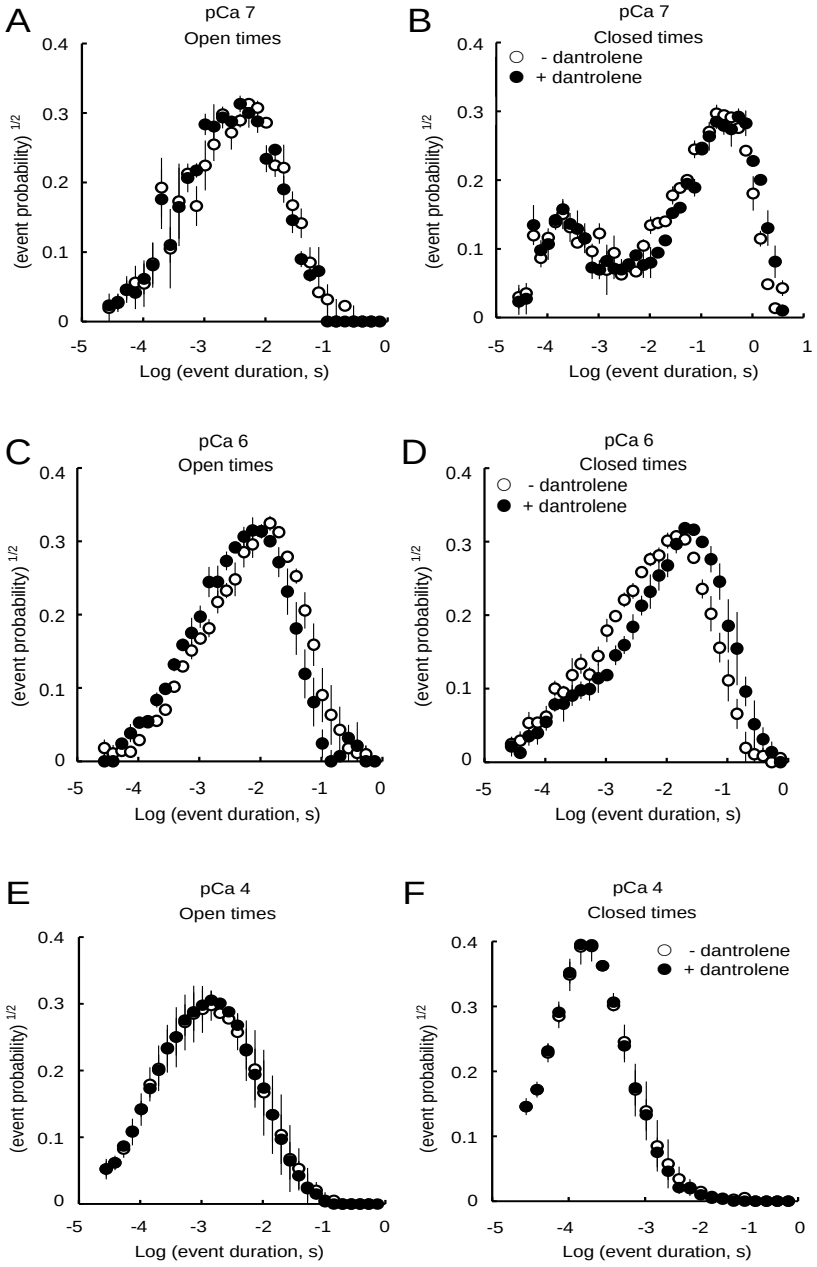

Figure 6.2: Effects of dantrolene on open and closed dwell-times of RyR2. (A,C,E) open and (B,D,F) closed dwell-time histograms compiled using the log-bin method of Sigworth and Sine [404] as described in the text (**6.3.2**). Histograms are averages of three experiments obtained in cytoplasmic [Ca^{2+}] (indicated by pCa in each panel) in the absence (O) or (●) presence of 10 μM dantrolene. The values are of exponential constant fits to the dwell-time histograms (**Table 6.1)**.

	Fit to open dwell times				Fit to closed dwell times			
Condition	A1	T1	A2	T2	A1	T1	A2	T2
	%	ms	%	ms	%	ms	%	ms
pCa7	73±16	3.8±0.6	27±16	22±6	11±3	0.77±0.18	89±3	500±100
pCa7+dan	81±12	4.4±1.0	19±12	22±5	8±4	0.37±0.04	92±4	700±150*
pCa6	37±7	8±2	63±7	27±9	31±5	5±2	69±5	27±6
pCa6+dan	41±17	5.2±0.5	59±18	16±1	35±10	15±9	65±10	50±20
pCa4	68±5	1.8±0.4	32±5	8±2	93±5	0.19±0.01	7±5	0.91±0.09
pCa4+dan	70±10	1.7±0.4	30±10	7±2	88±3	0.18±0.03	12±3	0.61±0.08

Table 6.1: Open and closed dwell-time histograms compiled using the log-bin method of Sigworth and Sine [404] as described in the text and shown in **Figure 6.2**. Histograms are averages of three experiments obtained in three different cytoplasmic [Ca^{2+}] (pCa 4, 6 and 7) in the absence and presence of 10 μM dantrolene. The values are exponential constant fits to dwell-time histograms. The asterisks indicate being significantly different to 100% (* $p<0.05$)

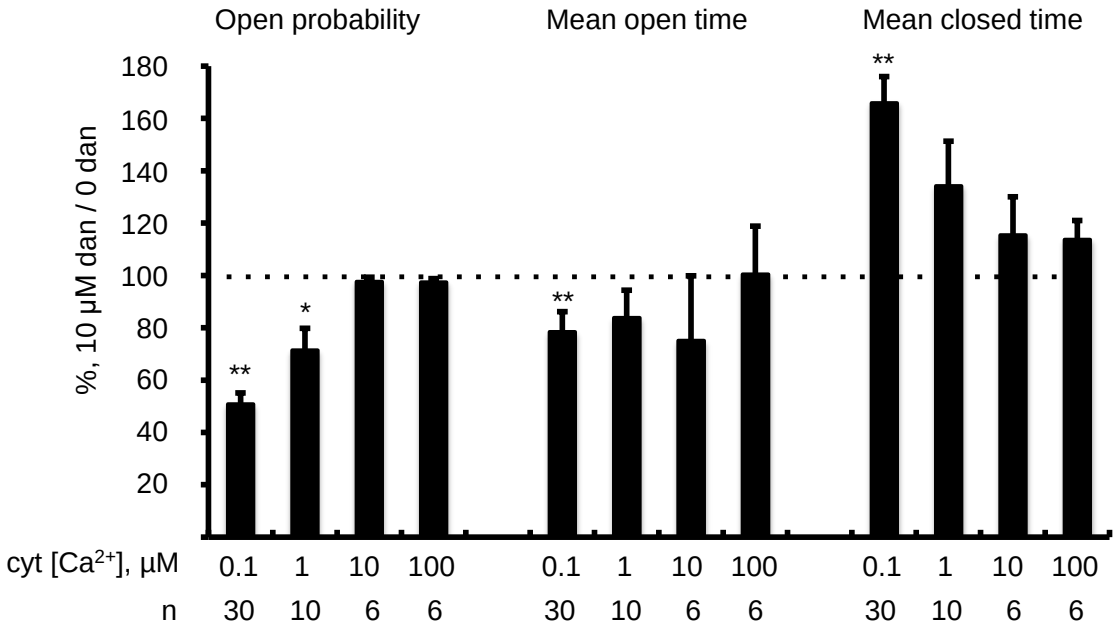

Figure 6.3: Statistical analysis of dwell-time histograms showing the relative changes in channel open probability, mean open and closed dwell-times induced by 10 µM dantrolene over a range of cytoplasmic [Ca^{2+}]. The luminal bath contains 0.1 mM [Ca^{2+}]. The asterisks indicate being significantly different to 100% (* $p<0.05$, ** $p<0.01$).

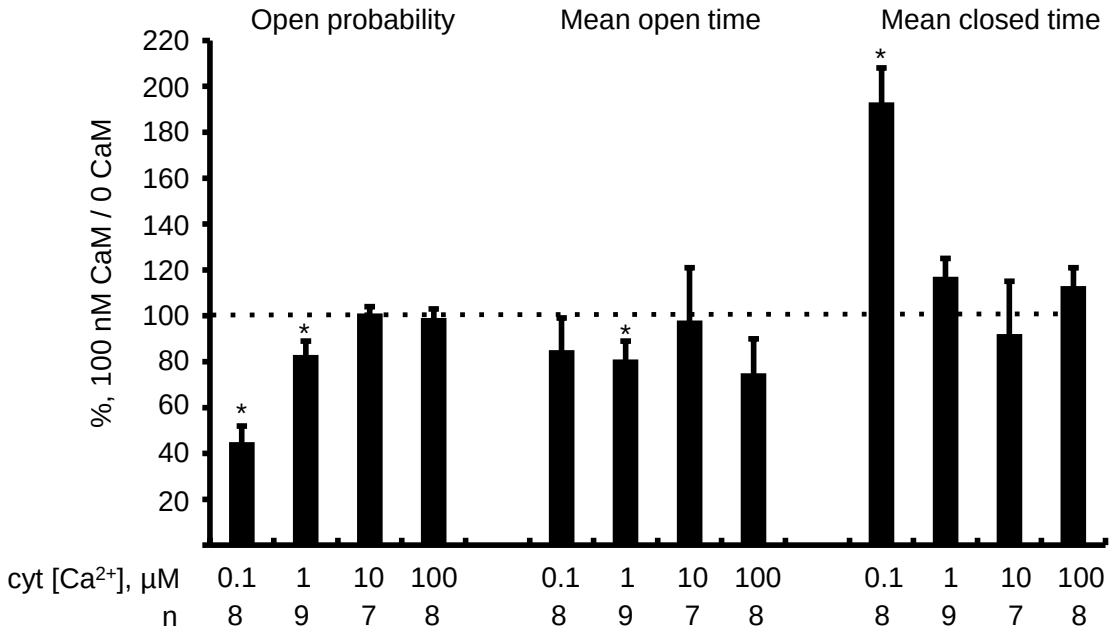

Figure 6.4: Statistical analysis of the relative inhibition of channel open probability, mean open and closed times induced by 100 nM CaM over a range of cytoplasmic [Ca^{2+}]. The luminal bath contained 0.1 mM [Ca^{2+}]. The asterisks indicate being significantly different to 100% (* $p<0.05$, **$p<0.01$).

6.3.3 Mutant CaM dose-response for facilitation of dantrolene inhibition

The concentration of CaM required to facilitate dantrolene inhibition was investigated. To do this dantrolene inhibition was measured at a fixed concentration (10 μM) in the presence of varying concentrations of N98S-CaM and a CPVT-CaM mutant that has no inhibitory effect on RyR2s (**Figure 6.5**, open circle). The advantage of this CVPT-CaM mutant was that it enabled examination of the effect of varying its concentration on facilitating dantrolene inhibition without the confounding the effect of CaM inhibition. In the absence of N98S CaM, dantrolene had no effect on RyR P_o. **Figure 6.5** shows the addition of only 5 nM N98S-CaM was sufficient to facilitate significant dantrolene inhibition of the RyR2. The N98S-CaM facilitation of dantrolene inhibition had a sigmoidal dependence on log-concentration with an IC_{50} of 5.9 ± 0.3 nM, a Hill coefficient of 5 ± 2.6 and an E_{max} of 53 ± 4 %.

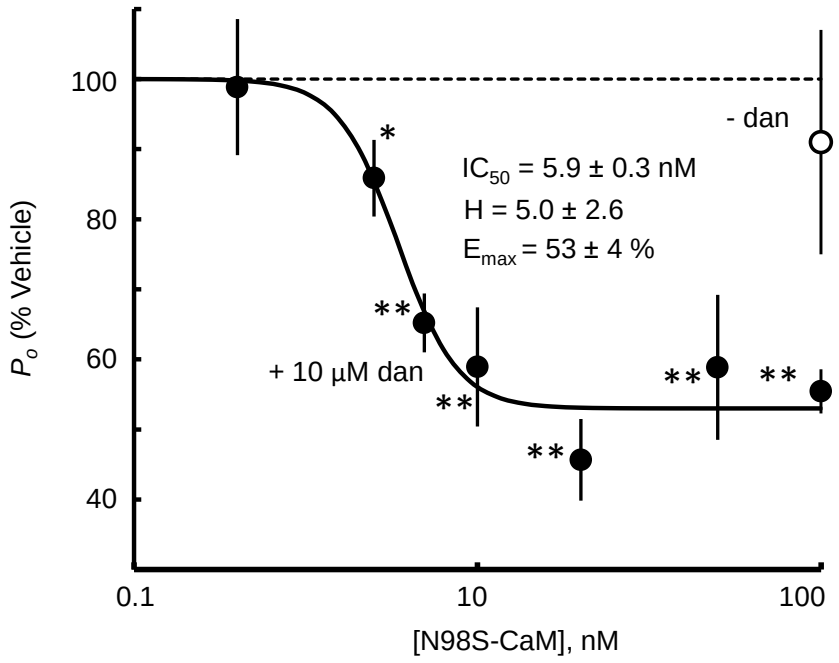

Figure 6.5: Facilitation of dantrolene (10 μM) inhibition by N98S-CaM (●). In the absence of dantrolene (○), N98S-CaM has no inhibiting action on RyR2s. The asterisks indicate being significantly different to 100% (* $p<0.05$, ** $p<0.01$). The luminal $[Ca^{2+}]$ was 0.1 mM and the cytoplasmic bath contained 2 mM ATP and 100 nM Ca^{2+}. The solid curve shows the fit of the Hill equation to the data (see caption of **Figure 6.1**).

6.4 Discussion

The study in this chapter provides the first dose-response of dantrolene inhibition using single channel recordings and the cytoplasmic [Ca^{2+}]-dependence effect of dantrolene. The maximum RyR2 inhibition by dantrolene (E_{max}= 50%) and IC_{50} (0.16 ± 0.03 μM, **Figure 6.1**) are in close agreement with dantrolene inhibition of Ca^{2+} wave frequency and amplitude in saponin permeablized cardiomyocytes (**Chapter 4, Figures 4.5 and 4.6,**) and inhibition of Ca^{2+} release in SR vesicles from failing dog heart (IC_{50} = 0.3 ± 0.07 μM, [283]). The dantrolene IC_{50} reported here coincides with the IC_{50} (0.3 ± 0.11 μM) for inhibiting DPc10-induced unzipping of the central and N-terminal domains of RyR2s [283]. The potency of dantrolene in our study was also consistent with the inhibitory action of 1 μM dantrolene (~40%) on Ca^{2+} spark frequency in isoproterenol-stimulated cardiomyocytes from R2474S knock-in mice [379].

Our finding that dantrolene inhibition is only seen at cytoplasmic [Ca^{2+}] =< 1 μM (**Figure 6.3**) is consistent with previous findings that dantrolene (1 μM) inhibits the frequency of Ca^{2+} sparks (and hence SR leak) but does not inhibit the amplitude of Ca^{2+} transients [323, 324]. Thus, dantrolene is a diastolic inhibitor of Ca^{2+} release in failing heart, which has the beneficial actions of increasing diastolic Ca^{2+} loading of the SR [323] and reducing diastolic SR Ca^{2+} leak after ventricular fibrillation [324].

Single channel recordings of dantrolene inhibition here provide a unique opportunity to probe the mechanism of dantrolene inhibition. RyR2 dwell-time distributions (**Figure 6.2**) indicate that dantrolene decreases the duration of channel openings and increases the duration of closures, characteristics typical of an allosteric inhibitor rather than a channel blocker like the local anesthetics that cause distinct blocking events in single channel recordings [405-407].

The RyR has a homotetrametic structure holding four dantrolene binding sites and at least four CaM binding sites. The dantrolene dose-response (**Figure 6.1**) exhibited a Hill coefficient ~1, consistent with values obtained from 3[H]-ryanodine binding assays [280]. Such a value indicates that the binding of only one dantrolene molecule is sufficient to cause inhibition of RyR2 activity. IC_{50} for CaM facilitation of dantrolene inhibition appears to be ~10 nM for wt-CaM (**Figure 6.1**) and 5.9 nM for N98S-CaM (**Figure 6.5**). These values are ~2-fold lower than the binding affinities for these CaMs on RyR2 [251] [387]. Interestingly, the dose-response of N98S-CaM facilitation of dantrolene inhibition (**Figure 6.5**) had a much higher Hill coefficient, consistent with a

requirement for multiple CaM molecules on the RyR2. The mechanism by which CaM facilitates dantrolene inhibition remains unclear. It is unlikely that dantrolene acts by binding to a site on CaM since that would not explain the different Hill-coefficients for the dantrolene and N98S-CaM dose responses. It is interesting to note that CaM inhibition and dantrolene inhibition have similar Ca^{2+} dependent effects on channel open and closed times. Therefore, even though dantrolene does not amplify CaM inhibition, this result does suggest some commonality in their allosteric mechanisms.

Chapter 7

General Discussion

7.1 Key findings

This study presents the essential role of CaM in dantrolene inhibition of RyR1s and RyR2s from recordings of a single RyR and permeablized cardiomyocytes. The principal finding was that 100 nM (physiological concentration) CaM was required for dantrolene inhibition, solving the long-standing problem of why dantrolene inhibition of RyR1 and RyR2 failed to be detected in previous single channel studies [292, 304, 381]. A similar requirement of CaM was discovered in dantrolene inhibition of calcium-release frequency and amplitude in mouse permeablized cardiomyocytes [388]. Interestingly, IC_{50} values for dantrolene inhibition of RyR2s and RyR1s in single channel recordings are in close agreement (IC_{50} of 0.16 ± 0.03 μM and IC_{50} of 0.20 ± 0.02 μM for RyR2 and RyR1 respectively) with that of calcium frequency and wave inhibition in permeablised cardiomyocytes (IC_{50} = 0.42 ± 0.18 μM and IC_{50} = 0.19 ± 0.04 μM). Dantrolene inhibition of both RyR1s and RyR2s had similar dependencies on cytoplasmic [Ca^{2+}] as in the case of CaM. Moreover, dantrolene inhibited RyR1s activated by halothane and DP4. This study also provided new insights into luminal Ca^{2+} and cytosolic Mg^{2+} modulation of CaM effects on RyR1s in the presence of low cytoplasmic [Ca^{2+}], and effects of CaM on RyR1 gating activity altered by ATP, halothane and DP4.

7.2 Can RyR2 be the therapeutic target of dantrolene?

Arrhythmogenic RyR2 defect was rescued by 10 μM dantrolene and it is thought that dantrolene restored normal Ca^{2+} spark properties in a stem cell model of human CPVT myocytes under basal conditions [378]. It also corrected S406L-RyR2 hyperactivity induced by adrenergic stimulation [378], and 20 μM dantrolene increased survival after ventricular fibrillation [324]. However, the studies here clearly showed that the maximum RyR2 inhibition (E_{max}) was 52 ± 4 % and the IC_{50} was 0.16 ± 0.03 μM in

single channel recordings. The IC_{50} values in single channel recordings match the dantrolene inhibition of Ca^{2+} wave frequency and amplitude in saponin permeablized cardiomyocytes (IC_{50} = 0.42 ± 0.18 μM and IC_{50} = 0.19 ± 0.04 μM). In addition, the values here agree well with the inhibition of Ca^{2+} release in SR vesicles from failing dog heart (IC_{50} = 0.3 ± 0.07 μM, [283]) and IC_{50} (0.3 ± 0.11 μM) for inhibiting the unzipping of the central and N-terminal domains of the RyR2 [283]. The potency of dantrolene in our study was also consistent with the inhibitory action of 1 μM dantrolene on Ca^{2+} spark frequency in isoproterenol-stimulated cardiomyocytes from R2474S knock-in mice [379]. In addition, 1 μM dantrolene reduced the Ca^{2+} spark frequency and prevented arrhythomgenic Ca^{2+} release in ventricular myocytes from rabbit failing hearts [323], and reduced Ca^{2+} spark frequency in aged mice [403]. Taken together, it could be concluded from our study that the RyR2 could possibly be the therapeutic target of dantrolene inhibition.

7.3 Can RyR1 be the therapeutic target of dantrolene?

Skeletal RyR IC_{50} concentration for dantrolene inhibition in single channel recordings was 0.20 ± 0.02 μM which is the same as that obtained for our RyR2s from sheep heart (0.16 ± 0.03 μM) [388]. This value also agrees well with IC_{50} values obtained using indirect assays of RyR activity: (1) the activity of purified RyR1 in ^{3}[H]-ryanodine binding assays (0.15 ± 0.02 μM) [280] and (2) the binding affinity of dantrolene to skeletal muscle SR vesicles (0.277 ± 0.025 μM) [288]. However, the potency of dantrolene in other studies is not consistent with the inhibitory action of dantrolene in our single channel recordings. For example, 10 μM dantrolene or more is required for 1) inhibition of the skeletal L-type Ca^{2+} current [306], 2) inhibition of the rate of Ca^{2+} release from MH and normal SR [280], 3) inhibition of abnormal unzipping of the domain switch induced by DP4 [313], 4) inhibition of excitation-coupled calcium entry in myotubes expressing the MH mutation R163C [300] and 5) inhibition of SR Ca^{2+} release in mouse skeletal muscle fibres [408]. These findings, taken together, have led others to consider alternative therapeutic mechanisms for dantrolene such as modulating store-operated Ca^{2+} entry [300] or by acting as an antioxidant [409] or regulating antioxidant enzymes [397, 398]. This speculation was further supported by the finding that dantrolene failed to inhibit RyR1 at intermediate [Ca^{2+}] of 10-100 μM at which

channels are fully activated. According to this finding, dantrolene could inhibit the initiation of SR Ca^{2+} release when the cytosolic [Ca^{2+}] is low but would not sustain its block during release. Since dantrolene is not an effective RyR inhibitor at high cytoplasmic [Ca^{2+}] then it is not surprising that other dantrolene mechanisms may also be important for suppressing Ca^{2+} release during skeletal muscle twitches [395] or suppressing MH episodes.

7.4 What could be suggested for the mechanism of dantrolene inhibition?

We tested the hypothesis that dantrolene just merely amplifies the effects of CaM. Therefore, the (CPVT-CaM) N54I mutant that activates RyR2 was used to investigate dantrolene action on the RyR2 activity. However, this is not the case and dantrolene only inhibits RyR2 activity in the presence of the N54I mutant. In addition, dantrolene inhibition was observed in RyR1 activated by wt-CaM at low cytosolic [Ca^{2+}]. Therefore, it is now clear that dantrolene required CaM for RyR1 and RyR2 inhibition but it inhibits the channel activities in its own way. The next question is how many dantrolene molecules are required to see the inhibitory effect on the RyR since RyRs have a homotetrametic structure holding four dantrolene binding sites and at least four CaM binding sites. The dantrolene dose-response curve exhibited a Hill coefficient of ~1 for both RyR1s and RyR2s, consistent with values obtained from ^{3}[H]-ryanodine binding assays [280]. Thus, it could be concluded from our data that binding of only one dantrolene molecule is sufficient to cause inhibition of both skeletal and cardiac RyR activity.

Dantrolene inhibition of the RyR2 was only seen at cytoplasmic [Ca^{2+}] ≤1 μM. This is consistent with previous findings that dantrolene inhibited the frequency of Ca^{2+} sparks (and hence SR leak) but did not inhibit the amplitude of Ca^{2+} transients [323, 324]. This is supporting evidence that dantrolene is a diastolic inhibitor of Ca^{2+} release in failing heart [323] and thatit reduces diastolic SR Ca^{2+} leak after ventricular fibrillation [324]. Similarly, dantrolene inhibition of RyR1s was also detected at cytoplasmic [Ca^{2+}] ≤ 1 μM and ≥ 0.2 mM.

7.5 Could dantrolene inhibition be species-dependent?

It is known that the effect of CaM on RyR2s is species specific phenomenon. Animal models for RyR2 function in sheep (~40% inhibition) [251] and dog (80% inhibition) [198] showed CaM binding had different effects on reducing RyR2 activity. Similarly, that our studies showed dantrolene inhibition (in the presence of CaM) in RyR2s from healthy sheep hearts (**Figure 4.1-4.3**) and mouse (**Figure 4.4-4.6**) but not from human (**Figure 4.9**), clearly demonstrated species-dependency.

7.6 Future Direction

The major finding of this thesis was that CaM is essential for dantrolene inhibition in both cardiac and skeletal muscle RyR. However, CaM alone is not enough to facilitate dantrolene inhibition of the channels so other undefined factors must also play a vital role. [^{3}H]-ryanodine binding assays have demonstrated that dantrolene reduced the CaM activation of purified pig RyR1 [280] which is consistent with CaM-mediated dantrolene inhibition of RyR1 channels in my study. However, a single channel bilayer study [300] using similar experimental conditions (100 nM cytoplasmic Ca^{2+} at 35^{o}C), failed to see dantrolene (20 μM) inhibition of purified rabbit RyR1 channels in the presence of exogenous FKBP12 and CaM. Therefore, it clearly highlights that the inhibitory effect of dantrolene on RyRs seen here not only requires CaM, but also other RyR-associated proteins that are present in native preparations but presumably absent in some purified RyR preparations. This hypothesis is supported by our finding that dantrolene inhibited RyR2s from failing human heart but had no effect on RyR2s from healthy human (non-failing) heart, even in the presence of CaM (**Figure 4.9**). This finding helped to gain insights into the different properties of the RyR2 macromolecular in healthy and failing human hearts.

There are some major differences between healthy and failing hearts. Loss of CaM binding to RyR2s has been suggested to be a feature of heart failure. Several studies showed that CaM binding to failing heart was reduced by 50% [410, 411]. Recently, Bers and his co-workers have shown that CaM binds to the RyR2 with high affinity (CaM is bound to >70% of RyR2 monomers), whereas RyR2s from failing hearts showed decreased CaM affinity [ref]. Interestingly, it is believed that decreased CaM

binding to RyR2s and subsequent abnormal RyR2 gating, complicates the pathogenesis of heart failure, and that they are the major causative factors for cardiac dysfunction, lethal arrhythmia and remodelling in heart failure [412]. Thus, it is possible to conclude that progression of heart failure results from depression of RyR2 activity associated with the loss of CaM binding. Progression of heart failure leads to remodelling that includes changes in RyR2 phosphorylation, nitrosylation and oxidation [92] as well as loss of regulatory co-proteins such as FKBP12.6 and PP1 in addition to CaM [219, 413]. Therefore, my future studies will probe the different states of phosphorylation, nitrosylation and oxidation, and presence and absence of co-proteins in healthy and failing heart RyR2s. As an example, RyR2s from healthy hearts will be phosphorylated to study how the phosphorylation state of the channel plays a role in dantrolene inhibition. If phosphorylation is the reason why dantrolene has differential effects in healthy and failing hearts, the next step would be to decipher the specific phosphorylation site that contributes to dantrolene inhibition. Kinases (PKA and CaMKII) will be used to phosphorylate RyR2 at Ser2808 and Ser2814 to investigate which specific phosphorylation site plays a key role in the mechanism of dantrolene inhibition.

My study was based on the fact that our single channel experiments were devoid of CaM since it dissociated within a minute during the isolation procedure. Therefore, it is also important to ascertain the effect of other anti-arrhythmic drugs such as flecainide and tetracaine on RyR2s in the presence of CaM to compare and validate the data with previous results that were done in the absence of CaM.

Lastly, my studies have shown that dantrolene inhibits RyR1 activity both in the absence and presence of DP4 and halothane so it was confirmed that dantrolene inhibition was independent of these regulators. In addition, dantrolene failed to inhibit RyR1 at 10 and 100 μM where the channels are fully activated (**Figure 5.6**) and dantrolene inhibition was not affected by Mg^{2+} inhibition (**Figure 5.12**). Zhao and his co-workers reported that dantrolene did not significantly change the IC_{50} for $MgCl_2$ inhibition of [^{3}H]-ryanodine binding both in normal and MH SR vesicles. However, my study did not include the effect of dantrolene on MH RyR1 in the presence of cytoplasmic [Mg^{2+}]. Therefore, it is very difficult to conclude from my data whether dantrolene might be working on MH channels that are presumably very active and where Mg^{2+} sensitivity is reduced. The foremost experiments would be to investigate whether dantrolene could inhibit the activity of MH RyR1 channels using MH RyR1

alleles that correspond to Arg615 and Cys615 using the previous methods [281, 393, 414]. The next step would be to investigate dantrolene inhibition on MH channels at both low and high calcium concentrations that cover the resting and contraction state of the muscle. Because Mg2+ sensitivity is reduced in MH channels [281], dantrolene inhibition of MH RyR1s will also be tested in the presence of a physiological range of cytoplasmic [Mg^{2+}] to see if dantrolene changes the sensitivity of cytoplasmic [Mg^{2+}]. There are a few other ways to investigate the function of RyR1 such as using [^{3}H]-ryanodine binding assays and SR Ca^{2+} release studies. However, single channel recording is a powerful technique that can directly measure single RyR1 activity in artificial lipid bilayers [347].

In summary, the first future direction is to probe the mechanism of dantrolene inhibition in failing human heart. Secondly, investigate the effects of other anti-arrhythmic drugs such as flecainide and tetracaine on RyR2 in the presence of CaM to see if CaM facilitates their therapeutic action; and finally, an attempt will be made to identify the therapeutic target of dantrolene using MH RyR1s.

REFERENCES

1. Bers, D.M., *Cardiac excitation-contraction coupling.* Nature, 2002. **415**(6868): p. 198-205.
2. Cannell, M.B. and C.H. Kong, *Local control in cardiac E-C coupling.* J Mol Cell Cardiol, 2012. **52**(2): p. 298-303.
3. Pogwizd, S.M., et al., *Arrhythmogenesis and contractile dysfunction in heart failure: Roles of sodium-calcium exchange, inward rectifier potassium current, and residual beta-adrenergic responsiveness.* Circ Res, 2001. **88**(11): p. 1159-67.
4. Flucher, B.E. and C. Franzini-Armstrong, *Formation of junctions involved in excitation-contraction coupling in skeletal and cardiac muscle.* Proc Natl Acad Sci U S A, 1996. **93**(15): p. 8101-6.
5. Marks, A.R., *Calcium and the heart: a question of life and death.* J Clin Invest, 2003. **111**(5): p. 597-600.
6. Wier, W.G., *Gain and cardiac E-C coupling: revisited and revised.* Circ Res, 2007. **101**(6): p. 533-5.
7. Cheng, H. and W.J. Lederer, *Calcium sparks.* Physiol Rev, 2008. **88**(4): p. 1491-545.
8. Reddy, L.G., et al., *Purified, reconstituted cardiac Ca2+-ATPase is regulated by phospholamban but not by direct phosphorylation with Ca2+/calmodulin-dependent protein kinase.* J Biol Chem, 1996. **271**(25): p. 14964-70.
9. MacLennan, D.H. and E.G. Kranias, *Phospholamban: a crucial regulator of cardiac contractility.* Nat Rev Mol Cell Biol, 2003. **4**(7): p. 566-77.
10. Armstrong, C.M., F.M. Bezanilla, and P. Horowicz, *Twitches in the presence of ethylene glycol bis(-aminoethyl ether)-N,N'-tetracetic acid.* Biochim Biophys Acta, 1972. **267**(3): p. 605-8.
11. Dulhunty, A.F. and P.W. Gage, *Effects of extracellular calcium concentration and dihydropyridines on contraction in mammalian skeletal muscle.* J Physiol, 1988. **399**: p. 63-80.
12. Franzini-Armstrong, C., F. Protasi, and V. Ramesh, *Comparative ultrastructure of Ca2+ release units in skeletal and cardiac muscle.* Ann N Y Acad Sci, 1998. **853**: p. 20-30.
13. Bers, D.M. and V.M. Stiffel, *Ratio of ryanodine to dihydropyridine receptors in cardiac and skeletal muscle and implications for E-C coupling.* Am J Physiol, 1993. **264**(6 Pt 1): p. C1587-93.
14. Block, B.A., et al., *Structural evidence for direct interaction between the molecular components of the transverse tubule/sarcoplasmic reticulum junction in skeletal muscle.* J Cell Biol, 1988. **107**(6 Pt 2): p. 2587-600.
15. Yano, M., Y. Ikeda, and M. Matsuzaki, *Altered intracellular Ca2+ handling in heart failure.* J Clin Invest, 2005. **115**(3): p. 556-64.
16. Tanabe, T., et al., *Repeat I of the dihydropyridine receptor is critical in determining calcium channel activation kinetics.* Nature, 1991. **352**(6338): p. 800-3.
17. Lamb, G.D., *Excitation-contraction coupling in skeletal muscle: comparisons with cardiac muscle.* Clin Exp Pharmacol Physiol, 2000. **27**(3): p. 216-24.
18. Meissner, G., E. Darling, and J. Eveleth, *Kinetics of rapid Ca2+ release by sarcoplasmic reticulum. Effects of Ca2+, Mg2+, and adenine nucleotides.* Biochemistry, 1986. **25**(1): p. 236-44.
19. Meissner, G., et al., *Regulation of skeletal muscle Ca2+ release channel (ryanodine receptor) by Ca2+ and monovalent cations and anions.* J Biol Chem, 1997. **272**(3): p. 1628-38.

20. Laver, D.R., T.M. Baynes, and A.F. Dulhunty, *Magnesium inhibition of ryanodine-receptor calcium channels: evidence for two independent mechanisms.* J Membr Biol, 1997. **156**(3): p. 213-29.
21. Laver, D.R. and G.D. Lamb, *Inactivation of Ca2+ release channels (ryanodine receptors RyR1 and RyR2) with rapid steps in [Ca2+] and voltage.* Biophys J, 1998. **74**(5): p. 2352-64.
22. Lamb, G.D., *Ca2+ inactivation, Mg2+ inhibition and malignant hyperthermia.* J Muscle Res Cell Motil, 1993. **14**(6): p. 554-6.
23. Schneider, M.F. and W.K. Chandler, *Voltage dependent charge movement of skeletal muscle: a possible step in excitation-contraction coupling.* Nature, 1973. **242**(5395): p. 244-6.
24. Nakai, J., et al., *Enhanced dihydropyridine receptor channel activity in the presence of ryanodine receptor.* Nature, 1996. **380**(6569): p. 72-5.
25. Sencer, S., et al., *Coupling of RYR1 and L-type calcium channels via calmodulin binding domains.* J Biol Chem, 2001. **276**(41): p. 38237-41.
26. Nakai, J., et al., *Two regions of the ryanodine receptor involved in coupling with L-type Ca2+ channels.* J Biol Chem, 1998. **273**(22): p. 13403-6.
27. Tanabe, T., et al., *Regions of the skeletal muscle dihydropyridine receptor critical for excitation-contraction coupling.* Nature, 1990. **346**(6284): p. 567-9.
28. Grabner, M., et al., *The II-III loop of the skeletal muscle dihydropyridine receptor is responsible for the Bi-directional coupling with the ryanodine receptor.* J Biol Chem, 1999. **274**(31): p. 21913-9.
29. Fill, M., et al., *Ryanodine receptor adaptation.* J Gen Physiol, 2000. **116**(6): p. 873-82.
30. Lanner, J.T., et al., *Ryanodine receptors: structure, expression, molecular details, and function in calcium release.* Cold Spring Harb Perspect Biol, 2010. **2**(11): p. a003996.
31. Takeshima, H., et al., *Primary structure and expression from complementary DNA of skeletal muscle ryanodine receptor.* Nature, 1989. **339**(6224): p. 439-45.
32. Zorzato, F., et al., *Molecular cloning of cDNA encoding human and rabbit forms of the Ca2+ release channel (ryanodine receptor) of skeletal muscle sarcoplasmic reticulum.* J Biol Chem, 1990. **265**(4): p. 2244-56.
33. Nakai, J., et al., *Primary structure and functional expression from cDNA of the cardiac ryanodine receptor/calcium release channel.* FEBS Lett, 1990. **271**(1-2): p. 169-77.
34. Otsu, K., et al., *Molecular cloning of cDNA encoding the Ca2+ release channel (ryanodine receptor) of rabbit cardiac muscle sarcoplasmic reticulum.* J Biol Chem, 1990. **265**(23): p. 13472-83.
35. Hakamata, Y., et al., *Primary structure and distribution of a novel ryanodine receptor/calcium release channel from rabbit brain.* FEBS Lett, 1992. **312**(2-3): p. 229-35.
36. Marks, A.R., S.O. Marx, and S. Reiken, *Regulation of ryanodine receptors via macromolecular complexes: a novel role for leucine/isoleucine zippers.* Trends Cardiovasc Med, 2002. **12**(4): p. 166-70.
37. Franzini-Armstrong, C. and A.O. Jorgensen, *Structure and development of E-C coupling units in skeletal muscle.* Annu Rev Physiol, 1994. **56**: p. 509-34.
38. Bers, D.M., *Macromolecular complexes regulating cardiac ryanodine receptor function.* J Mol Cell Cardiol, 2004. **37**(2): p. 417-29.
39. Serysheva, II, et al., *Structure of Ca2+ release channel at 14 A resolution.* J Mol Biol, 2005. **345**(3): p. 427-31.
40. Sorrentino, V. and P. Volpe, *Ryanodine receptors: how many, where and why?* Trends Pharmacol Sci, 1993. **14**(3): p. 98-103.
41. Yano, M., *Ryanodine receptor as a new therapeutic target of heart failure and lethal arrhythmia.* Circ J, 2008. **72**(4): p. 509-14.

42. Radermacher, M., et al., *Cryo-EM of the native structure of the calcium release channel/ryanodine receptor from sarcoplasmic reticulum.* Biophys J, 1992. **61**(4): p. 936-40.
43. Radermacher, M., et al., *Cryo-electron microscopy and three-dimensional reconstruction of the calcium release channel/ryanodine receptor from skeletal muscle.* J Cell Biol, 1994. **127**(2): p. 411-23.
44. Samso, M., T. Wagenknecht, and P.D. Allen, *Internal structure and visualization of transmembrane domains of the RyR1 calcium release channel by cryo-EM.* Nat Struct Mol Biol, 2005. **12**(6): p. 539-44.
45. Serysheva, II, et al., *Subnanometer-resolution electron cryomicroscopy-based domain models for the cytoplasmic region of skeletal muscle RyR channel.* Proc Natl Acad Sci U S A, 2008. **105**(28): p. 9610-5.
46. Samso, M., et al., *Coordinated movement of cytoplasmic and transmembrane domains of RyR1 upon gating.* PLoS Biol, 2009. **7**(4): p. e85.
47. Franzini-Armstrong, C., *STUDIES OF THE TRIAD : I. Structure of the Junction in Frog Twitch Fibers.* J Cell Biol, 1970. **47**(2): p. 488-99.
48. Efremov, R.G., et al., *Architecture and conformational switch mechanism of the ryanodine receptor.* Nature, 2015. **517**(7532): p. 39-43.
49. Van Petegem, F., *Ryanodine receptors: allosteric ion channel giants.* J Mol Biol, 2015. **427**(1): p. 31-53.
50. Scheres, S.H., *RELION: implementation of a Bayesian approach to cryo-EM structure determination.* J Struct Biol, 2012. **180**(3): p. 519-30.
51. Bai, X.C., et al., *Ribosome structures to near-atomic resolution from thirty thousand cryo-EM particles.* Elife, 2013. **2**: p. e00461.
52. Li, X., et al., *Electron counting and beam-induced motion correction enable near-atomic-resolution single-particle cryo-EM.* Nat Methods, 2013. **10**(6): p. 584-90.
53. Yan, Z., et al., *Structure of the rabbit ryanodine receptor RyR1 at near-atomic resolution.* Nature, 2015. **517**(7532): p. 50-5.
54. Groves, M.R. and D. Barford, *Topological characteristics of helical repeat proteins.* Curr Opin Struct Biol, 1999. **9**(3): p. 383-9.
55. Zalk, R., et al., *Structure of a mammalian ryanodine receptor.* Nature, 2015. **517**(7532): p. 44-9.
56. Xiong, L., et al., *A Ca2+-binding domain in RyR1 that interacts with the calmodulin binding site and modulates channel activity.* Biophys J, 2006. **90**(1): p. 173-82.
57. Zalk, R., S.E. Lehnart, and A.R. Marks, *Modulation of the ryanodine receptor and intracellular calcium.* Annu Rev Biochem, 2007. **76**: p. 367-85.
58. Laver, D.R., *Luminal Ca(2+) activation of cardiac ryanodine receptors by luminal and cytoplasmic domains.* Eur Biophys J, 2009. **39**(1): p. 19-26.
59. Laver, D.R. and B.N. Honen, *Luminal Mg2+, a key factor controlling RYR2-mediated Ca2+ release: cytoplasmic and luminal regulation modeled in a tetrameric channel.* J Gen Physiol, 2008. **132**(4): p. 429-46.
60. Laver, D.R., E.R. O'Neill, and G.D. Lamb, *Luminal Ca2+-regulated Mg2+ inhibition of skeletal RyRs reconstituted as isolated channels or coupled clusters.* J Gen Physiol, 2004. **124**(6): p. 741-58.
61. Laver, D.R., et al., *Cytoplasmic Ca2+ inhibits the ryanodine receptor from cardiac muscle.* J Membr Biol, 1995. **147**(1): p. 7-22.
62. Laver, D.R., G.K. Lenz, and G.D. Lamb, *Regulation of the calcium release channel from rabbit skeletal muscle by the nucleotides ATP, AMP, IMP and adenosine.* J Physiol, 2001. **537**(Pt 3): p. 763-78.
63. Lamb, G.D., *Voltage-sensor control of Ca2+ release in skeletal muscle: insights from skinned fibers.* Front Biosci, 2002. **7**: p. d834-42.

64. Meissner, G. and J.S. Henderson, *Rapid calcium release from cardiac sarcoplasmic reticulum vesicles is dependent on Ca2+ and is modulated by Mg2+, adenine nucleotide, and calmodulin.* J Biol Chem, 1987. **262**(7): p. 3065-73.
65. Sitsapesan, R. and A.J. Williams, *Regulation of current flow through ryanodine receptors by luminal Ca2+.* J Membr Biol, 1997. **159**(3): p. 179-85.
66. Gyorke, I. and S. Gyorke, *Regulation of the cardiac ryanodine receptor channel by luminal Ca2+ involves luminal Ca2+ sensing sites.* Biophys J, 1998. **75**(6): p. 2801-10.
67. Sitsapesan, R. and A.J. Williams, *The gating of the sheep skeletal sarcoplasmic reticulum Ca(2+)-release channel is regulated by luminal Ca2+.* J Membr Biol, 1995. **146**(2): p. 133-44.
68. Sitsapesan, R. and A.J. Williams, *Regulation of the gating of the sheep cardiac sarcoplasmic reticulum Ca(2+)-release channel by luminal Ca2+.* J Membr Biol, 1994. **137**(3): p. 215-26.
69. Tripathy, A. and G. Meissner, *Sarcoplasmic reticulum lumenal Ca2+ has access to cytosolic activation and inactivation sites of skeletal muscle Ca2+ release channel.* Biophys J, 1996. **70**(6): p. 2600-15.
70. Xu, L. and G. Meissner, *Regulation of cardiac muscle Ca2+ release channel by sarcoplasmic reticulum lumenal Ca2+.* Biophys J, 1998. **75**(5): p. 2302-12.
71. Laver, D.R., *Ca2+ stores regulate ryanodine receptor Ca2+ release channels via luminal and cytosolic Ca2+ sites.* Biophys J, 2007. **92**(10): p. 3541-55.
72. Meissner, G., *Ryanodine receptor/Ca2+ release channels and their regulation by endogenous effectors.* Annu Rev Physiol, 1994. **56**: p. 485-508.
73. Meissner, G., *Ryanodine activation and inhibition of the Ca2+ release channel of sarcoplasmic reticulum.* J Biol Chem, 1986. **261**(14): p. 6300-6.
74. Smith, J.S., R. Coronado, and G. Meissner, *Sarcoplasmic reticulum contains adenine nucleotide-activated calcium channels.* Nature, 1985. **316**(6027): p. 446-9.
75. Ashley, R.H. and A.J. Williams, *Divalent cation activation and inhibition of single calcium release channels from sheep cardiac sarcoplasmic reticulum.* J Gen Physiol, 1990. **95**(5): p. 981-1005.
76. Smith, J.S., R. Coronado, and G. Meissner, *Single channel measurements of the calcium release channel from skeletal muscle sarcoplasmic reticulum. Activation by Ca2+ and ATP and modulation by Mg2+.* J Gen Physiol, 1986. **88**(5): p. 573-88.
77. Meissner, G., *Adenine nucleotide stimulation of Ca2+-induced Ca2+ release in sarcoplasmic reticulum.* J Biol Chem, 1984. **259**(4): p. 2365-74.
78. Nagasaki, K. and M. Kasai, *Fast release of calcium from sarcoplasmic reticulum vesicles monitored by chlortetracycline fluorescence.* J Biochem, 1983. **94**(4): p. 1101-9.
79. Kermode, H., A.J. Williams, and R. Sitsapesan, *The interactions of ATP, ADP, and inorganic phosphate with the sheep cardiac ryanodine receptor.* Biophys J, 1998. **74**(3): p. 1296-304.
80. Laver, D.R., *Regulation of RyR Channel Gating by Ca(2+), Mg(2+) and ATP.* Curr Top Membr, 2010. **66**: p. 69-89.
81. Williams, A.J. and R.H. Ashley, *Reconstitution of cardiac sarcoplasmic reticulum calcium channels.* Ann N Y Acad Sci, 1989. **560**: p. 163-73.
82. Lamb, G.D. and D.G. Stephenson, *Effect of Mg2+ on the control of Ca2+ release in skeletal muscle fibres of the toad.* J Physiol, 1991. **434**: p. 507-28.
83. Lamb, G.D. and D.G. Stephenson, *Effects of intracellular pH and [Mg2+] on excitation-contraction coupling in skeletal muscle fibres of the rat.* J Physiol, 1994. **478 (Pt 2)**: p. 331-9.
84. Xin, H.B., et al., *Affinity purification of the ryanodine receptor/calcium release channel from fast twitch skeletal muscle based on its tight association with FKBP12.* Biochem Biophys Res Commun, 1995. **214**(1): p. 263-70.

85. Cornea, R.L., et al., *Mapping the ryanodine receptor FK506-binding protein subunit using fluorescence resonance energy transfer.* J Biol Chem, 2010. **285**(25): p. 19219-26.
86. Brilliantes, A.-M.B., et al., *Stabilization of calcium release channel (ryanodine receptor) function by FK506-binding protein.* Cell, 1994. **77**: p. 513-523.
87. Sewell, T.J., et al., *Inhibition of calcineurin by a novel FK-506-binding protein.* J Biol Chem, 1994. **269**(33): p. 21094-102.
88. Bers, D.M., *Macromolecular complexes regulating cardiac ryanodine receptor function.* Journal of Molecular and Cellular Cardiology, 2004. **37**: p. 417-429.
89. Marks, A.R., *Intracellular calcium-release channels: regulators of cell life and death.* Am J Physiol, 1997. **272**(2 Pt 2): p. H597-605.
90. Galfre, E., et al., *FKBP12 activates the cardiac ryanodine receptor Ca2+-release channel and is antagonised by FKBP12.6.* PLoS One, 2012. **7**(2): p. e31956.
91. Bultynck, G., et al., *The conserved sites for the FK506-binding proteins in ryanodine receptors and inositol 1,4,5-trisphosphate receptors are structurally and functionally different.* J Biol Chem, 2001. **276**(50): p. 47715-24.
92. Marx, S.O., et al., *PKA phosphorylation dissociates FKBP12.6 from the calcium release channel (ryanodine receptor): defective regulation in failing hearts.* Cell, 2000. **101**(4): p. 365-76.
93. Masumiya, H., et al., *Localization of the 12.6-kDa FK506-binding protein (FKBP12.6) binding site to the NH2-terminal domain of the cardiac Ca2+ release channel (ryanodine receptor).* J Biol Chem, 2003. **278**(6): p. 3786-92.
94. Jayaraman, T., et al., *FK506 binding protein associated with the calcium release channel (ryanodine receptor).* J. Biol. Chem., 1992. **267**: p. 9474-9477.
95. Timerman, A.P., et al., *The calcium release channel of sarcoplasmic reticulum is modulated by FK-506-binding protein. Dissociation and reconstitution of FKBP-12 to the calcium release channel of skeletal muscle sarcoplasmic reticulum.* J Biol Chem, 1993. **268**(31): p. 22992-9.
96. Timerman, A.P., et al., *Selective binding of FKBP12.6 by the cardiac ryanodine receptor.* J Biol Chem, 1996. **271**(34): p. 20385-91.
97. Marx, S.O. and A.R. Marks, *Dysfunctional ryanodine receptors in the heart: new insights into complex cardiovascular diseases.* J Mol Cell Cardiol, 2013. **58**: p. 225-31.
98. Ma, J., M.B. Bhat, and J. Zhao, *Rectification of skeletal muscle ryanodine receptor mediated by FK506 binding protein.* Biophys. J., 1995. **69**: p. 2398-2404.
99. Kaftan, E., A.R. Marks, and B.E. Ehrlich, *Effects of rapamycin on ryanodine receptor/Ca(2+)-release channels from cardiac muscle.* Circ Res, 1996. **78**(6): p. 990-7.
100. Xiao, R.P., et al., *The immunophilin FK506-binding protein modulates Ca2+ release channel closure in rat heart.* J Physiol, 1997. **500 (Pt 2)**: p. 343-54.
101. Wehrens, X.H., et al., *FKBP12.6 deficiency and defective calcium release channel (ryanodine receptor) function linked to exercise-induced sudden cardiac death.* Cell, 2003. **113**(7): p. 829-40.
102. Barg, S., J.A. Copello, and S. Fleischer, *Different interactions of cardiac and skeletal muscle ryanodine receptors with FK-506 binding protein isoforms.* Am J Physiol, 1997. **272**(5 Pt 1): p. C1726-33.
103. Reiken, S., et al., *beta-adrenergic receptor blockers restore cardiac calcium release channel (ryanodine receptor) structure and function in heart failure.* Circulation, 2001. **104**(23): p. 2843-8.
104. Ono, K., et al., *Altered interaction of FKBP12.6 with ryanodine receptor as a cause of abnormal Ca(2+) release in heart failure.* Cardiovasc Res, 2000. **48**(2): p. 323-31.
105. Yano, M., et al., *Altered stoichiometry of FKBP12.6 versus ryanodine receptor as a cause of abnormal Ca(2+) leak through ryanodine receptor in heart failure.* Circulation, 2000. **102**(17): p. 2131-6.

106. Wehrens, X.H., et al., *Ca2+/calmodulin-dependent protein kinase II phosphorylation regulates the cardiac ryanodine receptor.* Circ Res, 2004. **94**(6): p. e61-70.
107. Marx, S.O., et al., *Phosphorylation-dependent regulation of ryanodine receptors: a novel role for leucine/isoleucine zippers.* J Cell Biol, 2001. **153**(4): p. 699-708.
108. Hain, J., et al., *Phosphorylation modulates the function of the calcium release channel of sarcoplasmic reticulum from cardiac muscle.* J Biol Chem, 1995. **270**(5): p. 2074-81.
109. Valdivia, H.H., et al., *Rapid adaptation of cardiac ryanodine receptors: modulation by Mg2+ and phosphorylation.* Science, 1995. **267**(5206): p. 1997-2000.
110. Uehara, A., et al., *Gating kinetics and ligand sensitivity modified by phosphorylation of cardiac ryanodine receptors.* Pflugers Arch, 2002. **444**(1-2): p. 202-12.
111. Reiken, S., et al., *Protein kinase A phosphorylation of the cardiac calcium release channel (ryanodine receptor) in normal and failing hearts. Role of phosphatases and response to isoproterenol.* J Biol Chem, 2003. **278**(1): p. 444-53.
112. Carter, S., J. Colyer, and R. Sitsapesan, *Maximum phosphorylation of the cardiac ryanodine receptor at serine-2809 by protein kinase a produces unique modifications to channel gating and conductance not observed at lower levels of phosphorylation.* Circ Res, 2006. **98**(12): p. 1506-13.
113. Ullrich, N.D., H.H. Valdivia, and E. Niggli, *PKA phosphorylation of cardiac ryanodine receptor modulates SR luminal Ca2+ sensitivity.* J Mol Cell Cardiol, 2012. **53**(1): p. 33-42.
114. Xiao, B., et al., *Functional consequence of protein kinase A-dependent phosphorylation of the cardiac ryanodine receptor: sensitization of store overload-induced Ca2+ release.* J Biol Chem, 2007. **282**(41): p. 30256-64.
115. Reiken, S., et al., *PKA phosphorylation activates the calcium release channel (ryanodine receptor) in skeletal muscle: defective regulation in heart failure.* J Cell Biol, 2003. **160**(6): p. 919-28.
116. Gaburjakova, M., et al., *FKBP12 binding modulates ryanodine receptor channel gating.* J Biol Chem, 2001. **276**(20): p. 16931-5.
117. Maier, L.S. and D.M. Bers, *Calcium, calmodulin, and calcium-calmodulin kinase II: heartbeat to heartbeat and beyond.* J Mol Cell Cardiol, 2002. **34**(8): p. 919-39.
118. Braun, A.P. and H. Schulman, *The multifunctional calcium/calmodulin-dependent protein kinase: from form to function.* Annu Rev Physiol, 1995. **57**: p. 417-45.
119. Colbran, R.J. and T.R. Soderling, *Calcium/calmodulin-dependent protein kinase II.* Curr Top Cell Regul, 1990. **31**: p. 181-221.
120. Bronstein, J.M., D.B. Farber, and C.G. Wasterlain, *Regulation of type-II calmodulin kinase: functional implications.* Brain Res Brain Res Rev, 1993. **18**(1): p. 135-47.
121. Miller, S.G. and M.B. Kennedy, *Regulation of brain type II Ca2+/calmodulin-dependent protein kinase by autophosphorylation: a Ca2+-triggered molecular switch.* Cell, 1986. **44**(6): p. 861-70.
122. Lai, Y., A.C. Nairn, and P. Greengard, *Autophosphorylation reversibly regulates the Ca2+/calmodulin-dependence of Ca2+/calmodulin-dependent protein kinase II.* Proc Natl Acad Sci U S A, 1986. **83**(12): p. 4253-7.
123. Lou, L.L., S.J. Lloyd, and H. Schulman, *Activation of the multifunctional Ca2+/calmodulin-dependent protein kinase by autophosphorylation: ATP modulates production of an autonomous enzyme.* Proc Natl Acad Sci U S A, 1986. **83**(24): p. 9497-501.
124. Schworer, C.M., R.J. Colbran, and T.R. Soderling, *Reversible generation of a Ca2+-independent form of Ca2+(calmodulin)-dependent protein kinase II by an autophosphorylation mechanism.* J Biol Chem, 1986. **261**(19): p. 8581-4.
125. Witcher, D.R., et al., *Unique phosphorylation site on the cardiac ryanodine receptor regulates calcium channel activity.* J Biol Chem, 1991. **266**(17): p. 11144-52.

126. Lokuta, A.J., et al., *Modulation of cardiac ryanodine receptors of swine and rabbit by a phosphorylation-dephosphorylation mechanism.* J Physiol, 1995. **487 (Pt 3)**: p. 609-22.
127. Li, L., et al., *The effect of Ca(2+)-calmodulin-dependent protein kinase II on cardiac excitation-contraction coupling in ferret ventricular myocytes.* J Physiol, 1997. **501 (Pt 1)**: p. 17-31.
128. Huke, S. and D.M. Bers, *Temporal dissociation of frequency-dependent acceleration of relaxation and protein phosphorylation by CaMKII.* J Mol Cell Cardiol, 2007. **42**(3): p. 590-9.
129. Aydin, J., et al., *Activation of Ca(2+)-dependent protein kinase II during repeated contractions in single muscle fibres from mouse is dependent on the frequency of sarcoplasmic reticulum Ca(2+) release.* Acta Physiol (Oxf), 2007. **191**(2): p. 131-7.
130. Shi, Y., *Serine/threonine phosphatases: mechanism through structure.* Cell, 2009. **139**(3): p. 468-84.
131. Endo, S., et al., *Multiple structural elements define the specificity of recombinant human inhibitor-1 as a protein phosphatase-1 inhibitor.* Biochemistry, 1996. **35**(16): p. 5220-8.
132. Foulkes, J.G., et al., *A kinetic analysis of the effects of inhibitor-1 and inhibitor-2 on the activity of protein phosphatase-1.* Eur J Biochem, 1983. **132**(2): p. 309-13.
133. Franzini-Armstrong, C., L.J. Kenney, and E. Varriano-Marston, *The structure of calsequestrin in triads of vertebrate skeletal muscle: a deep-etch study.* J Cell Biol, 1987. **105**(1): p. 49-56.
134. Beard, N.A., D.R. Laver, and A.F. Dulhunty, *Calsequestrin and the calcium release channel of skeletal and cardiac muscle.* Prog Biophys Mol Biol, 2004. **85**(1): p. 33-69.
135. Beard, N.A., et al., *Calsequestrin is an inhibitor of skeletal muscle ryanodine receptor calcium release channels.* Biophys J, 2002. **82**(1 Pt 1): p. 310-20.
136. Zhang, L., et al., *Complex formation between junctin, triadin, calsequestrin, and the ryanodine receptor. Proteins of the cardiac junctional sarcoplasmic reticulum membrane.* J Biol Chem, 1997. **272**(37): p. 23389-97.
137. Mitchell, R.D., H.K. Simmerman, and L.R. Jones, *Ca2+ binding effects on protein conformation and protein interactions of canine cardiac calsequestrin.* J Biol Chem, 1988. **263**(3): p. 1376-81.
138. Park, H., et al., *Polymerization of calsequestrin. Implications for Ca2+ regulation.* J Biol Chem, 2003. **278**(18): p. 16176-82.
139. Fryer, M.W. and D.G. Stephenson, *Total and sarcoplasmic reticulum calcium contents of skinned fibres from rat skeletal muscle.* J Physiol, 1996. **493 (Pt 2)**: p. 357-70.
140. Wang, S., et al., *Crystal structure of calsequestrin from rabbit skeletal muscle sarcoplasmic reticulum.* Nat Struct Biol, 1998. **5**(6): p. 476-83.
141. Knollmann, B.C., *New roles of calsequestrin and triadin in cardiac muscle.* J Physiol, 2009. **587**(Pt 13): p. 3081-7.
142. Wei, L., et al., *The conformation of calsequestrin determines its ability to regulate skeletal ryanodine receptors.* Biophys J, 2006. **91**(4): p. 1288-301.
143. Gyorke, I., et al., *The role of calsequestrin, triadin, and junctin in conferring cardiac ryanodine receptor responsiveness to luminal calcium.* Biophys J, 2004. **86**(4): p. 2121-8.
144. Terentyev, D., et al., *Triadin overexpression stimulates excitation-contraction coupling and increases predisposition to cellular arrhythmia in cardiac myocytes.* Circ Res, 2005. **96**(6): p. 651-8.
145. Chopra, N., et al., *Ablation of triadin causes loss of cardiac Ca2+ release units, impaired excitation-contraction coupling, and cardiac arrhythmias.* Proc Natl Acad Sci U S A, 2009. **106**(18): p. 7636-41.
146. Kirchhefer, U., et al., *Impaired relaxation in transgenic mice overexpressing junctin.* Cardiovasc Res, 2003. **59**(2): p. 369-79.

147. Yuan, Q., et al., *Sarcoplasmic reticulum calcium overloading in junctin deficiency enhances cardiac contractility but increases ventricular automaticity.* Circulation, 2007. **115**(3): p. 300-9.
148. Meyers, M.B., et al., *Association of sorcin with the cardiac ryanodine receptor.* J Biol Chem, 1995. **270**(44): p. 26411-8.
149. Meyers, M.B., et al., *Sorcin associates with the pore-forming subunit of voltage-dependent L-type Ca2+ channels.* J Biol Chem, 1998. **273**(30): p. 18930-5.
150. Farrell, E.F., et al., *Sorcin inhibits calcium release and modulates excitation-contraction coupling in the heart.* J Biol Chem, 2003. **278**(36): p. 34660-6.
151. Lokuta, A.J., et al., *Modulation of cardiac ryanodine receptors by sorcin.* J Biol Chem, 1997. **272**(40): p. 25333-8.
152. Seidler, T., et al., *Effects of adenovirus-mediated sorcin overexpression on excitation-contraction coupling in isolated rabbit cardiomyocytes.* Circ Res, 2003. **93**(2): p. 132-9.
153. Valdivia, H.H., *Modulation of intracellular Ca2+ levels in the heart by sorcin and FKBP12, two accessory proteins of ryanodine receptors.* Trends Pharmacol Sci, 1998. **19**(12): p. 479-82.
154. Anthony, D.F., et al., *Interaction of calcium/calmodulin-dependent protein kinase IIdeltaC with sorcin indirectly modulates ryanodine receptor function in cardiac myocytes.* J Mol Cell Cardiol, 2007. **43**(4): p. 492-503.
155. Moore, B.W., *A soluble protein characteristic of the nervous system.* Biochem Biophys Res Commun, 1965. **19**(6): p. 739-44.
156. Prosser, B.L., E.O. Hernandez-Ochoa, and M.F. Schneider, *S100A1 and calmodulin regulation of ryanodine receptor in striated muscle.* Cell Calcium, 2011. **50**(4): p. 323-31.
157. Wright, N.T., et al., *The three-dimensional solution structure of Ca(2+)-bound S100A1 as determined by NMR spectroscopy.* J Mol Biol, 2005. **353**(2): p. 410-26.
158. Rustandi, R.R., et al., *Three-dimensional solution structure of the calcium-signaling protein apo-S100A1 as determined by NMR.* Biochemistry, 2002. **41**(3): p. 788-96.
159. Wright, N.T., et al., *S100A1 and calmodulin compete for the same binding site on ryanodine receptor.* J Biol Chem, 2008. **283**(39): p. 26676-83.
160. Goch, G., et al., *Affinity of S100A1 protein for calcium increases dramatically upon glutathionylation.* FEBS J, 2005. **272**(10): p. 2557-65.
161. Haimoto, H. and K. Kato, *S100a0 (alpha alpha) protein, a calcium-binding protein, is localized in the slow-twitch muscle fiber.* J Neurochem, 1987. **48**(3): p. 917-23.
162. Bers, D.M., *Calmodulin and S100A1 fine tune skeletal muscle E-C coupling. Focus on "Modulation of sarcoplasmic reticulum Ca2+ release in skeletal muscle expressing ryanodine receptor impaired in regulation by calmodulin and S100A1".* Am J Physiol Cell Physiol, 2011. **300**(5): p. C974-5.
163. Rebbeck, R.T., et al., *S100A1 does not compete with calmodulin for ryanodine receptor binding but structurally alters the ryanodine receptor/calmodulin complex.* J Biol Chem, 2016.
164. Remppis, A., et al., *Altered expression of the Ca(2+)-binding protein S100A1 in human cardiomyopathy.* Biochim Biophys Acta, 1996. **1313**(3): p. 253-7.
165. Most, P., et al., *Cardiac S100A1 protein levels determine contractile performance and propensity toward heart failure after myocardial infarction.* Circulation, 2006. **114**(12): p. 1258-68.
166. Pleger, S.T., et al., *S100A1 gene therapy preserves in vivo cardiac function after myocardial infarction.* Mol Ther, 2005. **12**(6): p. 1120-9.
167. Ritterhoff, J. and P. Most, *Targeting S100A1 in heart failure.* Gene Ther, 2012. **19**(6): p. 613-21.

168. Pepke, S., et al., *A dynamic model of interactions of Ca2+, calmodulin, and catalytic subunits of Ca2+/calmodulin-dependent protein kinase II.* PLoS Comput Biol, 2010. **6**(2): p. e1000675.
169. Wu, X. and D.M. Bers, *Free and bound intracellular calmodulin measurements in cardiac myocytes.* Cell Calcium, 2007. **41**(4): p. 353-64.
170. Saimi, Y. and C. Kung, *Calmodulin as an ion channel subunit.* Annu Rev Physiol, 2002. **64**: p. 289-311.
171. Babu, Y.S., et al., *Three-dimensional structure of calmodulin.* Nature, 1985. **315**(6014): p. 37-40.
172. Zhang, M. and H.J. Vogel, *Characterization of the calmodulin-binding domain of rat cerebellar nitric oxide synthase.* J Biol Chem, 1994. **269**(2): p. 981-5.
173. Barbato, G., et al., *Backbone dynamics of calmodulin studied by 15N relaxation using inverse detected two-dimensional NMR spectroscopy: the central helix is flexible.* Biochemistry, 1992. **31**(23): p. 5269-78.
174. Amelia, K., et al., *Analysis of common bean (Phaseolus vulgaris L., genotype BAT93) calmodulin cDNA using computational tools.* Pharmacognosy Res, 2015. **7**(2): p. 209-12.
175. Rhoads, A.R. and F. Friedberg, *Sequence motifs for calmodulin recognition.* FASEB J, 1997. **11**(5): p. 331-40.
176. Chin, D. and A.R. Means, *Calmodulin: a prototypical calcium sensor.* Trends Cell Biol, 2000. **10**(8): p. 322-8.
177. Fruen, B.R., et al., *Differential Ca(2+) sensitivity of skeletal and cardiac muscle ryanodine receptors in the presence of calmodulin.* Am J Physiol Cell Physiol, 2000. **279**(3): p. C724-33.
178. Yamaguchi, N., et al., *Molecular basis of calmodulin binding to cardiac muscle Ca(2+) release channel (ryanodine receptor).* J Biol Chem, 2003. **278**(26): p. 23480-6.
179. Tripathy, A., et al., *Calmodulin activation and inhibition of skeletal muscle Ca2+ release channel (ryanodine receptor).* Biophys J, 1995. **69**(1): p. 106-19.
180. Moore, C.P., et al., *Apocalmodulin and Ca2+ calmodulin bind to the same region on the skeletal muscle Ca2+ release channel.* Biochemistry, 1999. **38**(26): p. 8532-7.
181. Yamaguchi, N., C. Xin, and G. Meissner, *Identification of apocalmodulin and Ca2+-calmodulin regulatory domain in skeletal muscle Ca2+ release channel, ryanodine receptor.* J Biol Chem, 2001. **276**(25): p. 22579-85.
182. Gifford, J.L., M.P. Walsh, and H.J. Vogel, *Structures and metal-ion-binding properties of the Ca2+-binding helix-loop-helix EF-hand motifs.* Biochem J, 2007. **405**(2): p. 199-221.
183. Gangopadhyay, J.P. and N. Ikemoto, *Aberrant interaction of calmodulin with the ryanodine receptor develops hypertrophy in the neonatal cardiomyocyte.* Biochem J, 2011. **438**(2): p. 379-87.
184. sBalshaw, D.M., et al., *Calmodulin binding and inhibition of cardiac muscle calcium release channel (ryanodine receptor).* J Biol Chem, 2001. **276**(23): p. 20144-53.
185. Balshaw, D.M., N. Yamaguchi, and G. Meissner, *Modulation of intracellular calcium-release channels by calmodulin.* J Membr Biol, 2002. **185**(1): p. 1-8.
186. Balshaw, D.M., et al., *Calmodulin binding and inhibition of cardiac muscle calcium release channel (ryanodine receptor).* J Biol Chem, 2001. **276**(23): p. 20144-53.
187. Haiech, J., et al., *Restoration of the calcium binding activity of mutant calmodulins toward normal by the presence of a calmodulin binding structure.* J Biol Chem, 1991. **266**(6): p. 3427-31.
188. Gao, Z.H., et al., *Activation of four enzymes by two series of calmodulin mutants with point mutations in individual Ca2+ binding sites.* J Biol Chem, 1993. **268**(27): p. 20096-104.
189. Samso, M. and T. Wagenknecht, *Apocalmodulin and Ca2+-calmodulin bind to neighboring locations on the ryanodine receptor.* J Biol Chem, 2002. **277**(2): p. 1349-53.

190. Rodney, G.G., et al., *Calcium binding to calmodulin leads to an N-terminal shift in its binding site on the ryanodine Receptor.* J Biol Chem, 2001. **276**(3): p. 2069-74.
191. Yamaguchi, N., et al., *Different regions in skeletal and cardiac muscle ryanodine receptors are involved in transducing the functional effects of calmodulin.* J Biol Chem, 2004. **279**(35): p. 36433-9.
192. Yamaguchi, N., et al., *Calmodulin regulation and identification of calmodulin binding region of type-3 ryanodine receptor calcium release channel.* Biochemistry, 2005. **44**(45): p. 15074-81.
193. Huang, X., et al., *Calmodulin-binding locations on the skeletal and cardiac ryanodine receptors.* J Biol Chem, 2012. **287**(36): p. 30328-35.
194. Guo, T., et al., *Ca2+/Calmodulin-dependent protein kinase II phosphorylation of ryanodine receptor does affect calcium sparks in mouse ventricular myocytes.* Circ Res, 2006. **99**(4): p. 398-406.
195. Yamaguchi, N. and G. Meissner, *Does Ca2+/calmodulin-dependent protein kinase deltac activate or inhibit the cardiac ryanodine receptor ion channel?* Circ Res, 2007. **100**(3): p. 293-5.
196. Anderson, M.E., *Calcium and stunning: when, from where, and what next?* J Cardiovasc Electrophysiol, 2002. **13**(10): p. 1025-6.
197. Saucerman, J.J. and D.M. Bers, *Calmodulin mediates differential sensitivity of CaMKII and calcineurin to local Ca2+ in cardiac myocytes.* Biophys J, 2008. **95**(10): p. 4597-612.
198. Xu, L. and G. Meissner, *Mechanism of calmodulin inhibition of cardiac sarcoplasmic reticulum Ca2+ release channel (ryanodine receptor).* Biophys J, 2004. **86**(2): p. 797-804.
199. Rodney, G.G., et al., *The carboxy-terminal calcium binding sites of calmodulin control calmodulin's switch from an activator to an inhibitor of RYR1.* Biochemistry, 2001. **40**(41): p. 12430-5.
200. Hamilton, S.L., I. Serysheva, and G.M. Strasburg, *Calmodulin and Excitation-Contraction Coupling.* News Physiol Sci, 2000. **15**: p. 281-284.
201. Fruen, B.R., et al., *Regulation of the RYR1 and RYR2 Ca2+ release channel isoforms by Ca2+-insensitive mutants of calmodulin.* Biochemistry, 2003. **42**(9): p. 2740-7.
202. Boschek, C.B., et al., *Calcium occupancy of N-terminal sites within calmodulin induces inhibition of the ryanodine receptor calcium release channel.* Biochemistry, 2007. **46**(37): p. 10621-8.
203. Jiang, J., et al., *Site-specific modification of calmodulin Ca(2)(+) affinity tunes the skeletal muscle ryanodine receptor activation profile.* Biochem J, 2010. **432**(1): p. 89-99.
204. Wehrens, X.H. and A.R. Marks, *Novel therapeutic approaches for heart failure by normalizing calcium cycling.* Nat Rev Drug Discov, 2004. **3**(7): p. 565-73.
205. Xiao, B., et al., *Protein kinase A phosphorylation at serine-2808 of the cardiac Ca2+-release channel (ryanodine receptor) does not dissociate 12.6-kDa FK506-binding protein (FKBP12.6).* Circ Res, 2004. **94**(4): p. 487-95.
206. Seiler, S., et al., *High molecular weight proteins in cardiac and skeletal muscle junctional sarcoplasmic reticulum vesicles bind calmodulin, are phosphorylated, and are degraded by Ca2+-activated protease.* J Biol Chem, 1984. **259**(13): p. 8550-7.
207. Suko, J., et al., *Phosphorylation of serine 2843 in ryanodine receptor-calcium release channel of skeletal muscle by cAMP-, cGMP- and CaM-dependent protein kinase.* Biochim Biophys Acta, 1993. **1175**(2): p. 193-206.
208. Strand, M.A., C.F. Louis, and J.R. Mickelson, *Phosphorylation of the porcine skeletal and cardiac muscle sarcoplasmic reticulum ryanodine receptor.* Biochim Biophys Acta, 1993. **1175**(3): p. 319-26.

209. Chu, A., et al., *Specific association of calmodulin-dependent protein kinase and related substrates with the junctional sarcoplasmic reticulum of skeletal muscle.* Biochemistry, 1990. **29**(25): p. 5899-905.
210. Varsanyi, M. and H.E. Meyer, *Sarcoplasmic reticular Ca2+ release channel is phosphorylated at serine 2843 in intact rabbit skeletal muscle.* Biol Chem Hoppe Seyler, 1995. **376**(1): p. 45-9.
211. Sonnleitner, A., S. Fleischer, and H. Schindler, *Gating of the skeletal calcium release channel by ATP is inhibited by protein phosphatase 1 but not by Mg2+.* Cell Calcium, 1997. **21**(4): p. 283-90.
212. Dulhunty, A.F., et al., *Characteristics of irreversible ATP activation suggest that native skeletal ryanodine receptors can be phosphorylated via an endogenous CaMKII.* Biophys J, 2001. **81**(6): p. 3240-52.
213. Hain, J., et al., *Phosphorylation modulates the function of the calcium release channel of sarcoplasmic reticulum from skeletal muscle.* Biophys J, 1994. **67**(5): p. 1823-33.
214. Igami, K., N. Yamaguchi, and M. Kasai, *Regulation of depolarization-induced calcium release from skeletal muscle triads by cyclic AMP-dependent protein kinase.* Jpn J Physiol, 1999. **49**(1): p. 81-7.
215. Takasago, T., et al., *Regulation of the cardiac ryanodine receptor by protein kinase-dependent phosphorylation.* J Biochem, 1991. **109**(1): p. 163-70.
216. Takasago, T., T. Imagawa, and M. Shigekawa, *Phosphorylation of the cardiac ryanodine receptor by cAMP-dependent protein kinase.* J Biochem, 1989. **106**(5): p. 872-7.
217. Sutherland, E.W., *Studies on the mechanism of hormone action.* Science, 1972. **177**(4047): p. 401-8.
218. Yoshida, A., et al., *Phosphorylation of ryanodine receptors in rat myocytes during beta-adrenergic stimulation.* J Biochem, 1992. **111**(2): p. 186-90.
219. Xu, L., et al., *Activation of the cardiac calcium release channel (ryanodine receptor) by poly-S-nitrosylation.* Science, 1998. **279**(5348): p. 234-7.
220. Zima, A.V., J.A. Copello, and L.A. Blatter, *Differential modulation of cardiac and skeletal muscle ryanodine receptors by NADH.* FEBS Lett, 2003. **547**(1-3): p. 32-6.
221. Morad, M. and Y.J. Suzuki, *Redox regulation of cardiac muscle calcium signaling.* Antioxid Redox Signal, 2000. **2**(1): p. 65-71.
222. Menshikova, E.V. and G. Salama, *Cardiac ischemia oxidizes regulatory thiols on ryanodine receptors: captopril acts as a reducing agent to improve Ca2+ uptake by ischemic sarcoplasmic reticulum.* J Cardiovasc Pharmacol, 2000. **36**(5): p. 656-68.
223. Kawakami, M. and E. Okabe, *Superoxide anion radical-triggered Ca2+ release from cardiac sarcoplasmic reticulum through ryanodine receptor Ca2+ channel.* Mol Pharmacol, 1998. **53**(3): p. 497-503.
224. Ziolo, M.T., H. Katoh, and D.M. Bers, *Positive and negative effects of nitric oxide on Ca(2+) sparks: influence of beta-adrenergic stimulation.* Am J Physiol Heart Circ Physiol, 2001. **281**(6): p. H2295-303.
225. Barouch, L.A., et al., *Nitric oxide regulates the heart by spatial confinement of nitric oxide synthase isoforms.* Nature, 2002. **416**(6878): p. 337-9.
226. Xu, K.Y., et al., *Nitric oxide synthase in cardiac sarcoplasmic reticulum.* Proc Natl Acad Sci U S A, 1999. **96**(2): p. 657-62.
227. Arstall, M.A., et al., *Cytokine-mediated apoptosis in cardiac myocytes: the role of inducible nitric oxide synthase induction and peroxynitrite generation.* Circ Res, 1999. **85**(9): p. 829-40.
228. Zahradnikova, A., et al., *Inactivation of the cardiac ryanodine receptor calcium release channel by nitric oxide.* Cell Calcium, 1997. **22**(6): p. 447-54.
229. Stoyanovsky, D., et al., *Nitric oxide activates skeletal and cardiac ryanodine receptors.* Cell Calcium, 1997. **21**(1): p. 19-29.

230. Wang, P. and J.L. Zweier, *Measurement of nitric oxide and peroxynitrite generation in the postischemic heart. Evidence for peroxynitrite-mediated reperfusion injury.* J Biol Chem, 1996. **271**(46): p. 29223-30.
231. Cerrone, M., C. Napolitano, and S.G. Priori, *Catecholaminergic polymorphic ventricular tachycardia: A paradigm to understand mechanisms of arrhythmias associated to impaired Ca(2+) regulation.* Heart Rhythm, 2009. **6**(11): p. 1652-9.
232. Hayashi, M., et al., *The role of stress test for predicting genetic mutations and future cardiac events in asymptomatic relatives of catecholaminergic polymorphic ventricular tachycardia probands.* Europace, 2012. **14**(9): p. 1344-51.
233. Cerrone, M., et al., *Arrhythmogenic mechanisms in a mouse model of catecholaminergic polymorphic ventricular tachycardia.* Circ Res, 2007. **101**(10): p. 1039-48.
234. Cerrone, M., et al., *Bidirectional ventricular tachycardia and fibrillation elicited in a knock-in mouse model carrier of a mutation in the cardiac ryanodine receptor.* Circ Res, 2005. **96**(10): p. e77-82.
235. Jiang, D., et al., *Enhanced basal activity of a cardiac Ca2+ release channel (ryanodine receptor) mutant associated with ventricular tachycardia and sudden death.* Circ Res, 2002. **91**(3): p. 218-25.
236. Lahat, H., et al., *A missense mutation in a highly conserved region of CASQ2 is associated with autosomal recessive catecholamine-induced polymorphic ventricular tachycardia in Bedouin families from Israel.* Am J Hum Genet, 2001. **69**(6): p. 1378-84.
237. George, C.H., G.V. Higgs, and F.A. Lai, *Ryanodine receptor mutations associated with stress-induced ventricular tachycardia mediate increased calcium release in stimulated cardiomyocytes.* Circ Res, 2003. **93**(6): p. 531-40.
238. Nyegaard, M., et al., *Mutations in calmodulin cause ventricular tachycardia and sudden cardiac death.* Am J Hum Genet, 2012. **91**(4): p. 703-12.
239. Priori, S.G., et al., *Mutations in the cardiac ryanodine receptor gene (hRyR2) underlie catecholaminergic polymorphic ventricular tachycardia.* Circulation, 2001. **103**(2): p. 196-200.
240. Jiang, D., et al., *Enhanced store overload-induced Ca2+ release and channel sensitivity to luminal Ca2+ activation are common defects of RyR2 mutations linked to ventricular tachycardia and sudden death.* Circ Res, 2005. **97**(11): p. 1173-81.
241. Jiang, D., et al., *RyR2 mutations linked to ventricular tachycardia and sudden death reduce the threshold for store-overload-induced Ca2+ release (SOICR).* Proc Natl Acad Sci U S A, 2004. **101**(35): p. 13062-7.
242. Liu, Y., et al., *The CPVT-associated RyR2 mutation G230C enhances store overload-induced Ca2+ release and destabilizes the N-terminal domains.* Biochem J, 2013. **454**(1): p. 123-31.
243. Ikemoto, N. and T. Yamamoto, *Regulation of calcium release by interdomain interaction within ryanodine receptors.* Front Biosci, 2002. **7**: p. d671-83.
244. Uchinoumi, H., et al., *Catecholaminergic polymorphic ventricular tachycardia is caused by mutation-linked defective conformational regulation of the ryanodine receptor.* Circ Res, 2010. **106**(8): p. 1413-24.
245. Gyorke, S., *Molecular basis of catecholaminergic polymorphic ventricular tachycardia.* Heart Rhythm, 2009. **6**(1): p. 123-9.
246. Knollmann, B.C., et al., *Casq2 deletion causes sarcoplasmic reticulum volume increase, premature Ca2+ release, and catecholaminergic polymorphic ventricular tachycardia.* J Clin Invest, 2006. **116**(9): p. 2510-20.
247. Chopra, N., et al., *Modest reductions of cardiac calsequestrin increase sarcoplasmic reticulum Ca2+ leak independent of luminal Ca2+ and trigger ventricular arrhythmias in mice.* Circ Res, 2007. **101**(6): p. 617-26.

248. Kornyeyev, D., et al., *Calsequestrin 2 deletion shortens the refractoriness of Ca(2)(+) release and reduces rate-dependent Ca(2)(+)-alternans in intact mouse hearts.* J Mol Cell Cardiol, 2012. **52**(1): p. 21-31.
249. Ono, M., et al., *Dissociation of calmodulin from cardiac ryanodine receptor causes aberrant Ca(2+) release in heart failure.* Cardiovasc Res, 2010. **87**(4): p. 609-17.
250. Xu, X., et al., *Defective calmodulin binding to the cardiac ryanodine receptor plays a key role in CPVT-associated channel dysfunction.* Biochem Biophys Res Commun, 2010. **394**(3): p. 660-6.
251. Hwang, H.S., et al., *Divergent regulation of ryanodine receptor 2 calcium release channels by arrhythmogenic human calmodulin missense mutants.* Circ Res, 2014. **114**(7): p. 1114-24.
252. Heffron, J.J., *Malignant hyperthermia: biochemical aspects of the acute episode.* Br J Anaesth, 1988. **60**(3): p. 274-8.
253. Gronert, G.A., J. Mott, and J. Lee, *Aetiology of malignant hyperthermia.* Br J Anaesth, 1988. **60**(3): p. 253-67.
254. Halsall, P.J., P.A. Cain, and F.R. Ellis, *Retrospective analysis of anaesthetics received by patients before susceptibility to malignant hyperpyrexia was recognized.* Br J Anaesth, 1979. **51**(10): p. 949-54.
255. Mickelson, J.R., et al., *Abnormal sarcoplasmic reticulum ryanodine receptor in malignant hyperthermia.* J Biol Chem, 1988. **263**(19): p. 9310-5.
256. Jurkat-Rott, K., T. McCarthy, and F. Lehmann-Horn, *Genetics and pathogenesis of malignant hyperthermia.* Muscle Nerve, 2000. **23**(1): p. 4-17.
257. McCarthy, T.V., K.A. Quane, and P.J. Lynch, *Ryanodine receptor mutations in malignant hyperthermia and central core disease.* Hum Mutat, 2000. **15**(5): p. 410-7.
258. Sambuughin, N., et al., *Screening of the entire ryanodine receptor type 1 coding region for sequence variants associated with malignant hyperthermia susceptibility in the north american population.* Anesthesiology, 2005. **102**(3): p. 515-21.
259. Yano, M., *[Abnormal ryanodine receptor function in heart failure].* Nihon Yakurigaku Zasshi, 2005. **126**(6): p. 372-6.
260. Protasi, F., C. Paolini, and M. Dainese, *Calsequestrin-1: a new candidate gene for malignant hyperthermia and exertional/environmental heat stroke.* J Physiol, 2009. **587**(Pt 13): p. 3095-100.
261. Protasi, F., et al., *Lessons from calsequestrin-1 ablation in vivo: much more than a Ca(2+) buffer after all.* J Muscle Res Cell Motil, 2011. **32**(4-5): p. 257-70.
262. Dainese, M., et al., *Anesthetic- and heat-induced sudden death in calsequestrin-1-knockout mice.* FASEB J, 2009. **23**(6): p. 1710-20.
263. Capacchione, J.F., et al., *Exertional rhabdomyolysis and malignant hyperthermia in a patient with ryanodine receptor type 1 gene, L-type calcium channel alpha-1 subunit gene, and calsequestrin-1 gene polymorphisms.* Anesthesiology, 2010. **112**(1): p. 239-44.
264. Kraeva, N., et al., *CASQ1 gene is an unlikely candidate for malignant hyperthermia susceptibility in the North American population.* Anesthesiology, 2013. **118**(2): p. 344-9.
265. Carpenter, D., et al., *The role of CACNA1S in predisposition to malignant hyperthermia.* BMC Med Genet, 2009. **10**: p. 104.
266. Monnier, N., et al., *Presence of two different genetic traits in malignant hyperthermia families: implication for genetic analysis, diagnosis, and incidence of malignant hyperthermia susceptibility.* Anesthesiology, 2002. **97**(5): p. 1067-74.
267. Weiss, R.G., et al., *Functional analysis of the R1086H malignant hyperthermia mutation in the DHPR reveals an unexpected influence of the III-IV loop on skeletal muscle EC coupling.* Am J Physiol Cell Physiol, 2004. **287**(4): p. C1094-102.

268. Rosenberg, H., et al., *Malignant hyperthermia: a review.* Orphanet J Rare Dis, 2015. **10**: p. 93.
269. Gallant, E.M. and R.C. Jordan, *Porcine malignant hyperthermia: genotype and contractile threshold of immature muscles.* Muscle Nerve, 1996. **19**(1): p. 68-73.
270. Dietze, B., et al., *Malignant hyperthermia mutation Arg615Cys in the porcine ryanodine receptor alters voltage dependence of Ca2+ release.* J Physiol, 2000. **526 Pt 3**: p. 507-14.
271. Stamm, D.S., et al., *Native American myopathy: congenital myopathy with cleft palate, skeletal anomalies, and susceptibility to malignant hyperthermia.* Am J Med Genet A, 2008. **146A**(14): p. 1832-41.
272. Horstick, E.J., et al., *Stac3 is a component of the excitation-contraction coupling machinery and mutated in Native American myopathy.* Nat Commun, 2013. **4**: p. 1952.
273. Nelson, B.R., et al., *Skeletal muscle-specific T-tubule protein STAC3 mediates voltage-induced Ca2+ release and contractility.* Proc Natl Acad Sci U S A, 2013. **110**(29): p. 11881-6.
274. Polster, A., et al., *Stac adaptor proteins regulate trafficking and function of muscle and neuronal L-type Ca2+ channels.* Proc Natl Acad Sci U S A, 2015. **112**(2): p. 602-6.
275. Richter, M., et al., *Functional characterization of a distinct ryanodine receptor mutation in human malignant hyperthermia-susceptible muscle.* J Biol Chem, 1997. **272**(8): p. 5256-60.
276. Shomer, N.H., J.R. Mickelson, and C.F. Louis, *Caffeine stimulation of malignant hyperthermia-susceptible sarcoplasmic reticulum Ca2+ release channel.* Am J Physiol, 1994. **267**(5 Pt 1): p. C1253-61.
277. Kim, D.H., et al., *Kinetic studies of Ca2+ release from sarcoplasmic reticulum of normal and malignant hyperthermia susceptible pig muscles.* Biochim Biophys Acta, 1984. **775**(3): p. 320-7.
278. Fill, M., et al., *Abnormal ryanodine receptor channels in malignant hyperthermia.* Biophys J, 1990. **57**(3): p. 471-5.
279. Louis, C.F., et al., *The effects of volatile anesthetics on calcium regulation by malignant hyperthermia-susceptible sarcoplasmic reticulum.* Anesthesiology, 1992. **77**(1): p. 114-25.
280. Fruen, B.R., J.R. Mickelson, and C.F. Louis, *Dantrolene inhibition of sarcoplasmic reticulum Ca2+ release by direct and specific action at skeletal muscle ryanodine receptors.* J Biol Chem, 1997. **272**(43): p. 26965-71.
281. Laver, D.R., et al., *Reduced inhibitory effect of Mg2+ on ryanodine receptor-Ca2+ release channels in malignant hyperthermia.* Biophys J, 1997. **73**(4): p. 1913-24.
282. O'Driscoll, S., et al., *Calmodulin sensitivity of the sarcoplasmic reticulum ryanodine receptor from normal and malignant-hyperthermia-susceptible muscle.* Biochem J, 1996. **319 (Pt 2)**: p. 421-6.
283. Kobayashi, S., et al., *Dantrolene, a therapeutic agent for malignant hyperthermia, markedly improves the function of failing cardiomyocytes by stabilizing interdomain interactions within the ryanodine receptor.* J Am Coll Cardiol, 2009. **53**(21): p. 1993-2005.
284. Krause, T., et al., *Dantrolene--a review of its pharmacology, therapeutic use and new developments.* Anaesthesia, 2004. **59**(4): p. 364-73.
285. Loke, J. and D.H. MacLennan, *Malignant hyperthermia and central core disease: disorders of Ca2+ release channels.* Am J Med, 1998. **104**(5): p. 470-86.
286. Morgan, K.G. and S.H. Bryant, *The mechanism of action of dantrolene sodium.* J Pharmacol Exp Ther, 1977. **201**(1): p. 138-47.
287. Paul-Pletzer, K., et al., *Identification of a dantrolene-binding sequence on the skeletal muscle ryanodine receptor.* J Biol Chem, 2002. **277**(38): p. 34918-23.

288. Parness, J. and S.S. Palnitkar, *Identification of dantrolene binding sites in porcine skeletal muscle sarcoplasmic reticulum.* J Biol Chem, 1995. **270**(31): p. 18465-72.
289. Paul-Pletzer, K., et al., *Probing a putative dantrolene-binding site on the cardiac ryanodine receptor.* Biochem J, 2005. **387**(Pt 3): p. 905-9.
290. Wang, R., et al., *Localization of the dantrolene-binding sequence near the FK506-binding protein-binding site in the three-dimensional structure of the ryanodine receptor.* J Biol Chem, 2011. **286**(14): p. 12202-12.
291. Zhao, F., et al., *Dantrolene inhibition of ryanodine receptor Ca2+ release channels. Molecular mechanism and isoform selectivity.* J Biol Chem, 2001. **276**(17): p. 13810-6.
292. Diaz-Sylvester, P.L., M. Porta, and J.A. Copello, *Halothane modulation of skeletal muscle ryanodine receptors: dependence on Ca2+, Mg2+, and ATP.* Am J Physiol Cell Physiol, 2008. **294**(4): p. C1103-12.
293. Robinson, R., et al., *Mutations in RYR1 in malignant hyperthermia and central core disease.* Hum Mutat, 2006. **27**(10): p. 977-89.
294. Lanner, J.T., *Ryanodine receptor physiology and its role in disease.* Adv Exp Med Biol, 2012. **740**: p. 217-34.
295. Monnier, N., et al., *Malignant-hyperthermia susceptibility is associated with a mutation of the alpha 1-subunit of the human dihydropyridine-sensitive L-type voltage-dependent calcium-channel receptor in skeletal muscle.* Am J Hum Genet, 1997. **60**(6): p. 1316-25.
296. Pirone, A., et al., *Identification and functional characterization of malignant hyperthermia mutation T1354S in the outer pore of the Cavalpha1S-subunit.* Am J Physiol Cell Physiol, 2010. **299**(6): p. C1345-54.
297. Toppin, P.J., et al., *A report of fulminant malignant hyperthermia in a patient with a novel mutation of the CACNA1S gene.* Can J Anaesth, 2010. **57**(7): p. 689-93.
298. Zhao, X., et al., *Azumolene inhibits a component of store-operated calcium entry coupled to the skeletal muscle ryanodine receptor.* J Biol Chem, 2006. **281**(44): p. 33477-86.
299. Zhao, X., et al., *Increased store-operated Ca2+ entry in skeletal muscle with reduced calsequestrin-1 expression.* Biophys J, 2010. **99**(5): p. 1556-64.
300. Cherednichenko, G., et al., *Enhanced excitation-coupled calcium entry in myotubes expressing malignant hyperthermia mutation R163C is attenuated by dantrolene.* Mol Pharmacol, 2008. **73**(4): p. 1203-12.
301. Bannister, R.A., I.N. Pessah, and K.G. Beam, *The skeletal L-type Ca(2+) current is a major contributor to excitation-coupled Ca(2+) entry.* J Gen Physiol, 2009. **133**(1): p. 79-91.
302. Bannister, R.A. and K.G. Beam, *The cardiac alpha(1C) subunit can support excitation-triggered Ca2+ entry in dysgenic and dyspedic myotubes.* Channels (Austin), 2009. **3**(4): p. 268-73.
303. Ellis, K.O. and J.F. Carpenter, *Studies on the mechanism of action of dantrolene sodium. A skeletal muscle relaxant.* Naunyn Schmiedebergs Arch Pharmacol, 1972. **275**(1): p. 83-94.
304. Szentesi, P., et al., *Effects of dantrolene on steps of excitation-contraction coupling in mammalian skeletal muscle fibers.* J Gen Physiol, 2001. **118**(4): p. 355-75.
305. Prosser, B.L., et al., *The Qgamma component of intra-membrane charge movement is present in mammalian muscle fibres, but suppressed in the absence of S100A1.* J Physiol, 2009. **587**(Pt 18): p. 4523-41.
306. Bannister, R.A., *Dantrolene-induced inhibition of skeletal L-type Ca2+ current requires RyR1 expression.* Biomed Res Int, 2013. **2013**: p. 390493.
307. Avila, G. and R.T. Dirksen, *Functional impact of the ryanodine receptor on the skeletal muscle L-type Ca(2+) channel.* J Gen Physiol, 2000. **115**(4): p. 467-80.

308. Mickelson, J.R. and C.F. Louis, *Malignant hyperthermia: excitation-contraction coupling, Ca2+ release channel, and cell Ca2+ regulation defects.* Physiol Rev, 1996. **76**(2): p. 537-92.
309. Yamamoto, T. and N. Ikemoto, *Spectroscopic monitoring of local conformational changes during the intramolecular domain-domain interaction of the ryanodine receptor.* Biochemistry, 2002. **41**(5): p. 1492-501.
310. Yamamoto, T., R. El-Hayek, and N. Ikemoto, *Postulated role of interdomain interaction within the ryanodine receptor in Ca(2+) channel regulation.* J Biol Chem, 2000. **275**(16): p. 11618-25.
311. Kobayashi, S., et al., *Antibody probe study of Ca2+ channel regulation by interdomain interaction within the ryanodine receptor.* Biochem J, 2004. **380**(Pt 2): p. 561-9.
312. Murayama, T., et al., *Postulated role of interdomain interaction between regions 1 and 2 within type 1 ryanodine receptor in the pathogenesis of porcine malignant hyperthermia.* Biochem J, 2007. **402**(2): p. 349-57.
313. Kobayashi, S., et al., *Dantrolene stabilizes domain interactions within the ryanodine receptor.* J Biol Chem, 2005. **280**(8): p. 6580-7.
314. Kannankeril, P.J., et al., *Mice with the R176Q cardiac ryanodine receptor mutation exhibit catecholamine-induced ventricular tachycardia and cardiomyopathy.* Proc Natl Acad Sci U S A, 2006. **103**(32): p. 12179-84.
315. Oda, T., et al., *Defective regulation of interdomain interactions within the ryanodine receptor plays a key role in the pathogenesis of heart failure.* Circulation, 2005. **111**(25): p. 3400-10.
316. Ai, X., et al., *Ca2+/calmodulin-dependent protein kinase modulates cardiac ryanodine receptor phosphorylation and sarcoplasmic reticulum Ca2+ leak in heart failure.* Circ Res, 2005. **97**(12): p. 1314-22.
317. Terentyev, D., et al., *Redox modification of ryanodine receptors contributes to sarcoplasmic reticulum Ca2+ leak in chronic heart failure.* Circ Res, 2008. **103**(12): p. 1466-72.
318. Domeier, T.L., L.A. Blatter, and A.V. Zima, *Changes in intra-luminal calcium during spontaneous calcium waves following sensitization of ryanodine receptor channels.* Channels (Austin), 2010. **4**(2): p. 87-92.
319. Shannon, T.R., S.M. Pogwizd, and D.M. Bers, *Elevated sarcoplasmic reticulum Ca2+ leak in intact ventricular myocytes from rabbits in heart failure.* Circ Res, 2003. **93**(7): p. 592-4.
320. Pogwizd, S.M., et al., *Upregulation of Na(+)/Ca(2+) exchanger expression and function in an arrhythmogenic rabbit model of heart failure.* Circ Res, 1999. **85**(11): p. 1009-19.
321. Linder, M., et al., *Improved immobilization of fusion proteins via cellulose-binding domains.* Biotechnol Bioeng, 1998. **60**(5): p. 642-7.
322. Pieske, B., et al., *Ca2+ handling and sarcoplasmic reticulum Ca2+ content in isolated failing and nonfailing human myocardium.* Circ Res, 1999. **85**(1): p. 38-46.
323. Maxwell, J.T., T.L. Domeier, and L.A. Blatter, *Dantrolene prevents arrhythmogenic Ca2+ release in heart failure.* Am J Physiol Heart Circ Physiol, 2012. **302**(4): p. H953-63.
324. Zamiri, N., et al., *Dantrolene improves survival after ventricular fibrillation by mitigating impaired calcium handling in animal models.* Circulation, 2014. **129**(8): p. 875-85.
325. Ohta, T., S. Ito, and A. Ohga, *Inhibitory action of dantrolene on Ca-induced Ca2+ release from sarcoplasmic reticulum in guinea pig skeletal muscle.* Eur J Pharmacol, 1990. **178**(1): p. 11-9.
326. Palnitkar, S.S., et al., *[3H]Azidodantrolene: synthesis and use in identification of a putative skeletal muscle dantrolene binding site in sarcoplasmic reticulum.* J Med Chem, 1999. **42**(11): p. 1872-80.

327. Lacampagne, A., M.G. Klein, and M.F. Schneider, *Modulation of the frequency of spontaneous sarcoplasmic reticulum Ca2+ release events (Ca2+ sparks) by myoplasmic [Mg2+] in frog skeletal muscle.* J Gen Physiol, 1998. **111**(2): p. 207-24.
328. Herrmann-Frank, A., H.C. Luttgau, and D.G. Stephenson, *Caffeine and excitation-contraction coupling in skeletal muscle: a stimulating story.* J Muscle Res Cell Motil, 1999. **20**(2): p. 223-37.
329. Lamb, G.D. and D.G. Stephenson, *Control of calcium release from the sarcoplasmic reticulum.* Adv Exp Med Biol, 1992. **311**: p. 289-303.
330. Tong, J., et al., *Caffeine and halothane sensitivity of intracellular Ca2+ release is altered by 15 calcium release channel (ryanodine receptor) mutations associated with malignant hyperthermia and/or central core disease.* J Biol Chem, 1997. **272**(42): p. 26332-9.
331. Sitsapesan, R., et al., *Sheep cardiac sarcoplasmic reticulum calcium-release channels: modification of conductance and gating by temperature.* J Physiol, 1991. **434**: p. 469-88.
332. Miller, C. and E. Racker, *Ca++-induced fusion of fragmented sarcoplasmic reticulum with artificial planar bilayers.* J Membr Biol, 1976. **30**(3): p. 283-300.
333. Laver, D., *Electrical Methods for Determining Surface Charge Density and Electrolyte Composition at the Lipid Bilayer-Solution Interface.* Advances in Planar Lipid Bilayers and Liposomes, 2009. **9**: p. 87-105.
334. Miller, C. and E. Racker, *Ca^{++}-induced fusion of fragmented sarcoplasmic reticulum with artificial planar bilayers.* Cell, 1976. **9**: p. 283-300.
335. Mueller, P., et al., *Reconstitution of cell membrane structure in vitro and its transformation into an excitable system.* Nature, 1962. **194**: p. 979-80.
336. Laver, D., *The power of single channel recording and analysis: its application to ryanodine receptors in lipid bilayers.* Clin. Exp. Pharmacol. Physiol., 2001. **28**(8): p. 675-686.
337. Sies, H., *Glutathione and its role in cellular functions.* Free Radic Biol Med, 1999. **27**(9-10): p. 916-21.
338. Hwang, C., A.J. Sinskey, and H.F. Lodish, *Oxidized redox state of glutathione in the endoplasmic reticulum.* Science, 1992. **257**(5076): p. 1496-502.
339. Laver, D.R. and D.F. van Helden, *Three independent mechanisms contribute to tetracaine inhibition of cardiac calcium release channels.* J Mol Cell Cardiol, 2011. **51**(3): p. 357-69.
340. Smith, J.S., et al., *Purified ryanodine receptor from rabbit skeletal muscle is the calcium-release channel of sarcoplasmic reticulum.* J. Gen. Physiol., 1988. **92**: p. 1-26.
341. Tinker, A. and A.J. Williams, *Divalent cation conduction in the ryanodine receptor channel of sheep cardiac muscle sarcoplasmic reticulum.* J. Gen. Physiol., 1992. **100**: p. 479-493.
342. Smith, J.S., et al., *Purified ryanodine receptor from rabbit skeletal muscle is the calcium-release channel of sarcoplasmic reticulum.* J Gen Physiol, 1988. **92**(1): p. 1-26.
343. Coronado, R., et al., *Planar bilayer recording of ryanodine receptors of sarcoplasmic reticulum.* Methods Enzymol., 1992. **207**: p. 699-707.
344. Harrison, S.M. and D.M. Bers, *The effect of temperature and ionic strength on the apparent Ca- affinity of EGTA and the analogous Ca-chelators BAPTA and dibromo-BAPTA.* Biochim. Biophys. Acta, 1987. **925**: p. 133-143.
345. Brooks, S.P. and K.B. Storey, *Bound and determined: a computer program for making buffers of defined ion concentrations.* Anal Biochem, 1992. **201**(1): p. 119-26.
346. Marks, P.W. and F.R. Maxfield, *Preparation of solutions with free calcium concentration in the nanomolar range using 1,2-bis(o-aminophenoxy)ethane-N,N,N',N'-tetraacetic acid.* Anal. Biochem., 1991. **193**(1): p. 61-71.

347. Laver, D., *The power of single channel recording and analysis: its application to ryanodine receptors in lipid bilayers.* Clin Exp Pharmacol Physiol, 2001. **28**(8): p. 675-86.
348. Tsien, R.Y., *New calcium indicators and buffers with high selectivity against magnesium and protons: design, synthesis, and properties of prototype structures.* Biochemistry, 1980. **19**(11): p. 2396-404.
349. O'Neill, E.R., M.M. Sakowska, and D.R. Laver, *Regulation of the Calcium Release Channel from Skeletal Muscle by Suramin and the Disulfonated Stilbene Derivatives DIDS, DBDS, and DNDS.* Biophys. J., 2003. **84**(3): p. 1674-1689.
350. Franzini-Armstrong, C. and F. Protasi, *Ryanodine receptors of striated muscles: a complex channel capable of multiple interactions.* Physiol Rev, 1997. **77**(3): p. 699-729.
351. Fill, M. and J.A. Copello, *Ryanodine receptor calcium release channels.* Physiol Rev, 2002. **82**(4): p. 893-922.
352. Meissner, G., *Regulation of mammalian ryanodine receptors.* Front Biosci, 2002. **7**: p. d2072-80.
353. Coronado, R., et al., *Structure and function of ryanodine receptors.* Am J Physiol, 1994. **266**(6 Pt 1): p. C1485-504.
354. Meissner, G., *Molecular regulation of cardiac ryanodine receptor ion channel.* Cell Calcium, 2004. **35**(6): p. 621-8.
355. Yang, H.C., et al., *Calmodulin interaction with the skeletal muscle sarcoplasmic reticulum calcium channel protein.* Biochemistry, 1994. **33**(2): p. 518-25.
356. Wagenknecht, T., et al., *Localization of calmodulin binding sites on the ryanodine receptor from skeletal muscle by electron microscopy.* Biophys J, 1994. **67**(6): p. 2286-95.
357. Meissner, G., *Evidence of a role for calmodulin in the regulation of calcium release from skeletal muscle sarcoplasmic reticulum.* Biochemistry, 1986. **25**(1): p. 244-51.
358. Plank, B., et al., *Inhibition of calcium release from skeletal muscle sarcoplasmic reticulum by calmodulin.* Biochim Biophys Acta, 1988. **938**(1): p. 79-88.
359. Fuentes, O., et al., *Calcium-dependent block of ryanodine receptor channel of swine skeletal muscle by direct binding of calmodulin.* Cell Calcium, 1994. **15**(4): p. 305-16.
360. Damiani, E. and A. Margreth, *Pharmacological clues to calmodulin-mediated activation of skeletal ryanodine receptor using [3H]-ryanodine binding.* J Muscle Res Cell Motil, 2000. **21**(1): p. 1-8.
361. Buratti, R., et al., *Calcium dependent activation of skeletal muscle Ca2+ release channel (ryanodine receptor) by calmodulin.* Biochem Biophys Res Commun, 1995. **213**(3): p. 1082-90.
362. Rodney, G.G., et al., *Regulation of RYR1 activity by Ca(2+) and calmodulin.* Biochemistry, 2000. **39**(26): p. 7807-12.
363. Ford, L.E. and R.J. Podolsky, *Intracellular calcium movements in skinned muscle fibres.* J Physiol, 1972. **223**(1): p. 21-33.
364. Dunnett, J. and W.G. Nayler, *Calcium efflux from cardiac sarcoplasmic reticulum: effects of calcium and magnesium.* J Mol Cell Cardiol, 1978. **10**(5): p. 487-98.
365. MacLennan, D.H., *Ca2+ signalling and muscle disease.* Eur J Biochem, 2000. **267**(17): p. 5291-7.
366. Nelson, T.E., *Malignant hyperthermia: a pharmacogenetic disease of Ca++ regulating proteins.* Curr Mol Med, 2002. **2**(4): p. 347-69.
367. Louis, C.F., et al., *The effects of volatile anesthetics on calcium regulation by malignant hyperthermia-susceptible sarcoplasmic reticulum.* Anesthesiology, 1992. **77**(1): p. 114-125.
368. Nelson, T.E., *Halothane effects on human malignant hyperthermia skeletal muscle single calcium-release channels in planar lipid bilayers.* Anesthesiology, 1992. **76**(4): p. 588-95.

369. Jiang, D., et al., *Reduced threshold for luminal Ca2+ activation of RyR1 underlies a causal mechanism of porcine malignant hyperthermia.* J Biol Chem, 2008. **283**(30): p. 20813-20.
370. Shtifman, A., et al., *Interdomain interactions within ryanodine receptors regulate Ca2+ spark frequency in skeletal muscle.* J Gen Physiol, 2002. **119**(1): p. 15-32.
371. Laver, D.R., et al., *Cytoplasmic Ca^{2+} inhibits the ryanodine receptor from cardiac muscle.* J. Memb. Biol., 1995. **147**(1): p. 7-22.
372. Ikemoto, T., M. Iino, and M. Endo, *Enhancing effect of calmodulin on Ca(2+)-induced Ca2+ release in the sarcoplasmic reticulum of rabbit skeletal muscle fibres.* J Physiol, 1995. **487 (Pt 3)**: p. 573-82.
373. Ikemoto, T., et al., *Effect of calmodulin on Ca2+-induced Ca2+ release of skeletal muscle from mutant mice expressing either ryanodine receptor type 1 or type 3.* Pflugers Arch, 1998. **437**(1): p. 43-8.
374. Fabiato, A. and F. Fabiato, *Calcium release from the sarcoplasmic reticulum.* Circ Res, 1977. **40**(2): p. 119-29.
375. Oda, T., et al., *In cardiomyocytes, binding of unzipping peptide activates ryanodine receptor 2 and reciprocally inhibits calmodulin binding.* Circ Res, 2013. **112**(3): p. 487-97.
376. Hainaut, K. and J.E. Desmedt, *Effect of dantrolene sodium on calcium movements in single muscle fibres.* Nature, 1974. **252**(5485): p. 728-30.
377. McCarthy, T.V., et al., *Localization of the malignant hyperthermia susceptibility locus to human chromosome 19q12-13.2.* Nature, 1990. **343**(6258): p. 562-4.
378. Jung, C.B., et al., *Dantrolene rescues arrhythmogenic RYR2 defect in a patient-specific stem cell model of catecholaminergic polymorphic ventricular tachycardia.* EMBO Mol Med, 2012. **4**(3): p. 180-91.
379. Kobayashi, S., et al., *Dantrolene, a therapeutic agent for malignant hyperthermia, inhibits catecholaminergic polymorphic ventricular tachycardia in a RyR2(R2474S/+) knock-in mouse model.* Circ J, 2010. **74**(12): p. 2579-84.
380. Nelson, T.E., et al., *Dantrolene sodium can increase or attenuate activity of skeletal muscle ryanodine receptor calcium release channel. Clinical implications.* Anesthesiology, 1996. **84**(6): p. 1368-1379.
381. Wagner, L.E., 2nd, et al., *Characterization of ryanodine receptor type 1 single channel activity using "on-nucleus" patch clamp.* Cell Calcium, 2014. **56**(2): p. 96-107.
382. Chou, C.C., et al., *Dantrolene suppresses ventricular ectopy and arrhythmogenicity with acute myocardial infarction in a langendorff-perfused pacing-induced heart failure rabbit model.* J Cardiovasc Electrophysiol, 2014. **25**(4): p. 431-9.
383. Salata, J.J., J.A. Wasserstrom, and J. Jalife, *Dantrolene sodium: effects on isolated cardiac tissues.* J Mol Cell Cardiol, 1983. **15**(4): p. 233-43.
384. Balshaw, D.M., et al., *Calmodulin binding and inhibition of cardiac muscle calcium release channel (ryanodine receptor).* J. Biol. Chem., 2001. **276**(23): p. 20144-53.
385. Tripathy, A., et al., *Calmodulin activation and inhibition of skeletal muscle Ca^{2+} release channel (ryanodine receptor).* Biophys. J., 1995. **69**: p. 106-119.
386. Huang, X., et al., *Two potential calmodulin-binding sequences in the ryanodine receptor contribute to a mobile, intra-subunit calmodulin-binding domain.* J Cell Sci, 2013. **126**(Pt 19): p. 4527-35.
387. Guo, T., et al., *FRET detection of calmodulin binding to the cardiac RyR2 calcium release channel.* Biophys J, 2011. **101**(9): p. 2170-7.
388. Oo, Y.W., et al., *Essential Role of Calmodulin in RyR Inhibition by Dantrolene.* Mol Pharmacol, 2015. **88**(1): p. 57-63.
389. Walweel, K., et al., *Differences in the regulation of RyR2 from human, sheep, and rat by Ca(2)(+) and Mg(2)(+) in the cytoplasm and in the lumen of the sarcoplasmic reticulum.* J Gen Physiol, 2014. **144**(3): p. 263-71.

390. Yang, Y., et al., *Cardiac myocyte Z-line calmodulin is mainly RyR2-bound, and reduction is arrhythmogenic and occurs in heart failure.* Circ Res, 2014. **114**(2): p. 295-306.
391. Galimberti, E.S. and B.C. Knollmann, *Efficacy and potency of class I antiarrhythmic drugs for suppression of Ca(2+) waves in permeabilized myocytes lacking calsequestrin.* J Mol Cell Cardiol, 2011. **51**(5): p. 760-8.
392. Suetomi, T., et al., *Mutation-linked defective interdomain interactions within ryanodine receptor cause aberrant Ca(2)(+)release leading to catecholaminergic polymorphic ventricular tachycardia.* Circulation, 2011. **124**(6): p. 682-94.
393. Owen, V.J., N.L. Taske, and G.D. Lamb, *Reduced Mg2+ inhibition of Ca2+ release in muscle fibers of pigs susceptible to malignant hyperthermia.* Am J Physiol, 1997. **272**(1 Pt 1): p. C203-11.
394. Yarotskyy, V., F. Protasi, and R.T. Dirksen, *Accelerated activation of SOCE current in myotubes from two mouse models of anesthetic- and heat-induced sudden death.* PLoS One, 2013. **8**(10): p. e77633.
395. Flewellen, E.H., et al., *Dantrolene dose response in awake man: implications for management of malignant hyperthermia.* Anesthesiology, 1983. **59**(4): p. 275-80.
396. Ward, A., M.O. Chaffman, and E.M. Sorkin, *Dantrolene. A review of its pharmacodynamic and pharmacokinetic properties and therapeutic use in malignant hyperthermia, the neuroleptic malignant syndrome and an update of its use in muscle spasticity.* Drugs, 1986. **32**(2): p. 130-68.
397. Buyukokuroglu, M.E., et al., *Mechanism of the beneficial effects of dantrolene sodium on ethanol-induced acute gastric mucosal injury in rats.* Pharmacol Res, 2002. **45**(5): p. 421-5.
398. Ucuncu, H., et al., *Effect of dantrolene on lipid peroxidation, lutathione and glutathione-dependent enzyme activities in experimental otitis media with effusion in guinea pigs.* Hum Exp Toxicol, 2005. **24**(11): p. 567-71.
399. Laver, D.R., et al., *Termination of calcium-induced calcium release by induction decay: an emergent property of stochastic channel gating and molecular scale architecture.* J Mol Cell Cardiol, 2013. **54**: p. 98-100.
400. Palade, P., *Drug-induced Ca2+ release from isolated sarcoplasmic reticulum. II. Releases involving a Ca2+-induced Ca2+ release channel.* J Biol Chem, 1987. **262**(13): p. 6142-8.
401. Nelson, T.E., et al., *Dantrolene sodium can increase or attenuate activity of skeletal muscle ryanodine receptor calcium release channel. Clinical implications.* Anesthesiology, 1996. **84**(6): p. 1368-79.
402. Yang, T., et al., *Pharmacologic and functional characterization of malignant hyperthermia in the R163C RyR1 knock-in mouse.* Anesthesiology, 2006. **105**(6): p. 1164-75.
403. Domeier, T.L., et al., *Dantrolene suppresses spontaneous Ca2+ release without altering excitation-contraction coupling in cardiomyocytes of aged mice.* Am J Physiol Heart Circ Physiol, 2014. **307**(6): p. H818-29.
404. Sigworth, F.J. and S.M. Sine, *Data transformations for improved display and fitting of single- channel dwell time histograms.* Biophys. J., 1987. **52**: p. 1047-1054.
405. Xu, L., R. Jones, and G. Meissner, *Effects of local anesthetics on single channel behavior of skeletal muscle calcium release channel.* J Gen Physiol, 1993. **101**(2): p. 207-33.
406. Tsushima, R.G., J.E. Kelly, and J.A. Wasserstrom, *Subconductance activity induced by quinidine and quinidinium in purified cardiac sarcoplasmic reticulum calcium release channels.* J Pharmacol Exp Ther, 2002. **301**(2): p. 729-37.
407. Tinker, A. and A.J. Williams, *Charged local anesthetics block ionic conduction in the sheep cardiac sarcoplasmic reticulum calcium release channel.* Biophys. J., 1993. **65**: p. 852-864.

408. Ikemoto, T., et al., *Effects of dantrolene and its derivatives on Ca(2+) release from the sarcoplasmic reticulum of mouse skeletal muscle fibres.* Br J Pharmacol, 2001. **134**(4): p. 729-36.
409. Buyukokuroglu, M.E., et al., *In vitro antioxidant properties of dantrolene sodium.* Pharmacol Res, 2001. **44**(6): p. 491-4.
410. Ono, M., et al., *Dissociation of calmodulin from cardiac ryanodine receptor causes aberrant Ca(2+) release in heart failure.* Cardiovascular research, 2010. **87**(4): p. 609-17.
411. Hino, A., et al., *Enhanced binding of calmodulin to the ryanodine receptor corrects contractile dysfunction in failing hearts.* Cardiovascular research, 2012. **96**(3): p. 433-43.
412. Yano, M., et al., *Abnormal ryanodine receptor function in heart failure.* Pharmacology & therapeutics, 2005. **107**(3): p. 377-91.
413. Ide, T., et al., *Mitochondrial electron transport complex I is a potential source of oxygen free radicals in the failing myocardium.* Circ Res, 1999. **85**(4): p. 357-63.
414. Otsu, K., et al., *Refinement of diagnostic assays for a probable causal mutation for porcine and human malignant hyperthermia.* Genomics, 1992. **13**(3): p. 835-7.